SKELETAL TOURMALINE, UNDERCOOLING, AND CRYSTALLIZATION HISTORY OF THE STONE MOUNTAIN GRANITE

by

KRISTEN MICHELLE LONGFELLOW

(Under the Direction of Samuel E. Swanson)

ABSTRACT

Stone Mountain is composed of a light colored, fine-grained two-mica granite to granodiorite. Large (3-15cm) skeletal tourmaline crystals occur singly or in clusters and are surrounded by a white halo of biotite-free granite. Skeletal tourmaline occurs in granite and in pegmatite-aplite dikes. Euhedral tourmaline (.1-3cm) occurs in cores of pegmatite-aplites. The skeletal tourmaline crystals display a morphology typically associated with crystallization from undercooled melts. Halos surrounding the skeletal tourmaline crystals are consistent with growing tourmaline that depleted local melt environment in Fe, suggesting a magmatic origin for the skeletal crystals. The appearance of skeletal crystals in the granite and early-formed parts of the pegmatite suggest a link between the crystallization history of these units. Microprobe compositions indicate little compositional variation in the different textures of the schorl tourmaline. Crystallization of the aplite began by removal of B, and the remaining melt crystallized to form a euhedral core at low undercooling.

INDEX WORDS: Stone Mountain Georgia, pegmatite-aplite dikes, skeletal tourmaline, tourmaline, undercooling.

SKELETAL TOURMALINE, UNDERCOOLING, AND CRYSTALLIZATION HISTORY OF THE STONE MOUNTAIN GRANITE

by

KRISTEN MICHELLE LONGFELLOW

B.S., Valdosta State University, 2007

A Thesis Submitted to the Graduate Faculty of The University of Georgia in Partial Fulfillment of the Requirements for the Degree

MASTER OF SCIENCE

ATHENS, GEORGIA

2010

SKELETAL TOURMALINE, UNDERCOOLING, AND CRYSTALLIZATION HISTORY OF THE STONE MOUNTAIN GRANITE

by

KRISTEN MICHELLE LONGFELLOW

Major Professor: Samuel E. Swanson

Committee: Douglas Crowe
Alberto Patiño-Douce

Electronic Version Approved:

Maureen Grasso
Dean of the Graduate School
The University of Georgia
May 2010

ACKNOWLEDGEMENTS

First I would like to thank Stone Mountain Park for allowing me free access to the mountain and the extraction of samples. They were very accommodating and interested in my research. Assistance with sample extraction and tool transportation was provided by Mark T. Longfellow and David C. Gholson. Their muscle power and an eagerness to learn about my project made field work a great experience. Microprobe analysis would not have been possible without Chris Fleisher. His patience and expertise helped me to generate promising data. Funding was provided by the Miriam Watts-Wheeler travel and research fund.

I would like to acknowledge my undergraduate professor, Dr. Mark Groszos, for introducing me to the world of Geology. A field trip including a stop at Stone Mountain, GA in 2006 introduced me to what my future MS Thesis topic would entail. Many thanks also to the other members of my committee, Dr. Doug Crowe and Dr. Alberto Patino-Douce for their review of my manuscript and guidance. Finally, I would like to express my utmost gratitude to my advisor, Sam Swanson, for all of his support. His efforts to keep me on track and extensive knowledge made this study possible.

TABLE OF CONTENTS

Page

LIST OF TABLES

Page

LIST OF FIGURES

Page

CHAPTER 1

INTRODUCTION

The word "pegmatite" originally referred to the intergrowth of quartz and perthitic microcline (Brongniart, 1813) to form graphic granite. Haidinger (1845) broadened the meaning to include very coarse-grained dikes regardless of the presence of graphic granite. Scientific exploration of pegmatites began in the late 19th century with Sorby (1858) investigating pegmatite minerals and inclusions, followed by Brush's (1862, 1863) studies on the Hebron, Main, and Branchville, Connecticut pegmatites (London 2008). For the last 50 years or so, Cameron *et al.* (1949) has held the most widely accepted model for pegmatite origin and classification. A historical review by Jahns (1955) and study of internal evolution (Jahns and Burnham, 1969) were also very influential to the study of pegmatites.

As described by London (2008), there is only one unique textural occurrence that sets pegmatites apart from other igneous rocks, namely graphic intergrowths in the form of skeletal crystals. According to London (2008) the fine-grained margin of a pegmatite is accompanied by skeletal crystals formed by crystallization of an undercooled magma. Undercooling arises because of sluggish nucleation rates common to granitic melts (Fenn, 1977; Swanson, 1977). The presence of fluxing components, in the case of this study B, and a hydrous vapor phase, inhibits nucleation of crystals and decreases the melting temperature (solidus) of the melt (Swanson and Fenn, 1992). When the supersaturated

melt begins to nucleate crystals, which could take hours to days, if undercooling is high enough skeletal crystals will result. The transition from euhedral to skeletal crystals occurs within 100°C of undercooling in several silicate minerals (plagioclase, Lofgren, 1974; olivine, Donaldson, 1976; quartz, Swanson and Fenn, 1986).

Typically skeletal intergrowth occurs between the major granitic phases, quartz and feldspar, forming graphic granite. Skeletal crystals can also include muscovite, apatite, or tourmaline. Skeletal tourmaline is reported in several granites (Hub Kapong, Manning, 1982; Capo Bianco, Perugini and Poli, 2007; Seagull batholith, Sinclair and Richardson, 1992). A study on the Hub Kapong batholith of Thailand reveals skeletal and euhedral tourmalin found in pegmatite-aplite systems. The Hub Kapong batholith also exhibits "hollow" (skeletal) tourmaline crystals. This Sn and W rich system shows extensive zoning of individual tourmaline crystals from early schorl toward an alkali-free tourmaline (Manning, 1982).

Dendritic tourmaline in nodules or orbicules occurs in the relatively shallow Capo Bianco aplitic granite of the Elba Island, Italy (Perugini and Poli, 2007) and near the roof of the Seagull batholith in the Yukon Territory (Sinclair and Richardson, 1992). In both locations, tourmaline forms fine-grained skeletal crystals, surrounded by a leucocratic halo devoid of Fe-bearing minerals. Tourmaline in the Elba nodules consists of one optically continuous tourmaline crystal while the Yukon tourmaline replaces feldspar and quartz in the granite. Both authors (Sinclair and Richardson, 1992; Perugini and Poli, 2007) argue for a late-stage magmatic origin for the tourmaline nodules.

Various studies of Stone Mountain tourmaline propose a metasomatic (Grant, 1986; Watson 1902; and Size and Kahairallah, 1989), or magmatic origin (Swanson et al,

2001). Determining a relationship between skeletal tourmaline crystals in pegmatites and skeletal crystals in granite is essential in order to understand this system. Currently this system is at odds with London's (2008) model for pegmatites. Not only is undercooling found in the margin of pegmaite-aplites and tips of early dikes (line rock), but it is also found in granite. The occurrence is well documented in pegmatite-aplite systems, but little is know about lone skeletal tourmaline in granite. This study aims to use tourmaline textures as a guide to crystallization history of Stone Mountain granite.

CHAPTER 2

GEOLOGIC BACKGROUND

Stone Mountain

The Stone Mountain pluton (Figure 2.1) is one of approximately 60 Alleghanian intrusions in the Southern Appalachian region (Speer *et al.* 1994). The Alleghanian orogeny marks the suturing of Laurentia and Gondwana and produced westward-directed thrusts and dextral strike-slip faults (Hatcher, 1989). The Alleghanian deformation and abundant magmatic activity in the Southern Appalachians started at 327 Ma. and lasted for about 45 million years (Speer *et al.* 1994). This magmatic event began and ended with deformation, and produced a bimodal suite of plutonic igneous rocks dominated by granites with no apparent associated volcanism. These plutons were dispersed over an area 10,500 km^2 extending from Georgia to eastern Virginia. Plutons, strike-slip faults, and Bouguer gravity anomalies in Georgia and central North Carolina all have northeasterly trends (Speer *et al.* 1994).

The Stone Mountain pluton is an oval shaped sheet-like intrusion, which was emplaced into the core of a N65W anticline system (Grant, 1986). The fine-grained Stone Mountain granite is resistant to weathering and forms a monadnock rising nearly 250 m above the surrounding metamorphic rocks of the Piedmont. It is an asymmetrical dome with a nearly vertical slope on the north, 0 - 45° grade on the west, and 10 - 35° grade on

the south and east. The west slope is the only hiking area open to the public. Exfoliation is responsible for the rounded form of Stone Mountain and exfoliation continues today. Large lenticular slabs 10's of cm thick and 10's of meters long continually cleave off the sides of the mountain (Figure 2.2). This exfoliation creates excellent nearly 100 percent exposure of the granite. Stone Mountain has been uplifted 11.5 km via the unroofing of 11,000 m of rock over the past 71 m.y. Dallmeyer (1978) calculated the erosion rate for Stone Mountain to be 0.16 mm/yr.

The Stone Mountain pluton intrudes sillimanite-grade gneiss and schist of the Lithonia Gneiss (Hermann,1954). Stone Mountain granite has moderate to poor foliation, defined by the orientation of the biotite and muscovite (Whitney *et al.* 1976; Grant, 1986), although flow features are found in the granite (Figure 2.3). Relations between the Stone Mountain granite and Lithonia Gneiss have been described by Buddington (1959) as an example of a transitional mesozone-catazone depth of intrusion. Xenoliths of mica-schist and biotite gneiss are strongly oriented parallel to the flow structure (Grant, 1986).

Mineralogy/Petrology

Stone Mountain granite is light grey and fine to medium-grained (1 - 3mm). The granite is composed of quartz, oligoclase, potassium feldspar, and muscovite, with minor biotite. Characteristic accessory minerals include epidote, apatite, zircon, garnet, beryl, thulite, calcite, and skeletal and euhedral tourmaline. The granite is mineralogically homogeneous, with very little variation (Whitney et al. 1976). This granite is noted for it's skeletal tourmaline crystals and tourmaline-bearing pegmatite dikes. Known to local geologists as "cat's paws", these skeletal crystals range in size from 2 - 3 cm in width and

4 - 15 cm in length. The core of the pod is a skeletal black, schorl-type tourmaline crystal intergrown with feldspar and quartz. A white, Fe-depleted halo in the enclosing granite surrounds each pod. The amount of iron "missing" from the halo is equal to the calculated amount of iron tourmaline in the skeletal crystal (Size and Kahairallah, 1989). Tourmaline-bearing dikes and skeletal crystals are more prominent near the western margin of the granite, but do occur sporadically throughout the pluton. Table 2.1 (Whitney et al. 1976) gives the modal mineralogical composition of the Stone Mountain granite. Magmatic conditions of 600 - 700°C and 10 - 15 km intrusion depth were estimated using early existence of the assemblage of muscovite and quartz in granitic melt (Whitney et al. 1976).

Whitney et al. (1976) explains the petrology of the Stone Mountain granite. The plagioclase is oligoclase (An_{10-18}). It forms euhedral to anhedral crystals, commonly with inclusions of potassium feldspar, quartz, and muscovite. Potassium feldspar occurs as euhedral to subhedral crystals, commonly with inclusions of quartz, oligoclase, and muscovite. Quartz forms anhedral crystals, almost devoid of fluid inclusions. A few minor intergrowths with potassium feldspar are present. Muscovite occurs as tabular, anhedral crystals, commonly intergrown with biotite. Biotite forms inclusions in all major minerals. Epidote is found intergrown with biotite and muscovite. Almandine-rich garnet is found as thin layers along the edges of early dikes as well as pegmatite-aplites. Zircon is commonly found included in biotite as well as apatite. Dark green beryl is found in some pegmatites. Tourmaline occurs as previously described as skeletal crystals in granite and as skeletal to euhedral crystals within pegmatite and aplite dikes. Iron-titanium oxides are completely absent in Stone Mountain granite (Whitney et al. 1976).

Geochemistry

The Stone Mountain granite is peraluminous, with 1 - 3 percent corundum by weight in the norm, and shows limited compositional variation, ranging from 72 - 76 weight percent SiO_2 (Whitney *et al.* 1976; Grant *et al.* 1980). FeO, MgO, and TiO_2 are all low, less than 1 weight percent. Na and K are present in nearly equal amounts (Table 2.2). The age of Stone Mountain granite is given by a whole-rock Rb-Sr isochron as 271 Ma with an initial $^{87}Sr/^{86}Sr$ isotope ratio of 0.7250 (Whitney *et al.* 1976). The presence of modal muscovite, normative corundum, and high initial Sr isotope ratios indicate the Stone Mountain granite is an S-type granite.

Trace element concentrations were determined by Whitney (*et al.* 1976). Rb ranges from 210 - 285 ppm, Sr from 84 - 107 ppm, and Ba from 240 - 310ppm. Such high ratios of K/Rb and Rb/Sr indicate a highly differentiated granitic melt (Whitney *et al.* 1976) and partial melting of the host Lithonia Gneiss to produce the Stone Mountain granite. La/Lu ratios range from 22.8 - 91.7 (Grant *et al.* 1980) also showing a fractionated pattern.

Pegmatite-Aplite Dikes

The granite is host to at least three generations of thin (mms to cms) pegmatite-aplite dikes (Table 2.3). Early dikes (ED) are composed of fine- to coarse-grained quartz and feldspar. Coarse-grained ED are less abundant than fine-grained ED and occur on all sides of the mountain. They are on average 6cm wide, variable in length, and contain coarse-grained, euhedral, inward-projecting potassium feldspar crystals. Fine-grained ED are much more abundant relative to coarse-grained ED, and are composed of fine-grained

quartz and feldspar, with occasional local development of marginal garnet. Fine-grained ED range from 1 – 90 cm in width and bifurcate along strike. Individual dikes can be traced for 10s to 100s m.

Composite pegmatite-aplite dikes (PAD) contain tourmaline and have sharp, anastomosing contacts with the enclosing granite. Isolated pegmatite dikes, lacking an aplite unit, were not observed at Stone Mountain. These PAD have a distinct 1 – 5 cm leucocratic halo in the granite adjacent to the dike. Quartz, feldspar, tourmaline and white mica are the main constituents. Pegmatite units can contain accessory apatite, beryl, thulite, garnet, calcite, and zircon. Tourmaline occurs as euhedral grains up to 3 cm in length in the core of pegmatite units and as skeletal crystals in the aplite zone and granite halo. Most PAD show a gradation from euhedral to skeletal tourmaline textures, and from coarse-grained to fine-grained from the core to the rim.

Tourmaline-bearing aplite dikes, lacking a pegmatite unit, are common at Stone Mountain. These dikes contain a leucocratic halo zone in the adjacent granite. The aplite dikes are rich in quartz and feldspar. Tourmaline is present as fine-grained skeletal crystals. Very fine-grained euhedral crystals tourmaline crystals occur in core of thin (mm to cm) quartz feldspar veins. These veins are also enclosed by a leucocratic halo zone. These thin veins may actually represent the distal ends of aplite dikes, but the veins do locally cross-cut the composite pegmatite-aplite dikes. Grant (1986) noted similar veins in Mount Arabia migmatite in South DeKalb County (Grant, 1986).

Skeletal Tourmaline

Skeletal tourmaline crystals are a hallmark of Stone Mountain granite. They are elliptical in shape, and range in size from 4 - 15 cm in length and 2 - 3 cm in width. These crystals occur singly or in clusters and may appear with in a short distance of a pegmatite or ED. They have no preferred orientation of the long axis. Skeletal tourmaline occur in granite, within the leucocratic halo zone of all composite PAD (Figure 2.4), and in some cases as part of the marginal end of a pegmatite. Size and Khairallah (1989) and Whitney *et al.* (1976) argue a metasomatic origin for the skeletal tourmaline in granite, suggest that the tourmaline clusters probably formed through an interaction between boron-rich solutions and the crystalline material in the later stages of crystallization. Whitney et al. (1999) asks, "What evidence can be seen in support of this idea? Did the tourmaline form relatively early or late in the crystallization history of the granite?" This study aims to answer this very question.

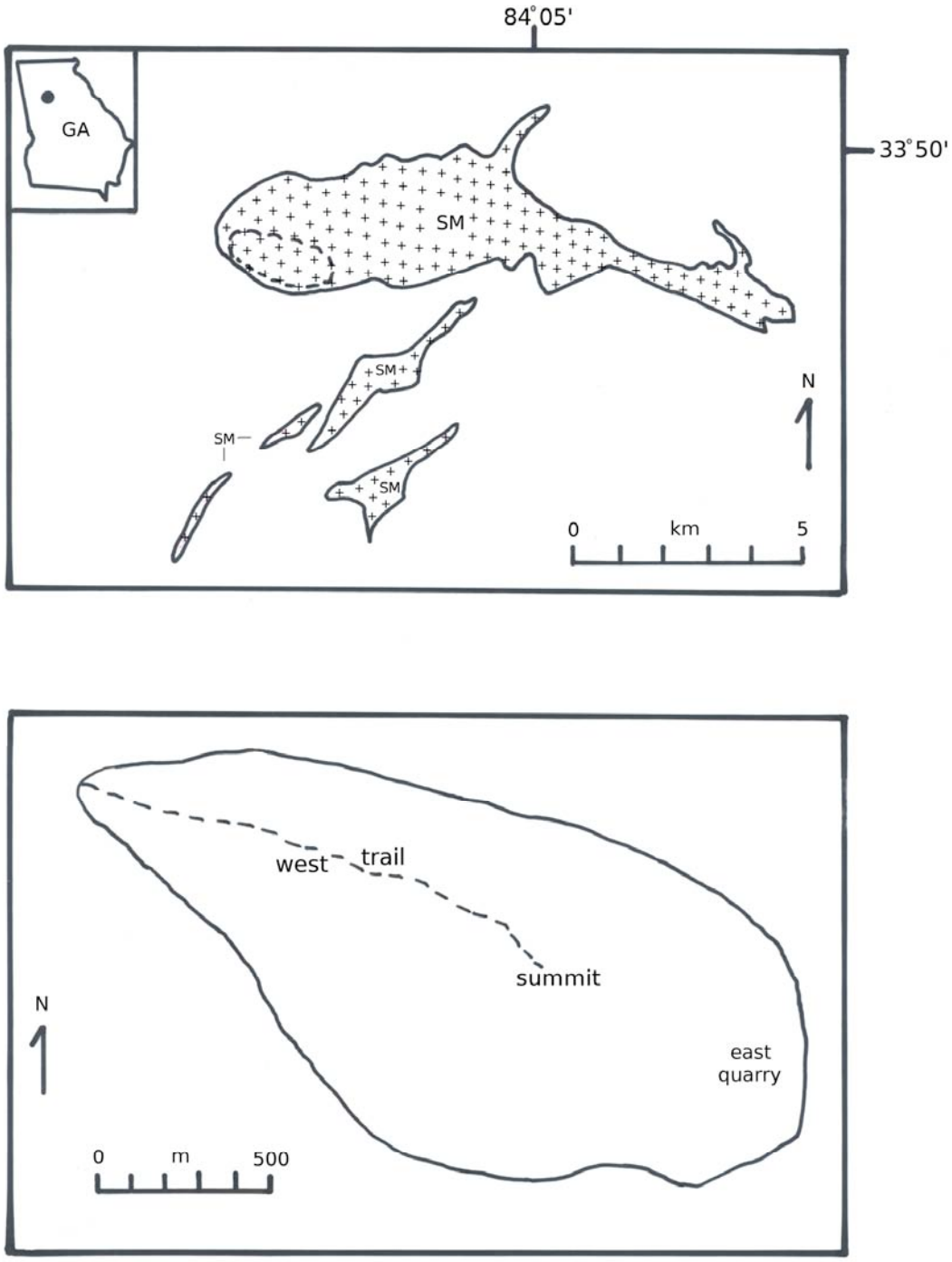

Figure 2.1 Geologic map of the Stone Mountain pluton, GA.

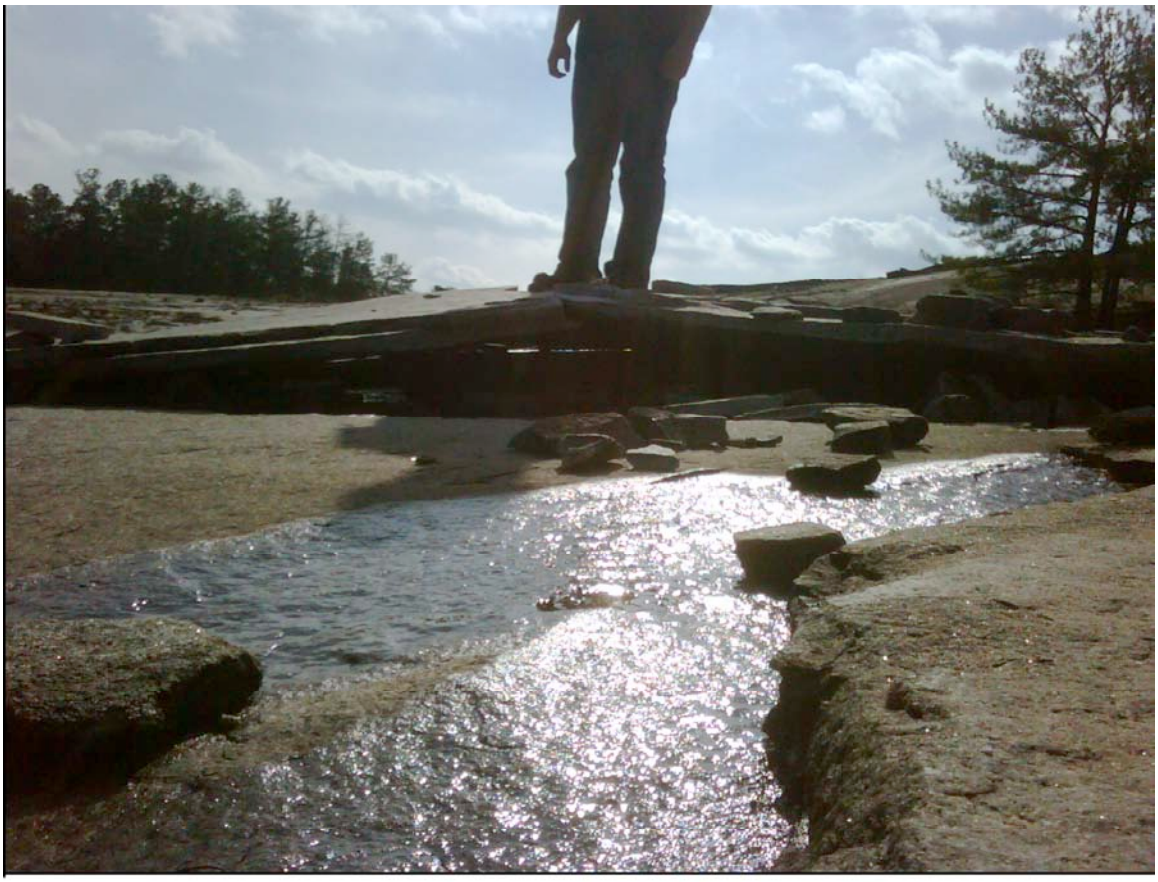

Figure 2.2 Exfoliation of Stone Mountain Granite, East Quarry, Stone Mountain, GA. Slabs are approximately two inches thick.

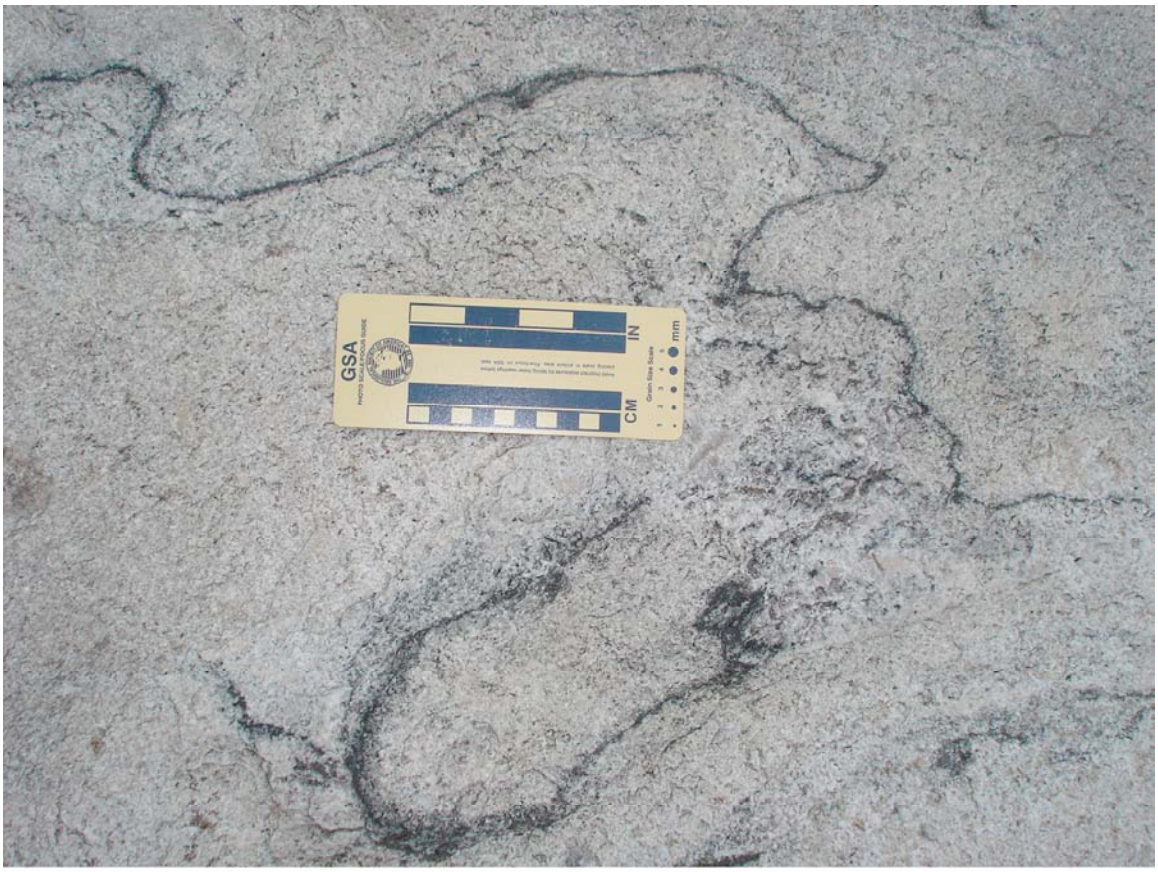

Figure 2.3 Evidence of flow within Stone Mountain pluton, Summit, Stone Mountain, GA. Black, anastomosing, very fine-grained tourmaline is rare in the granite.

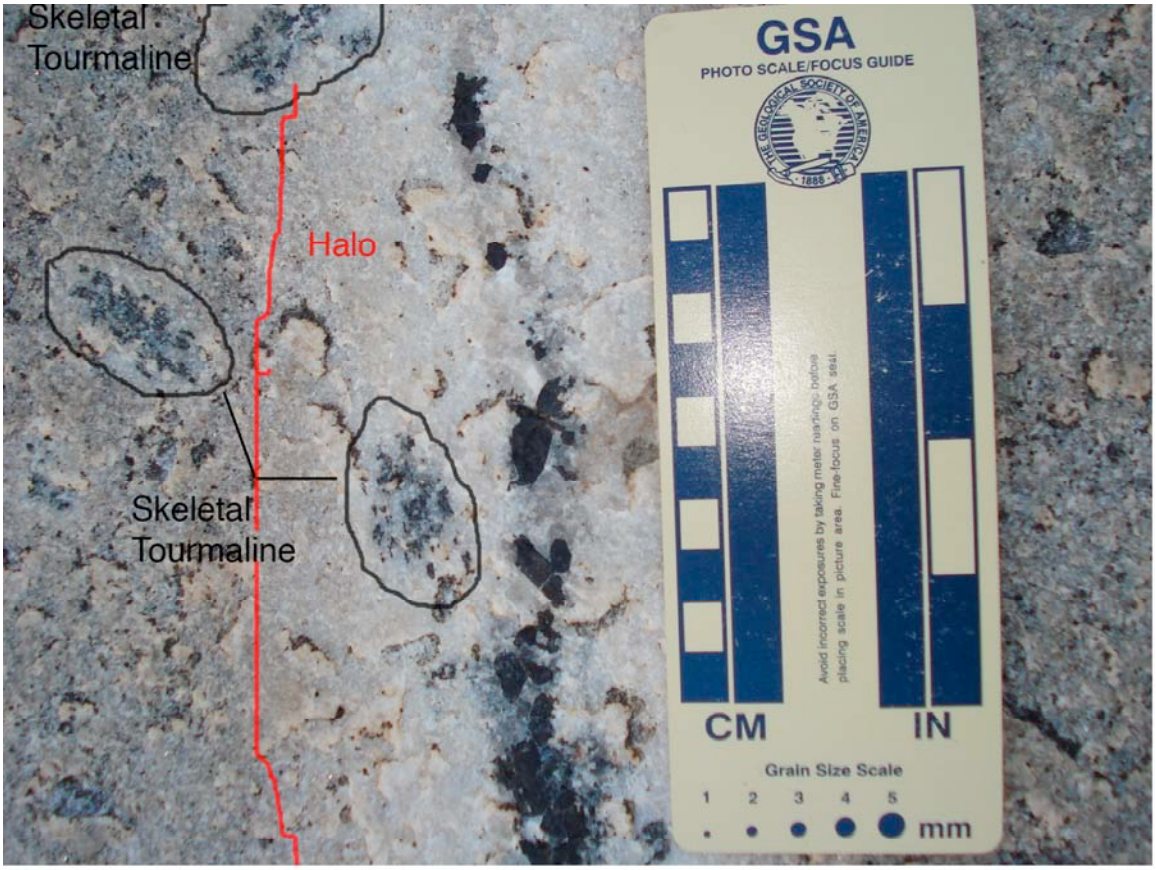

Figure 2.4 Skeletal tourmaline in halo of PA. East quarry, Stone Mountain, GA

Table 2.1 Modal mineralogical composition of the Stone Mountain granite. (Whitney et al. 1976)

	1	2A	3A	4B	5	6
Quartz	29.8	32.8	31.9	33.1	32.4	30.8
Microline	26.5	22.3	23.1	19.2	25.7	27.9
Oligoclase	35.8	34.8	34.0	38.0	28.8	31.1
Muscovite	6.1	8.4	8.5	9.0	11.5	8.7
Biotite	1.5	1.0	1.9	0.3	1.2	1.4
Epidote	0.2	0.6	0.4	0.3	0.3	0.1
Apatite	tr.	0.1	0.2	0.1	tr.	tr.
Zircon	tr.	tr.	tr.	tr.	tr.	tr.
Tourmaline	0.0	0.0	0.0	0.0	0.3	0.0
Color Index	1.7	1.6	2.3	0.6	1.8	1.5

Table 2.2 Chemical analysis and normative minerals for Stone Mountain granite. (Grant et al. 1980)

Oxide %	1A	2B	3C	4C	6A
Si02	72.5	72.0	75.5	73.3	74.0
TiO2	0.19	0.15	0.15	0.15	0.12
Al2O3	16.2	15.8	15.4	14.6	15.6
FeO	2.0	1.39	0.89	1.22	0.98
MnO	0.04	0.03	0.02	0.02	0.03
MgO	0.15	0.22	0.24	0.25	0.25
CaO	0.80	0.45	0.78	0.84	1.26
Na2O	3.24	2.27	2.27	4.18	4.49
K2O	4.37	5.30	4.59	4.75	4.42
H2O	0.42	0.52	0.35	0.36	0.35
Total	99.91	98.13	100.6	99.87	101.5
Normative					
Q	34.99	36.71	39.8	28.42	27.54
C	4.69	5.51	4.54	1.06	1.14
Or	25.83	31.32	27.13	28.07	26.12
Ab	27.42	19.21	23.02	35.37	37.99
An	3.97	2.23	3.87	4.17	6.25
Hy	0.37	1.66	1.22	1.53	1.40
Mt	0.61	0.68	0.43	0.61	0.48
Il	0.36	0.28	0.28	0.28	0.23
DI	88.2	87.2	90.0	91.9	91.7

DI = Differentiation Index = ΣQ + Or + Ab in the norm.

Table 2.3 Mineralogy of dikes

type	grain size (mm)	abundance	mineralogy	tourmaline texture
Early dikes	<1	Abundant	Qtz, Kfs, Pl, Ms, Bt, Srl, Grt	Rare euhedral, 5 mm
Pegmatite-aplite dikes	<1 to >30	Very abundant	Qtz, Kfs, Pl, Ms, Bt, Srl, Grt, Zo, Ap, Brl	Common skeletal 0.5 – 15 cm
Tourmaline veins	<1	Rare	Qtz, Kfs, Srl	Euhedral, 0.05 mm

Ap = apatite, Brl = Berly, Bt = biotite, Grt = garnet, Kfs = Potassium fedspar, Ms = muscovite, Pl = plagioclase, Qtz = quartz, Srl = schorl, Zo = zoisite

CHAPTER 3

METHODS

Field work was confined to the slopes and summit of Stone Mountain proper in order to take advantage of the excellent (100 percent) bare rock exposure. The study was divided into three main focus areas: the easy quarry, the west trail, and the summit. Samples were taken from ED, pegmatite dikes, PAD, skeletal tourmaline in granite, and tourmaline veins for microprobe analysis. Textures, field relations, sketch maps, photographs, strike and dip, GPS location, mineralogy, and orientation were collected from at least 30 dike/vein occurrences (Appx. C). Presence of skeletal versus euhedral tourmaline crystals was noted along with size and orientation of tourmaline crystals.

Due to the exfoliation-controlled, smooth surface of Stone Mountain, it was difficult to determine dips of planar features, such as dikes or veins. A few dips were measured, but the majority of dike/vein orientations consist only of strike. Cross-cutting relationships are well exposed on the bare outcrop and provide a crystallization history for the various units. Dikes and veins were categorized based on mineralogy and texture (Table 2.3). Microprobe analysis was performed on all samples taken from Stone Mountain.

In this study, Stone Mountain granite analysis was conducted using prepared slides used by Swanson *et al.* (2001). Samples from a tourmaline-bearing PA dike EQO (Appx. B), a Tourmaline-bearing vein from site WTE4 (Figure 5.9)(Appx. B), and

euhedral tourmaline crystals extracted from site EQO (Figure 5.17)(Appx. B) were analyzed in this study on the JEOL 8600 EMPA. Euhedral tourmaline crystals extracted from pegmatites were cut perpendicular and parallel to the c-axis in order to observe zoning patterns. Crystal fragments were set in epoxy, polished, and analyzed in the microprobe.

Samples were analyzed with the University of Georgia Department of Geology JEOL 8600 electron microprobe using a 15 KV accelerating voltage and a 15-20 nA beam current. Quantitative analyses were performed with a wavelength dispersive spectrometer (WDS) automated with Geller Microanalytical Laboratory's dQUANT software using 10 second counting times, and natural and synthetic mineral standards. Analyses were calculated using the Phi-Rho-Z matrix correction model (Armstrong, 1988). Backscattered electron images (BEI) and secondary electron images were acquired using Gheller Microanalytical Laboratory's dPICT imaging software.

Boron, lithium, and hydrogen were not able to be analyzed in this study. A normalization scheme was needed because of an incomplete data set. Structural formulae were calculated using a spreadsheet made by Andy Tindle from his web address: http://www.open.ac.uk/earthresearch/tindle/AGTWebPages/AGTSoft.html Calculations were made for 31 anions, and assumed three atoms of B^{3+} *apfu*, and Fe = Fe^{2+}.

CHAPTER 4

SKELETAL TOURMALINE, UNDERCOOLING, AND CRYSTALLIZATION HISTORY OF THE STONE MOUNTAIN GRANITE, GEORGIA, U.S.A.

[1]Skeletal Tourmaline, Undercooling, and Crystallization History of Stone Mountain Granite, K. M. Longfellow & S. E. Swanson, submitted to *The Canadian Mineralogist*, 11/17/2009.

SKELETAL TOURMALINE, UNDERCOOLING, AND CRYSTALLIZATION HISTORY OF THE STONE MOUNTAIN GRANITE, GEORGIA, U. S. A.

By

Kristen M. Longfellow and Samuel E. Swanson'

Department of Geology

University of Georgia

Athens, GA 30602

U. S. A.

'

E-mail address: sswanson@uga.edu

ABSTRACT

The Stone Mountain pluton is composed of tourmaline-bearing biotite-muscovite granite. Tourmaline occurs as large skeletal crystals in the granite in the same areas as late-stage aplite and aplite-pegmatite dikes. Skeletal tourmaline also occurs in the aplite zone of aplite-pegmatite dikes. Pegmatites and feldspar-quartz-tourmaline veins contain euhedral tourmaline. Isolated skeletal tourmaline crystals in the granite and tourmaline-bearing dikes are surrounded by a fine-grained leucocratic halo of feldspar and quartz. The halo is depleted in Fe and represents granite and/or magma that was depleted in tourmaline-forming components. Skeletal tourmaline shows a brown (early) to blue (late) pleochroism. Euhedral tourmaline has blue cores and brown rims. Microprobe compositions indicate little compositional variation and chemical zoning in the different textures of the tourmaline. Tourmaline textures indicate an initial crystallization at undercoolings of 40-100 ºC. Removal of B from the melt raises the solidus temperature and initiated crystallization to form aplite. Remaining, B (and water) depleted magma has a higher solidus temperature and tourmaline (and other phases) crystallize at a low undercooling to form euhedral crystals in pegmatites.

Specifics of the origin of the granite-hosted skeletal crystals are problematic. They may represent crystallization from some B-enriched fluid that replaces existing granite. Alternatively, they may form from localized pools of melt formed in the granite by the fluxing of B-enriched fluids.

INTRODUCTION

Skeletal crystals are an integral part of granitic pegmatites (London, 2008). Granitic melts are known to be sluggish to nucleate crystals (e.g. Fenn, 1977; Swanson, 1977). Nucleation is found to be inhibited by the presence of a hydrous vapor phase or even by the presence of fluxing components, such as F, that lower solidus and liquidus temperatures of the melts Swanson and Fenn, 1992). The delay in nucleation apparently results from the modification of the Si-O framework within the melts related to the solution of the fluxing components. Cooling of silicate melts coupled with the delay in nucleation produces undercooled melts without crystals. Ultimately undercooled melts nucleate crystals, but if the undercooling is high enough, the crystals have skeletal habits. The transition from euhedral to skeletal crystals (Fig. 1) occurs at less than 100 ºC of undercooling in several rock-forming silicate minerals (plagioclase, Lofgren, 1974; olivine, Donaldson, 1976; and quartz, Swanson & Fenn, 1986).

Undercooling in pegmatitic systems is associated with an overall cooling of the system related to intrusion in cold host rocks or is associated with local diffusion-related compositional gradients in the melt in front of advancing crystals (London, 2008). Typically skeletal crystals in pegmatites are the major phases in granitic pegmatites, K-feldspar and quartz of graphic granite and the clevelandite variety of albitic plagioclase. Other accessory minerals, such as muscovite and apatite, also exhibit skeletal forms (London, 2008).

Tourmaline is an accessory mineral, found in peraluminous granitic rocks and pegmatites. The composition of tourmaline is complex with 9 different species recognized (Clark, 2007). Compositional variations are common within a given tourmaline occurrence (e.g. London and Manning, 1995) and are related to fractionation trends in magmatic systems and/or fluctuations of hydrothermal fluids during crystallization. Compositional variation in tourmaline is a sensitive guide to petrogenesis of pegmatites (Jolliff *et al.* 1986) and hydrothermal (Demirel *et al.* 2009) systems.

Skeletal tourmaline is reported in several granites (Manning, 1982, Sinclair & Richardson, 1992; Perugini & Poli, 2007,). Small aplite dikes associated with Sn and W mineralization in the Hub Kapong batholith of Thailand contain fine-grained tourmaline in the aplite and coarse-grained skeletal tourmaline in thin pegmatitic lenses. The skeletal tourmaline is cored by quartz or alklai feldspar. Tourmaline shows extensive zoning from early schrol toward an alkali-free tourmaline.

Crystallization of dendritic tourmaline in nodules or orbicules occur in the relatively shallow Capo Bianco aplite of the Elba Island, Italy (Perugini & Poli, 2007) and in granite near the roof of the Seagull batholith in the Yukon Territory (Sinclair& Richardson, 1992). In both cases the nodules consist of fine-grained, dendritic tourmaline and are surrounded by a leucocratic halo depleted in Fe (biotite-absent). Tourmaline in the Elba nodules consists of a single, optically continuous crystal of tourmaline. The Yukon tourmaline replaces feldspar and quartz in the granite. In both cases the authors argue for a late stage magmatic origin for the tourmaline nodules. The purpose of this paper is to use the textural variation of tourmaline as a guide to the crystallization history of the Stone Mountain granite.

REGIONAL GEOLOGICAL SETTING

Stone Mountain is an isolated, bare-rock outcrop that rises some 200 meters above the metamorphic rocks of the Georgia Piedmont near Atlanta, Georgia (Fig. 2). The Mountain is 0.9 km at its widest point and some 2.6 km long and forms an asymmetrical dome with a nearly vertical slope on the north, 0-45 degree grade on the west, and steeper on the south and east. The bare rock outcrop is in stark contrast to the heavily vegetated surrounding countryside. The mountain known as Stone Mountain corresponds to the western end of the outcrop of the Stone Mountain granite pluton. Exfoliation of Stone Mountain Granite produces a smooth outcrop surface, rarely showing three-dimensional faces required in order to measure dip.

The Stone Mountain granite (Fig. 2) is one of approximately 60 Alleghanian plutons in the Southern Appalachian region (Speer *et al*. 1994). The Alleghanian orogeny marked the suturing of Laurentia and Gondwana and produced westward-directed thrusts and dextral strike-slip faults (Hatcher *et al*. 1989). Alleghanian magmatic activity in the southern Appalachians started at 327 Ma. and lasted for about 45 million years (Speer *et al*. 1994). The magmatic event produced a bimodal suite of plutonic igneous rocks dominated by granites with apparently no associated volcanism. Granitoid rocks comprise 95 % of the Alleghanian plutons and about 20 % of the granitoids are peraluminous S-type granites (Speer *et al*. 1994). These plutons were dispersed over an area 10,500 km^2 extending from Georgia to eastern Virginia. Plutons, strike-slip faults,

and Bouguer gravity anomalies in Georgia and central North Carolina have northeasterly trends while Alleghanian plutons and structures in eastern North Carolina and Virginia trend north-south (Speer *et al*. 1994).

High-grade, migmatitc granite gneiss, the Lithonia Gneiss, is the host rock for the Stone Mountain pluton. Contacts between the granite and host rock vary from concordant to sharply cross cutting suggesting a mid-crustal depth of pluton emplacement. Relations between the Stone Mountain granite and the Lithonia Gneiss were cited by Buddington (1959) as an example of a transitional meszone-catazone depth of intrusion. Contact metamorphism in the form of K-feldspar porphyroclasts in the gneiss adjacent to the Stone Mountain granite is reported in at least one location (Grant, 1986). Tourmaline is not noted in the gneiss in contact with the granite.

STONE MOUNTAIN GRANITE

The Stone Mountain granite is light grey and fine-medium-grained, typical grain sizes ranges from 1-3 mm. It is an S-type granite composed of quartz, oligoclase, microcline, muscovite, and minor biotite. Accessory minerals include tourmaline, epidote, apatite, zircon and garnet. Tourmaline occurs in pegmatite-aplite dikes and in pods in the granite. Tourmaline pods consist of a inner, coarse-grained (3-15 cm) skeletal tourmaline crystal surrounded by a leucocratic aplitic zone identical to the granite except for the absence of biotite and lower modal muscovite. Tourmaline pods and tourmaline pegmatite-aplite dikes occur in the same areas and are generally more abundant near the western edge of the Stone Mountain pluton, including the area of Stone Mountain (Fig. 2).

Geochemically, the Stone Mountain granite is peraluminous and shows limited compositional variation, ranging from 72 to 76 weight percent SiO_2 (Whitney *et al*. 1976; Grant *et al*. 1980). Contents of FeO + MgO are low, less than 1 weight percent and Na and K are present in about equal amounts. Age of the Stone Mountain granite is given by a whole rock Rb-Sr isochron as 271 Ma with an initial Sr isotope ratio of 0.7250 (Whitney *et al*. 1976). The peramuminous composition and high initial Sr isotope ratio indicate a anatectic origin and Whitney *(et al*. 1976) proposed melting of the enclosing Lithonia Gneiss to produce the Stone Mountain magma. Feldspar compositions combined with solidus phase relations yield a estimate of the depth of emplacement of the Stone Mountain granite at about 0.5 Gpa. (Whitney *et al*. 1976).

Pegmatite/Aplite

The granite is host to at least three generations of thin (mms to cms) pegmatite-aplite dikes (Figs. 3, 4 & 5). Early dikes (Figs.3, 4 & 5) are composed of fine- to coarse-grained quartz and feldspar and can have marginal garnet. Later dikes, composite pegmatite-aplite dikes, contain quartz, feldspar, and tourmaline. A somewhat arbitrary distinction is made between thin veins of tourmaline, K-feldspar, and quartz and the more complex tourmaline-bearing pegmatite-aplite dikes.

Tourmaline-bearing pegmatite-aplite dikes form sharp contacts with the enclosing granite (Figs. 5b & 5c). The pegmatite portion of the dikes is coarser-grained than the granite with grains up to 3 cm in length. Tourmaline occurs as euhedral and skeletal forms in the dikes. Euhedral tourmaline in the pegmatite is enclosed by leucocratic aplite zone with skeletal tourmaline in the outer part of the composite dikes (Fig.5b). The thin

tourmaline veins (Fig. 5d) also are enclosed by a leucocratic aplitic zone between the vein and the granite.

Tourmaline

Tourmaline is a common phase in both the Stone Mountain granite and in the aplite-pegmatites. Pods of skeletal tourmaline are scattered through the granite. Skeletal tourmaline occurs in marginal aplite zone of the pegmatites, while euhedral tourmaline only occurs in pegmatite cores or in the tourmaline veins. The origin of the skeletal tourmaline is problematic and prompted one worker to state a detailed description of the development of the tourmaline pods is "beyond the scope of this study" (Whitney *et al*. 1976). This paper will shed some light on the development of tourmaline textures in the Stone Mountain granite.

METHODS

Field work was confined to the slopes and summit of Stone Mountain proper in order to take advantage of the excellent (100 percent) exposures afforded by the bare rock outcrop. Stone Mountain was divided into three study areas for this project: the east quarry, the west trail, and the summit (Fig. 2). Textures, mineralogy, orientation, strike and dip, GPS location, sketch map, and photographs were collected from 30 dikes/ vein occurrences. Early dikes (ED) occur in the east quarry and west trail areas (Fig. 2), but were not observed on the summit. Fine-grained ED are more common than coarse-grained ED. Composite aplite-pegmatite dikes are more common than coarse-grained ED. Aplite-pegmatites are most abundant in the east quarry, but occur in all areas.

Presence of skeletal or euhedral tourmaline crystals, along with their size, was noted during the field studies. The smooth, exfoliation-controlled outcrop surface at Stone Mountain makes determination of the dip of planar features, such as dikes or veins, difficult. Most measurements vein and dike orientations consist of only the strike. Only a few isolated dips were measurable. Dikes and veins in the granite were classified based on their texture and mineralogy (Table 1). Cross-cutting relations (Fig. 4) are well exposed at Stone Mountain and provide a crystallization history for the magma. Samples of all the textural varieties of tourmaline were collected for microprobe analysis.

Samples were analyzed with the University of Georgia Department of Geology JEOL 8600 electron microprobe using a 15 KV accelerating voltage and 15-20 nA beam current. Quantitative analyses were performed with wavelength dispersive spectrometers (WDS) automated with Geller Microanalytical Laboratory's dQANT software, using 10 second counting times, and natural and synthetic mineral standards. Analyses were calculated using Armstrong's (1988) Phi-Rho-Z matrix correction model. Backscattered electron (BEI) and secondary electron images were acquired using Geller Microanalytical Laboratory's dPICT imaging software.

RESULTS

Field Studies

Several varieties of dikes and veins can be distinguished in the Stone Mountain pluton based on mineralogy (Table 1). The early dikes (ED) are composed of feldspar and quartz and are devoid of skeletal tourmaline (Fig. 3). Rare euhedral tourmaline occurs in one ED. These dikes are cut by tourmaline veins and pegmatites (Fig. 4), hence

the name early dikes. Most ED are fine-grained (Fig. 3b) with local development of garnet layers (line rock) parallel to the dike contact. A few ED are coarse-grained (pegmatitic) and contain unidirectional, inward-projecting, K-feldspar crystals (Fig. 3a). Early dikes bifurcate and can be traced for long (10's to 100's of meters) distances. ED in the east quarry strike in the range 45-62^{o} NE. Along the west trail (Fig. 2), ED strike are in the range 20-42^{o} NE. All ED found on the summit have a more notherly trend and strike 0-14^{o} NE.

Tourmaline-bearing pegmatite dikes (TP) are zoned from an outer, finer-grained (aplitic) zone (A), composed of feldspar + quartz + skeletal tourmaline, to a coarse-grained pegmatitic core (P) of quartz + euhedral tourmaline (Figs. 5b & 5c). Some dike outcrops lack a pematitic core and are composed only of the leucocratic aplite with skeletal tourmaline (Fig. 5b). The aplitic zone forms a fine-grained leucocratic halo that is devoid of biotite and contains less muscovite than the granite. Rare accessory minerals include fine-grained garnet, apatite, and a carbonate mineral. Tourmaline-bearing pegmatite dikes are typically less than one meter wide and rarely extend for more than 10 meters. TP cross-cut the ED (Fig. 4a). Pegmatites found on the summit strike 0-20^{o} NE. Pegmatites in the east quarry measured strike 0-35^{o} NW. One pegmatite was found on the west trail with a variable strike of 0-10^{o} NW.

Tourmaline veins (Figs. 4b & 5d) are very-fine grained and composed of euhedral tourmaline crystals in a matrix of K-feldspar and quartz. A white Fe-depleted halo encloses the tourmaline veins. The term vein is used to connote a fracture filled with one or two minerals as opposed to a dike (fracture filled with rock). Tourmaline veins only

occur on the west flank of the mountain. The veins are thin and branch to follow local joints (Fig. 5d). Veins cross cut early dikes and pegmatite dikes (Fig. 4b).

Tourmaline pods occur within the Stone Mountain granite (Fig. 5a & 6a) in the same areas as TP (Figs. 6c & 6d) and the ends of the ED (Fig.6a). The pods are composed of a large, single skeletal crystals of tourmaline surrounded by a fine-grained leucocratic aplitic halo devoid of biotite. The lack of any Fe-bearing phases in the halo results in the white color. Minerals in the halo are similar to the same phases in the granite in term of texture and composition. Width of the halo is proportional to the width of the tourmaline crystal.

On the summit, skeletal tourmaline density is approximately 65 crystals per square meter**.** The crystals are elongate along the c-axis and have a poikiloblastic texture with abundant inclusions of quartz and feldspar grains. None of the dikes or tourmaline veins appear to cross cut the tourmaline pods.

MINERALOGY OF TOURMALINE

Euhedral tourmaline

Crystals of euhedral tourmaline up to 3 cm long occur in the pegmatite cores (Fig. 6d). The crystals show extensive color zoning from blue cores to brown rims (Fig. 7c), but the zoning patters are complex (Figs. 7b & 7d). Some sector zoning is apparent in the tourmaline cores (Fig.7c). Mineral inclusions in euhedral pegmatite tourmaline include: quartz, Ca-rich garnet, and apatite. Euhedral, very fine-grained tourmaline in the veins (Fig. 7a) does not contain any mineral inclusions.

Skeletal tourmaline

Very coarse-grained (3-15 cm) skeletal tourmaline crystals in the granite are composed of numerous small (0.5-6 mm), disconnected cellular tourmaline grains all in optical continuity. A few of these grains show some development of euhedral crystal faces. Very fine-grained inclusions in the cellular tourmaline grains are mostly quartz, but feldspar is also common. Locally the tourmaline grains cross cut feldspar-quartz grain boundaries or twin lamella in the feldspars. Most of a skeletal crystal is brown in plane polarized light (PPL), but some blue color occurs on some grain terminations.

Skeletal tourmaline crystals in the aplite zone of aplite-pegmatite dikes are coarse-grained (2-9 mm). The crystals are each individual crystals, not like the disconnected grains of the larger granite-hosted skeletal crystals. The aplite skeletal crystals have a euhedral outer form and a distinct hollow interior filled with quartz and feldspar (Fig. 7d). Fine-grained inclusions of quartz and feldspar also occur in the skeletal crystals. Aplite tourmaline is mostly brown in PPL, but some blue is found toward the grain centers; reminiscent of the color zoning in the euhedral tourmaline of the pegmatite (Fig. 7c).

Composition of tourmaline

Tourmaline compositions show little variation in the Stone Mountain granite and pegmatites (Table 2). The tourmaline is a schorl variety with a restricted range of FeO (10.5 - 13.4 wt.%) and relatively low MgO (2.9 - 4.0 wt. %). Color variations correlate with Ti content; low Ti (0.2 - 0.4 wt % TiO_2) tourmaline is blue in plain light, higher Ti tourmaline (1.0 - 1.4 wt % TiO_2) is brown.

Compositions of euhedral tourmaline reveal only subtle changes in composition, in contrast to the distinct patterns of optical zoning. Maximum observed variation is

about 3 weight percent FeO. This pattern of dramatic color zoning of Fe-rich tourmaline, but a weak chemical signature for the zoning is noted in other systems (e.g. Slack & Coad, 1989; Sinclair & Richardson, 1992). Vein tourmaline crystals are not zoned (Table 2).

DISCUSSION

The presence of skeletal tourmaline in the granite and in pegmatite-aplite dikes at Stone Mountain prompted earlier workers to propose a metasomatic origin (Watson, 1902; Grant *et al*., 1980; Grant, 1986; Size & Khairallah, 1989). Tourmaline formed from hydrothermal fluids shows fine-scale, oscillatory-type zoning (Samson & Sinclair, 1992; London & Manning, 1995; Demirel *et al*. 2009). Lack of appreciable zoning is a mark of magmatic tourmaline (Manning, 1982; London & Manning, 1995). Stone Mountain tourmaline shows little zoning. There is no textural evidence that skeletal Stone Mountain tourmaline replaced preexisting phases. These facts, together with the moderate emplacement depth (reduced hydrothermal activity) argue for a magmatic origin for the Stone Mountain tourmaline (Swanson *et al*. 2001).

Most of the Stone Mountain skeletal tourmaline from both aplite and granite is composed of single crystals of tourmaline. Some skeletal crystals within the aplite are oriented perpendicular to the contact of the aplite with the granite (Figs. 5c, 6c & 6d). Clusters of skeletal crystals in the granite show a outward directed radial pattern resulting from outward growth from a common nucleation center. Oriented crystal growth is consistent with crystallization from a magma with a compositional and/or thermal gradient (London, 2008).

Growth of skeletal silicate crystals requires an undercooling of at least 30-40 ºC (Fig. 1b). Higher undercoolings produce dendritic crystals (Figs. 1c & 1d), lower underecoolings produce euhedral crystals (Fig. 1a). The skeletal crystals of tourmaline record undercoolings on the order of 30-40 ºC during the crystallization of the Stone Mountain granite, while euhedral tourmaline occurring in the core of the pegmatite dikes and veins represents crystallization at lower undercooling. Skeletal tourmaline in the granite is only found in areas with dikes (either ED or aplite-pegmatite). Skeletal tourmaline in the granite is most abundant in areas with skeletal tourmaline in aplites. No evidence of cross-cutting relations between skeletal tourmaline in granite and dikes found during the field work. The uniformity of tourmaline compositions implies some uniformity to the crystallization suggesting the skeletal tourmaline in the granite and the aplite zone of the pegmatite crystallized at the same time.

Model for tourmaline crystallization

Skeletal tourmaline crystals occur in the aplite zone of pegmatite-aplite dikes (Figs 5a, 5b, 6c, 6d) and in the granite in areas surrounding dikes (Figs. 5b, 5c 6c, & 6d). These skeletal crystals grew in a oversaturated melt. The transition from skeletal tourmaline in the aplites to euhedral tourmaline in pegmatite cores (Figs. 5b, 6c & 6d) represents the transition to a less oversaturated melt.

Formation of ED is initiated as magma moves into a propagating fracture. Magma in the ED is a fractionated melt, left after crystallization of the Stone Mountain granite at some depth below the present level of exposure. This melt is enriched in incompatible components, such as B and H_2O, but depleted in other components, such as Ca and Fe. The ED magma cools along the sides of the fracture and begins to crystallize,

locally forming line rock. Inward crystallization of coarse-grained feldspar occurs in some ED at Stone Mountain while other ED are fine-grained. Incompatible components are concentrated near the end of the fracture causing local enrichment in B in the immediately enclosing granite. Skeletal tourmaline crystallizes in this undercooled environment. Removal of B (and water) from the ED magma raises the solidus temperature (the so called "boron quench" discussed by London, 1986a, 1986b, 2008), promoting crystallization of the magma remaining in the dike.

Crystallization of skeletal tourmaline in the edges of the aplite-pegmatite dike depletes the magma in B (also Fe & Mg). Depletion in B also reduces the solubility of water and the remaining magma is "quenched" to form the aplite enclosing the skeletal tourmaline. Expulsion of H_2O-rich fluid during aplite crystallization produces a water-rich vapor phase that concentrates toward the center of the crystallizing dike. Crystallization of silicate melts in the presence of hydrous vapor phase produces fewer nuclei and slower growth rates than in vapor-absent systems (Fenn, 1977; Swanson, 1977). The resultant rise of the solidus temperature reduces the tourmaline undercooling promoting the nucleation and growth of euhedral tourmaline in the core of the pegmatite. Ultimately crystallization of the remaining melt in the presence of a H_2O-rich fluid produces the larger, euhedral crystals (few nuclei, slower growth rate) of the pegmatite zone. B-enriched fluid from a pegmatite magma depleted in Fe & Mg may permeate the granite surrounding the aplite-pegmatite and crystallize tourmaline in undercooled conditions (and low # of nuclei, high growth rate). This model explains the association of skeletal tourmaline in the granite with areas that contain dikes. It also accounts for the

concentration of skeletal tourmaline immediately adjacent to the ends of pegmatites (Fig. 5a), an area of concentrated fluid flow.

CONCLUSIONS

This paper presents a model for the crystallization of late-stage melts in the Stone Mountain granite using tourmaline as a guide to crystallization conditions. The proposed development of skeletal tourmaline in dikes is easily imagined as long as a melt phase is involved. The formation of skeletal tourmaline in the granite is more problematic. All of the late-stage melts occur in fractures with a more-or-less coherent orientation. This implies that the granite was cool enough to fracture. Yet the skeletal tourmaline crystals hosted by the granite appear to require crystallization from a melt. How can a granite that is hot enough to grow skeletal tourmaline fracture? Perhaps the hot granite is fluxed by the presence of a B-enriched fluid and locally melts? Perhaps the skeletal crystals hosted by the granite represent replacement in response to some magmatic-hydrothermal fluid?

Testing of the proposed model, with a special emphasis on the origin of the granite-hosted skeletal crystals, is currently underway. More field work is being done in an effort to constrain the timing of dikes vs. granite-hosted skeletal tourmaline crystallization. Stable isotope analysis of tourmaline and associated phases is planned to look for a difference in fluids that accompanied skeletal tourmaline crystallization in different settings.

ACKNOWLEDGMENTS

The Stone Mountain Memorial Association provided access to Stone Mountain and allowed collection of samples. Chris Fleisher assisted with the electron microprobe analyses. We thank Alberto Patino Douce and Doug Crowe for their reviews. This paper is part of Longfellow's Masters thesis at the University of Georgia.

REFERENCES

Armstrong, J.T. (1988): Quantitative analysis of silicate and oxide materials: comparison of Monte Carlo, ZAF, and phi-rho-z procedures. Microbeam Analysis, 239-246.

Buddington, A. F. (1959): Granite emplacement with special reference to North America. *Geol. Soc. Am. Bull*. **70**, 671-747.

Clark, C. M. (2007): Tourmaline: structural formula calculations. *Can. Mineral*. **45**, 229-237.

Demirel, S., Göncüoluc◌̧lu, M. C., Topuz, G., & Isik, V. (2009): Geology and chemical variations in tourmaline from the quartz-tourmaline breccias within the Kerkenez granite-monzonite massif, central Anatolian crystalline complex, Turkey. *Can. Mineral*. **47,** 787-799.

Donaldson, C.H. (1976) An experimental investigation of olivine morphology. *Contrib. Mineral. Pet.* **57**, 187-213.

Fenn, P. M. (1977): The nucleation and growth of alkali feldspar from hydrous melts. *Can. Mineral.* **62**, 135-1671.

Grant, W. H., Size, W. B. & O'Connor, B. J. (1980): Petrology and structure of the Stone Mountain Granite and Mount Arabia Migmatite, Lithonia, Georgia. *Geol. Soc. Am. 1980 Atlanta Field Trip* no. 3, **17**, 41-57.

Grant, W. H. (1986): Structural and petrologic features of the Stone Mountain granite pluton, Georgia. *Geol. Soc. Am. Centennial Field Guide - Southeastern Section* 285-290.

Hatcher, R. D., Jr., Thomas, W A., Geiser, P. A., Snoke, A. W., Mosher, S. & Wiltschko, D. V. (1989): Alleghanian orogen. *In* The Appalachian-Ouachita Orogen in the United States (R. D. Hatcher, Jr., W. A. Thomas & G. W Viele, eds.). *The geology of North America*, **F-2**, 233-318.

Jolliff, B. L., Papike, J. J. & hearer, C. K. (1986): Tourmaline as a recorder of pegmatite evolution: Bob Ingersoll pegmatite, Black Hills, South Dakota. *Am. Mineral.* **71**, 472-500.

Lofgren, G. E. (1974): An experimental study of plagioclase crystal morphology. *Am. J. Sci.* **274,** 243-273.

London, D. (1986a): The magmatic-hydrothermal transition in the Tanco rare-element pegmatite: evidence from fluid inclusions and phase equilibrium experiments. *Am. Mineral*. **71,** 376-395.

London,D. (1986b): Formation of tourmaline-rich gem pockets in miarolitic pegmatites. *Am. Mineral*. **71,** 396-405.

London, D. (2008): *Pegmatites*. The Canadian Mineralogist Special Publication **10**.

London, D. & Manning, D. A. C. (1995): Chemical variation and significance of tourmaline from southwest England. *Econ. Geol*. **90,** 495-519.

Manning, D. A. C. (1982): Chemical and morphological variation in tourmaline from the Hub Kapong batholith of peninsular Thailand. *Mineral. Mag*. **45**, 139-147.

Perugini, D. & Poli, G. (2007): Tourmaline nodules from Capo Bianco aplite (Elba Island, Italy): an example of diffusion limited aggregation growth in a magmatic system. *Contrib. Mineral. Pet.* **153**, 493-508.

Samson, I. M. & Sinclair, W. D. (1992): magmatic hydrothermal fluids and the origin of quartz-tourmaline orbicules in the Seagull Batholith, Yukon Territory. *Can. Mineral*. **30**, 937-954.

Sinclair, W. D. & Richardson, J. M. (1992): Quartz-tourmaline orbicules in the Seagull batholith, Yukon Territory. *Can. Mineral*. **30**, 923-935.

Size, W. B. & Khairallah, N. (1989): Geology of the Stone Mountain granite and Mount Arabia migmatite, Georgia. *In* Excursions in Georgia Geology (W. J. Fritz, ed.). Georgia geological Society Guidebooks, **9**, 149-177.

Slack, J. F. & Coad, P. R. (1989): Multiple hydrothermal and metamorphic events in the Kidd Creek volcanogenic massive sulfide deposit, Timmins, Ontario: evidence from tourmalines and chlorites. *Can. J. Earth Sci*. **26**, 694-715.

Speer, J. A., McSween H. Y., Jr., & Gates, A. E. (1994): Generation, segregation, ascent and emplacement of Alleghanian plutons in the southern Appalachians. *J. Geol*. **102**, 249-267.

Swanson, S.E. (1977): Relation of nucleation and crystal growth rate to the development of granitic textures. *Am. Mineral.* **62**, 966-978.

Swanson, S. E. & Fenn, P. M. (1986): Quartz crystallization in igneous rocks. *Am. Mineral.* **71**, 331-342.

Swanson, S. E. & Fenn, P. M. (1992): The effect of F and Cl on the kinetics of albite crystallization: a model for granitic pegmatites ? *Can. Mineral*. **30**, 549-559.

Swanson, S. E., Mirante, D. C., Schrader, C. M., Tracy, B. J., Wolak, C. E. & Roden, M. F. (2001): Undercoling in granitoid systems: an example from Stone Mtn., GA. *Geol Soc. Am. Abs. Prog.* **33**, A-29.

Watson, T. L. (1902): On the occurrence of aplite, pegmatite, and tourmaline bunches in the Stone Mountain granite of Georgia. *J. Geol*. **10**, 186-193.

Whitney, J. A., Jones, L. M., & Walker, R.L. (1976): Age and origin of the Stone Mountain granite, Lithonia district, Georgia. *Geol. Soc. Am. Bull*. **87**, 1067-1077.

Figure Captions

Fig.1. Quartz crystals grown from various silicate melts at various pressures and temperatures. Quenched melt is represented by the red color under first order red accessory plate. (a) euhedral crystals and (b) skeletal crystals at the same undercooling in different experiments. (c) Quartz dendrites, (d) dendritic quartz (note margins of experimental charge).

Fig. 2. (a) Stone Mountain pluton. Location of Stone Mountain is shown by the dashed line. (b) Stone Mountain (outline in (a)) showing locations mentioned in text.

Fig. 3. (a) Coarse-grained early dike (ED) with inward-directed K-feldspar crystals in granite (GR). (b) Fine-grained early dike (ED) in granite (GR).

Fig. 4. Field relations of dikes in Stone Mountain pluton. (a) Early dike (ED) cut by tourmaline-bearing pegmatite-aplite (TP). (b) Early dike (ED) cut by tourmaline vein (V).

Fig. 5. Tourmaline-bearing dikes in the Stone Mountain pluton. Locations are given in Fig. 2. (a) Skeletal tourmaline crystals near end of aplite (A) dike in east quarry. (b) Composite pegmatite-aplite dike in granite with skeletal and euhedral tourmaline, east quarry. (c) Aplite dike with skeletal tourmaline in the center of the dike, summit area. (d) Tourmaline veins in granite, near the west trail.

Fig. 6. Textures of tourmaline in the Stone Mountain pluton.(a) Skeletal tourmaline crystals (S) near end of early dike (ED) in east quarry. (b) Cluster of skeletal tourmaline in granite on the summit. (c) Euhedral tourmaline (E) in pegmatite core and skeletal tourmaline (S) in aplite and granite, east quarry. (d) Map of aplite-pegmatite zones in (c).

Fig. 7. Images of Stone Mountain tourmaline. (a) BSI image of tourmaline (T) in matrix of K-feldspar (Or) and quartz (Qtz) in tourmaline vein. (b) BSI image of zoning in euhedral toruramline (Tur) from pegmatite. (c) Plane light photomicrogaph of zoning in euhedral tourmaline in pegmatite. (d) Photomicrograph of zoning in skeletal tourmaline from granite.

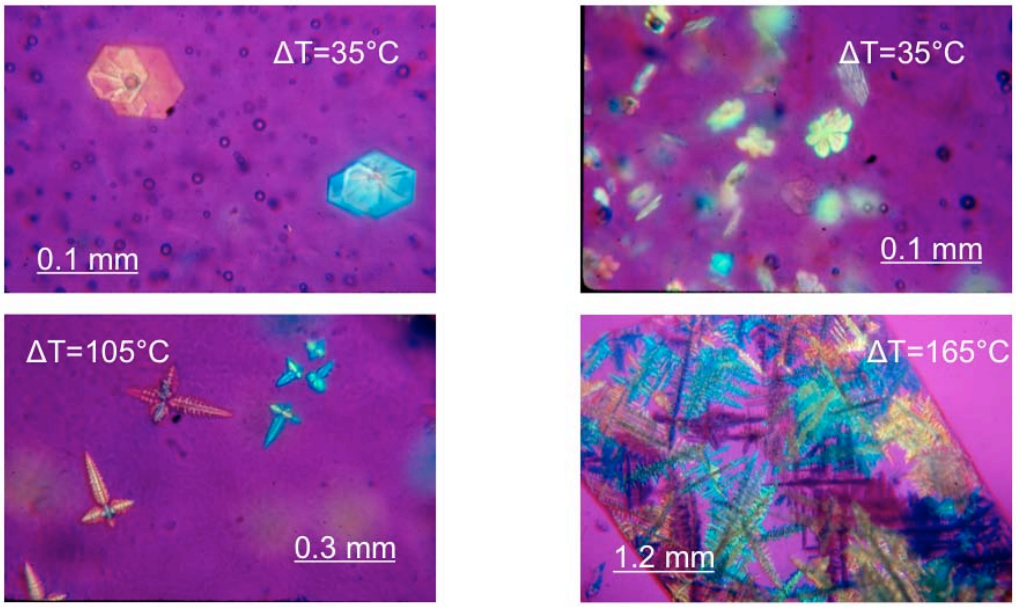

Figure 4.1 Silicate Crystals at Various Temperatures.

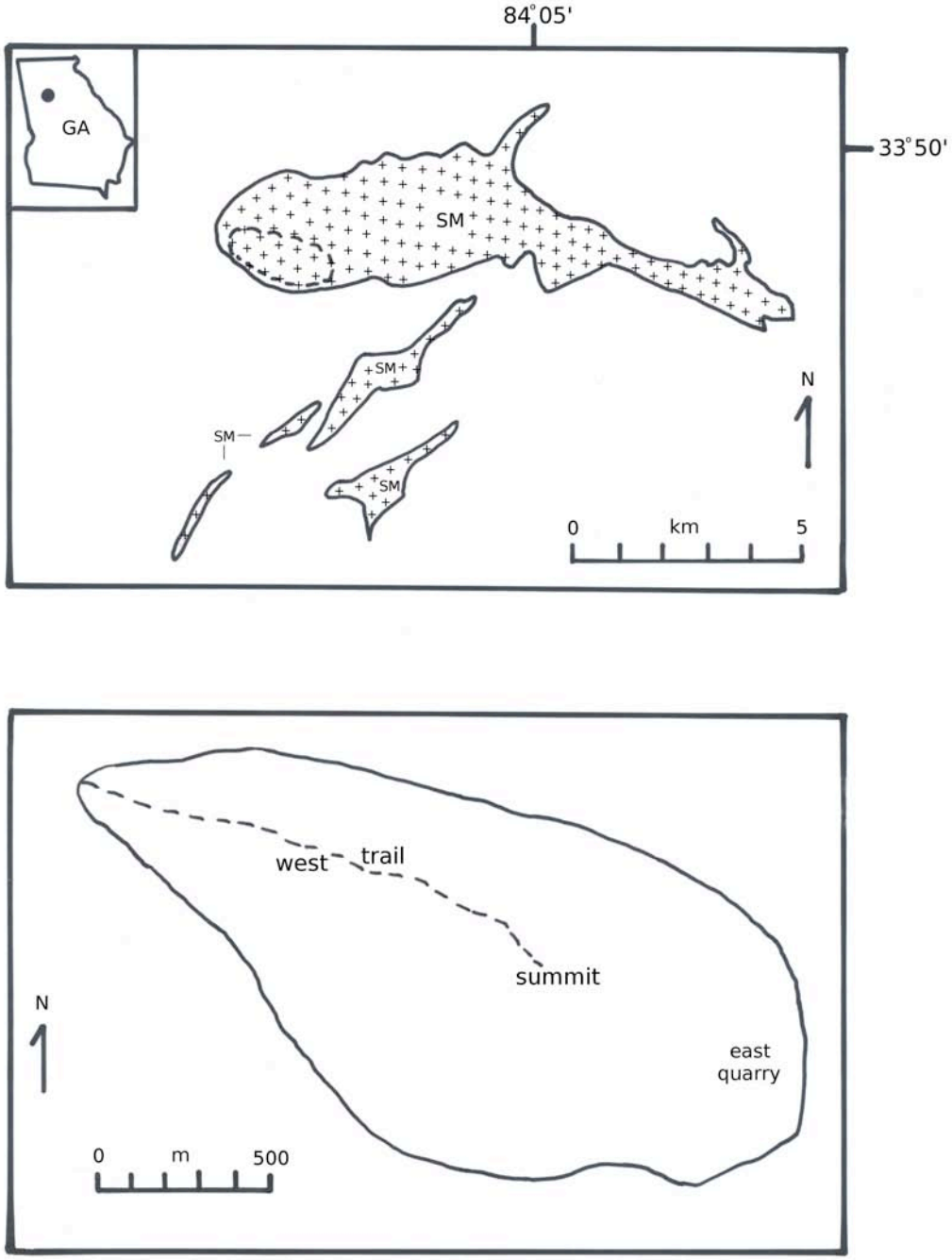

Figure 4.2 Stone Mountain Pluton.

A

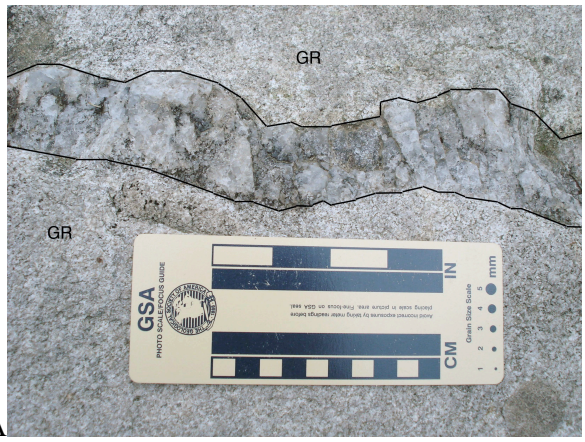

B

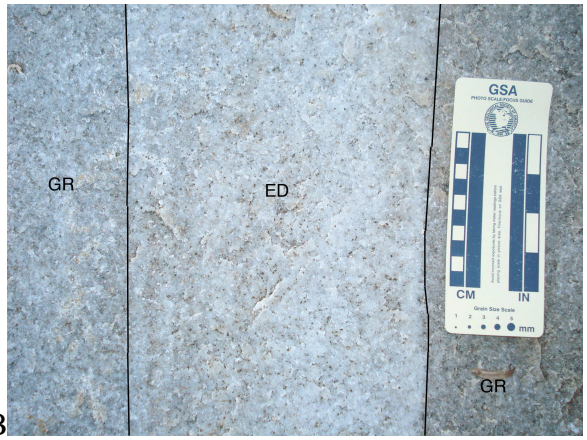

Figure 4.3 Coarse-grained and find-grained ED.

A

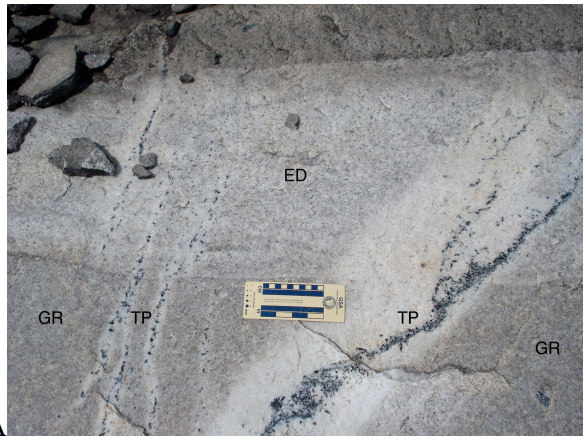

B

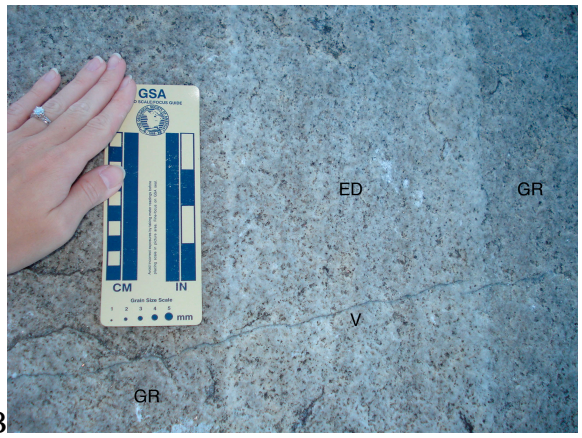

Figure 4.4 Field Relations of Dikes in Stone Mountain Pluton

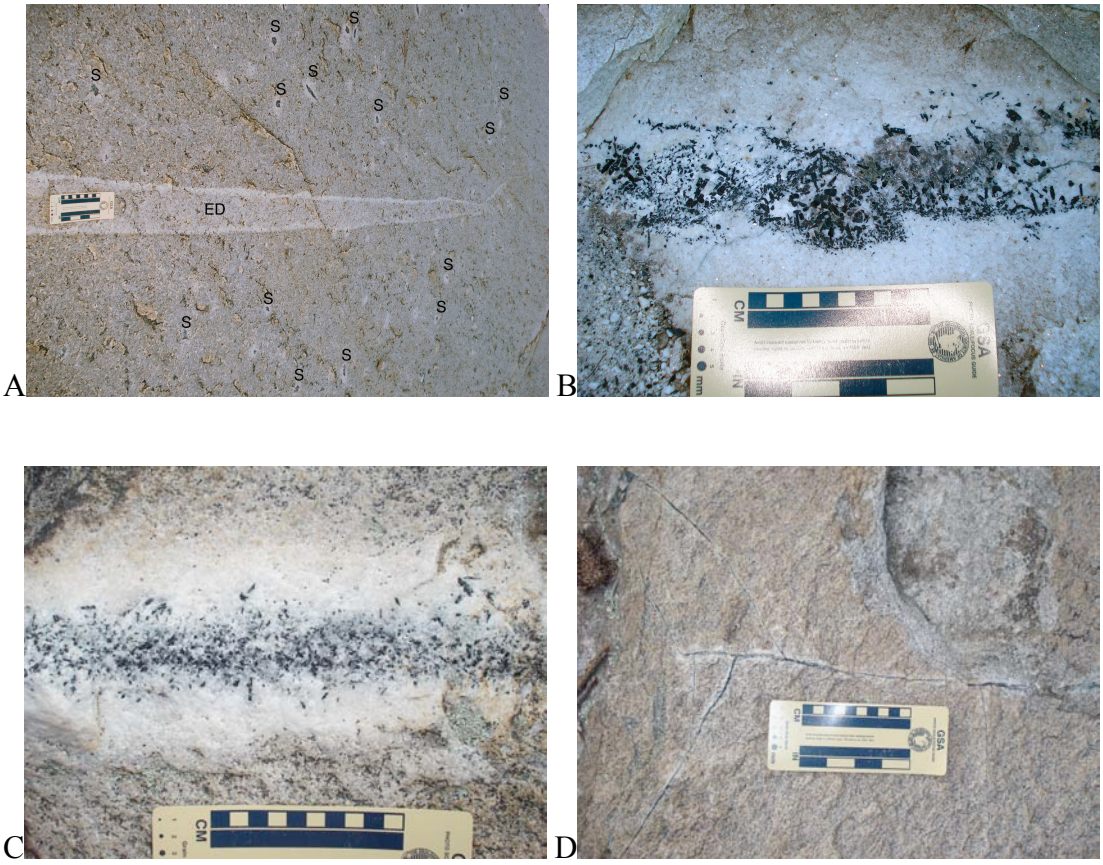

Figure 4.5 Tourmaline-bearing Dikes in the Stone Mountain Pluton

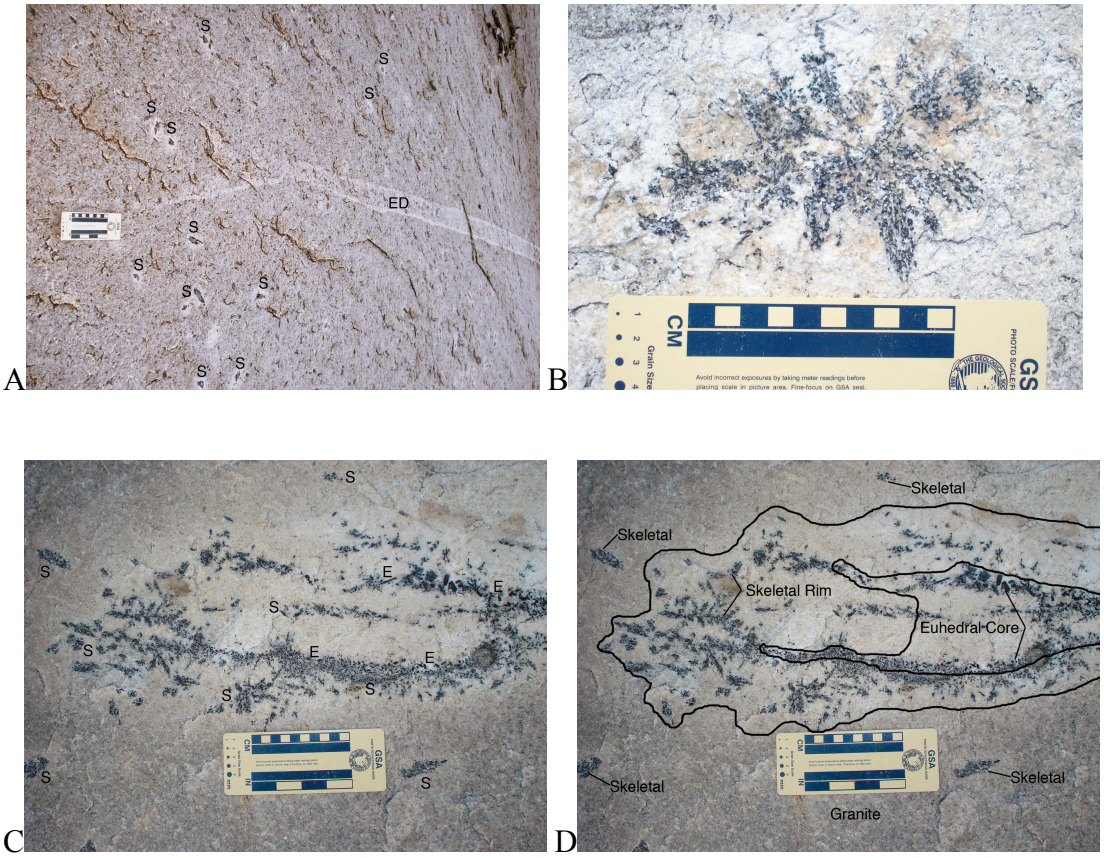

Figure 4.6 Textures of Tourmaline in the Stone Mountain Pluton

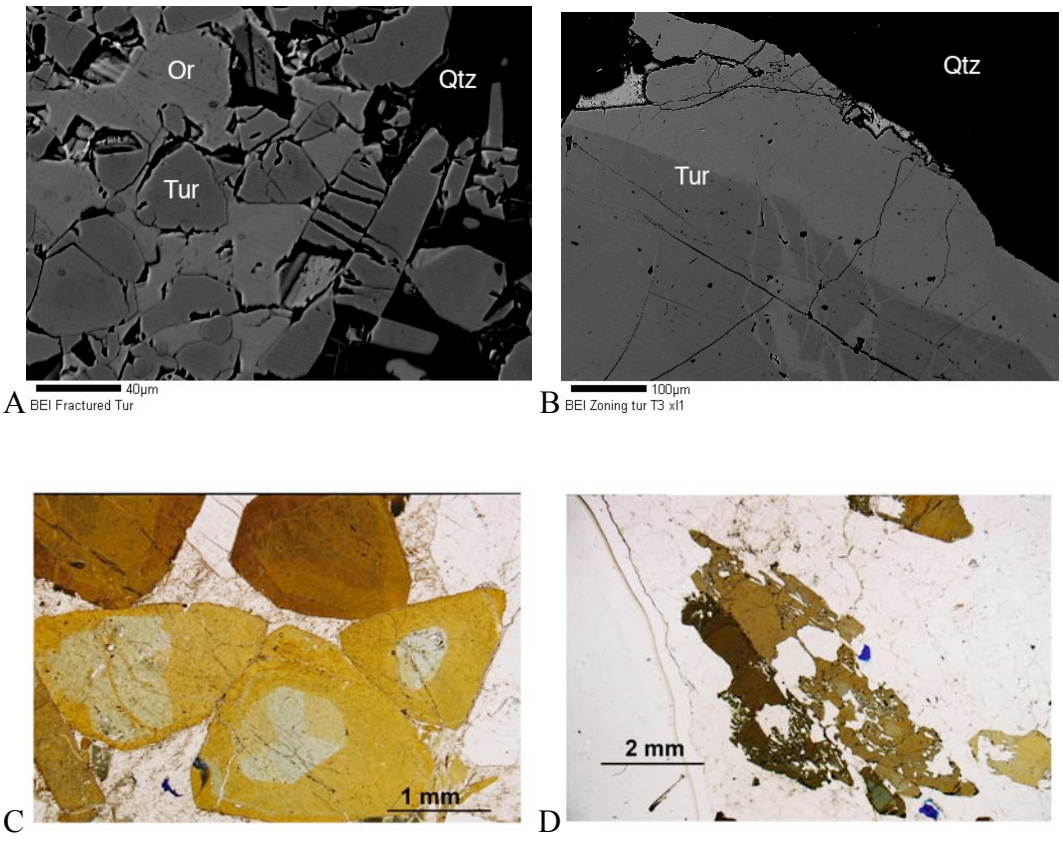

Figure 4.7 Images of Stone Mountain Tourmaline

TABLE 4.1 MINERALOGY OF DIKES

type	grain size (mm)	abundance	mineralogy	tourmaline texture
Early dikes	<1	Abundant	Qtz, Kfs, Pl, Ms, Bt, Srl, Grt	Rare euhedral, 5 mm
Pegmatite-aplite dikes	<1 to >30	Very abundant	Qtz, Kfs, Pl, Ms, Bt, Srl, Grt, Zo, Ap, Brl	Common skeletal 0.5 – 15 cm
Tourmaline veins	<1	Rare	Qtz, Kfs, Srl	Euhedral, 0.05 mm

Ap = apatite, Brl = Berly, Bt = biotite, Grt = garnet, Kfs = Potassium fedspar, Ms = muscovite, Pl = plagioclase, Qtz = quartz, Srl = schorl, Zo = zoisite

TABLE 4.2 REPRESENTATIVE MICROPROBE ANALYSES OF TOURMALINE

	Pegmatite				Vein		Granite	
grain	1c	1r	2c	2r	3c	4c	5c	5r
texture	Eu	Eu	Sk	Sk	Eu	Eu	Sk	Sk
color	blu	brn	blu	brn	nd	nd	brn	blu
SiO_2	36.63	33.73	35.79	34.61	35.45	35.17	35.53	36.25
TiO_2	0.15	1.35	0.35	1.15	1.05	1.20	1.16	0.29
Al_2O_3	32.94	31.63	33.66	32.02	31.33	31.31	32.74	33.97
FeO	11.72	13.14	11.81	11.73	11.90	11.57	12.07	10.53
MnO	bdl	0.26	0.24	0.23	bdl	0.26	bdl	0.20
MgO	3.58	3.32	2.88	3.57	3.81	3.40	3.76	3.59
CaO	0.38	0.57	0.23	0.51	0.52	0.54	0.45	0.35
Na_2O	1.73	2.01	1.78	2.01	2.04	2.05	1.71	1.80
K_2O	bdl	0.06	bdl	0.07	0.06	0.08	0.04	0.05
total	87.17	86.07	86.75	85.90	86.32	85.58	87.60	87.03

C = core, r = rim, Eu = euhedral, Sk = skeletal, blu = blue, brn = brown, bdl = below detection limit, MDL = silicon, 0.051; titanium, 0.068; aluminum, 0.042; iron, 0.129; manganese, 0.171; magnesium, 0.032; calcium, 0.035; sodium, 0.061; potassium, 0.030; fluorine, 0.124; and chlorine, 0.024

CHAPTER 5

DIKES AND A MODEL FOR EMPLACEMT

Field Studies

Several dike varieties can be distinguished based on mineralogy in the Stone Mountain pluton (Table 2.3). Early dikes (ED) contain only rare crystals of tourmaline and are associated with a tourmaline-bearing zone in the host granite only near the tip of the dike. Composite pegmatite-aplite dikes contain tourmaline throughout the dikes and in a zone in the enclosing granite. Tourmaline veins contain tourmaline in the center of the vein.

Early Dikes (ED)

Early dikes (ED) are very fine grained (<1mm) and are reasonably abundant throughout the Stone Mountain granite. They range from 1 to over 90 cm wide and from 10's to 100's of meters long (Figures 5.1, 5.2). ED are composed of quartz, plagioclase, potassium feldspar, muscovite, and minor biotite with accessory schorl and garnet. ED are cross-cut by all other tourmaline veins and composite pegmatite-aplite dikes, hence the name, "early dike". Euhedral tourmaline occur rarely within ED. A few ED are very coarse-grained and contain inward-projecting K-feldspar (Figure 5.3), and occasionally inward-projecting muscovite and biotite. The coarse-grained ED have irregular contacts with the granite and are short, ranging from 6 - 8 meters long and 5 to 9 cm wide.

Orientations of 22 ED found in the east quarry, west trail, and summit of the mountain were measured. Overall, strike for all fine-grained ED ranges from 2.5 - 65° NE. In the east quarry strike ranges from 49 - 63° NE, west trail 10 - 42° NE, and on the summit 2.5 - 20° NE. When occurring side by side, ED look nearly parallel. The east quarry has a set of three very distinct ED that run up slope and appear parallel. Locally strikes differ only 13°. Along the west trail ED appear perpendicular to the walking path and occur very frequently. Many ED stand above the enclosing granite due to differential weathering on the west trail. A similar set of three nearly parallel ED occur along the west trail at about 364m (1194 ft) elevation (Figure 5.2). Strike varies only 8° between the three ED. The three ED are 28 to >55 meters long and are cross-cut by a thin quartz-tourmaline vein (Figure 5.4). ED on the summit are thinner and shorter (Figure 5.5), but exact lengths could not be measured due to dangerous slopes.

Composite Pegmatite-Aplite Dikes

Tourmaline-bearing pegmatite-aplite dikes (PAD) are abundant in some areas on Stone Mountain. Grain-size ranges from 1 - 30 mm and euhedral and skeletal tourmaline are usually both present. PAD range from 2 - 14.2 meters in length, and 12-550 cm in width. A white halo in the enclosing granite forms an envelope around the PAD. The halo is composed of quartz, feldspar, and minor muscovite. These halos range from 2 - 11cm in width. These leucocratic halo zones lack biotite, and contain much less muscovite than the typical granite.

Modal analyses of quartz, feldspars, micas in PAD and within the granite-hosted skeletal tourmaline and the associated halo were done on thin sections. Approximately

150 points were counted per area. Results of these analyses are compared to previously determined modes on the Stone Mountain granite taken from the literature (Whitney et al., 1976, Wright, 1966, Hermann, 1954) on Table 5.1. The Stone Mountain granite shows quartz, plagioclase, potassium feldspar, muscovite, and biotite present in nearly equal amounts (Table 5.1). The halo enclosing the skeletal tourmaline crystal in the granite contains more muscovite than the core of the skeletal crystal and nearly the same amount as in granite. Skeletal tourmaline crystals in granite contain more plagioclase that PAD but less than granite. Interstitial grains within PAD show more potassium feldspar and less plagioclase than skeletal tourmaline (core and halo) in granite, and also less than granite. More quartz is present in skeletal tourmaline and PAD than in granite.

Skeletal tourmaline is associated with all PAD, either within the halo zone and/or internally with the PAD. PAD are zoned from an outer fine-grained aplitic zone composed of quartz, feldspar, and skeletal tourmaline, to a coarse-grained pegmatitic core containing euhedral tourmaline (schorl) and quartz. Some accessory minerals in the pegmatitic zones include garnet, apatite, thulite, beryl, zircon, and a rhombohedral carbonate mineral. Some PAD lack a pegmatitic zone and consist entirely of aplitic granite with skeletal tourmaline (Figure 5.6). Skeletal tourmaline occurs in the enclosing granite halo, followed by euhedral tourmaline in the core (Figure 5.7). Coarse and fine-grained PAD cross-cut fine-grained ED (Figure 5.8). Coarse-grained pegmatite-aplites stand out as the most abundant dike in the Stone Mountain granite.

One large (2.25 m wide and 5.9 m long) PAD in the east quarry exhibits all texture zones found in Stone Mountain PAD (Figure 5.9). It has a pronounced pegmatitic core composed of a zone of monomineralic white-gray quartz and an adjacent zone of

euhedral tourmaline in quartz. The tourmaline grades outward from the core to skeletal crystals in the aplitic zone along the ends and margins of the dike. Skeletal tourmaline is also found in the leucocratic halo in the granite adjacent to the dike. All units in the PAD are cut by very thin quartz-tourmaline veins.

Strike was measured for 14 individual PAD. The trend of the PAD is more variable than that of the ED with a range of strikes of 53° NW – 10 NE°. The strike of PA dikes in the east quarry is between 5 - 53° NW, on the west trail, PA dikes strike from 4° NW to 9.5° NE, and on the summit from 2.5° to 10° NE.

Tourmaline Veins

Rare tourmaline veins are thin and extremely fine-grained. The tourmaline is euhedral with itherstitial K-feldspar and an envelope of quartz (Figure 5.10). A white, iron-depleted halo encloses the vein. Only three were documented in this study. Veins are 1 – 2 cm wide and vary in length. Veins cut all other dikes in the Stone Mountain granite. Veins appear in the east quarry and west trail. In the east quarry, veins cross cut ED, PAD, and skeletal tourmaline. Veins along the west trail cut ED. Strike of the veins range from 8 - 11° NE.

Grain Sizes

Grain size of the Stone Mountain granite and ED is very similar to the point where it is impossible to distinguish dike from granite in a thin section of the contact. Grain size within the inner coarse-grained core of PAD can vary from .8 – 4.4mm, however most grains exceed 2.5mm in length. The aplitic skeletal tourmaline zone of

PAD range in grain size from 0.7 – 4mm, with the majority of grains less than 1mm; very similar to the Stone Mountain granite. PAD halo and granite show no apparent difference in grain size. Tourmaline-bearing veins and granite show a drastic grain size difference. Vein grain size is on average 40μm, the enclosing granite averages about 2mm.

Skeletal Tourmaline

Skeletal tourmaline crystals occur not only in aplites and PAD, but also in the granite. Skeletal tourmaline occurs as a "bloom" at terminating ends of ED in the east quarry (Figure 5.11). Clusters (2.4 by 3.4 meters) of skeletal tourmaline make up the terminating tips of ED. Skeletal tourmaline is not found in the granite adjacent to the margins of ED, only at terminating ends.

Skeletal tourmaline is typically associated with aplites and PAD, and all PAD contain or are proximal to skeletal tourmaline. Overall, in the east quarry skeletal tourmaline crystals are elliptical and tend to become more elongate and narrow (Figure 5.12) toward the west and summit of the mountain. The largest skeletal crystal found was 15 cm long and 1.5 cm wide (Figure 5.13). Sometimes crystals appear to overlap one another and share a halo in a "starburst" shape (Figure 5.6). Granite, such as the southeast side of the East Quarry, is devoid of PAD and ED is also devoid of skeletal tourmaline (Figure 5.14). All occurrences of skeletal tourmaline crystals in granite are localized around ED or PAD.

Skeletal tourmaline occurs in halo zones of PAD, and within PAD in a gradation from a euhedral core to a more aplitic margin (Figure 5.15). Granitic hosted skeletal

tourmaline crystals appear coeval with PAD, and no cross-cutting relationships are evident. Only the late stage tourmaline veins cross-cut skeletal tourmaline.

Brittle Magmas and Dike Propagation

Silicate melts and glasses have similar molecular structures (Rubin, 1993), suggesting that melts can fracture. A study on the viscoelasticity and the glass transition in magma by Dingwell (1997), suggests that the width of the transition zone between fully glassy and fully liquid response of the melt is on the order of tens of degrees, several log units of viscosity, and several log units of strain rate. Between 600 and 675° C, the transition between solid-like and liquid-like behavior is in transition. Thus granitic magmas may behave as a brittle or ductile material.

Intrusions in the Iberian Massif show evidence of viscous flow and brittle failures of granitic magmas during intrusion of multiple magma batches (Fernandez and Castro, 1999). Rubin's 1993 model of pressurized dike intrusion explains the main structural features of the Iberian Massif (Fernandez and Castro,1999). New, low viscosity melt can intrude as a dike into a still viscous, magma host. The predicted aspect ratios (dike thickness at center divided by dike length) for the Iberian Massif are 10^{-1}, which correlates with horizontal aspect ratio measured in the field. The growth of the Iberian Massif batholith was marked by episodic magma intrusion into previously emplaced magma bodies. This intrusion occurred at depth of about 14km where stress levels were in the field of brittle behavior of magmas with large tensile strengths (Fernandez and Castro, 1999). The Stone Mountain pluton was also emplaced at 12 - 15km (Whitney *et al.* 1976), within the range of conditions needed for brittle failure of a magma.

Late Stage Crystallization History of Stone Mountain Dikes and Tourmaline

The ED have sharp contacts and a uniform strike over their outcrop length (10's to 100' of meters, (Figure 5.1). Early dikes rarely contain tourmaline. Later pegmatite-aplite dikes also show consistent strikes and sharp contacts, but the internal structure of pegmatitic and aplitic units is irregular and some of these internal units sometimes cross-cut the dike margins. The PAD contain tourmaline. Saturation of the granitic magma with tourmaline-forming components occurred between the time of ED emplacement and crystallization of the PAD.

The ED in Stone Mountain granite have long, straight contacts. This is an indication of dike emplacement into a brittle Stone Mountain magma or granite. The earliest dikes in the Stone Mountain granite are slightly more evolved when compared to the granite itself, evidenced by small amounts of garnet and tourmaline along dike margins. Skeletal tourmaline enclosed by a leucocratic halo, adjoin tips of ED (Figure 5.11). This indicates ED intrusion into a magma where boron and other incompatible components migrated ahead of the propagating dike into the surrounding magma (Rubin, 1993), and crystallize skeletal tourmaline crystals around the tip of the ED.

Boron is present in the ED system mainly as skeletal crystals at the ends of ED. The addition of boron to a granitic system not only lowers the crystallization temperature of the melt, but also lowers viscosity (Dingwell, 1997). Dike propagation stops when dike magma overpressure is reduced (Rubin, 1993). When dike cracking stops at the very end of the crack there may be a gap between the dike tip and magma front (Barenblatt, 1962). This tip cavity is filled, at low pressure, with volatiles exsolving from the magma (Lister,

1990) and may account for pegmatitic zones at the tip of some granitic dikes (Rubin 1993). At Stone Mountain, this pressure gradient was higher at the tips of ED and volatiles (including B) that form the skeletal tourmaline crystals accumulated ahead of the advancing dike in the host granite.

The formation of skeletal tourmaline at the very end of ED in Stone Mountain granite results when B is combined with other components, including Fe, in residual melt. The scavenging of Fe from the melt to produce skeletal tourmaline is responsible for Fe-depleted halos and shows that the ED were emplaced in magma (as opposed to solid granite). This skeletal texture of the tourmaline indicates crystallization in an undercooled environment.

Pegmatite-aplite dikes intruded after the ED. They represent a more evolved melt propagating through cracks in the still partially molten host rock. Saturation of PAD magma with B is indicated by the early crystallization of tourmaline. Initially the tourmaline crystallized in an undercooled setting producing skeletal crystals in the margins of the PAD. Diffusion of some of the B into host granitic magma produced skeletal tourmaline with Fe-depleted halos. The crystallization of skeletal tourmaline depleted the magma of B and other incompatibles, raised the solidus temperature, reduced the solubility of water, and the depleted magma was “quenched” and formed the enclosing aplite halo (London, 2008). With the resulting rise of solidus temperature, undercooling is suppresses and the PAD core nucleates and grows large euhedral crystals at low undercooling.

PAD contain accessory green beryl, calcite, pink thulite, epidote, and titanium oxides not found in the granite. PAD are marked by a predominately northwesterly

pegmatite-aplite trend (Figure 5.16) and cut the northeasterly trend of ED. The PAD melt is more enriched in incompatible elements (e.g. boron) than the magma that crystallized ED. The occurrence of calcite (Figure 5.17) as a late-stage, apparently magmatic phase, is consistent with experimental studies showing calcite is stable above 0.3 GPa in granitic magmas with small amounts of carbon dioxide (Swanson, 1979).

Model/Cartoon

During late stage crystallization of the Stone Mountain granite, residual magmas were irregularly distributed within the Stone Mountain pluton. Some areas accumulated more residual melt, began to fracture, resulting in the propagation of the ED. These areas of residual melt began to fractionate over time to produce more evolved melts, resulting in the tourmaline-rich PAD. Large areas of Stone Mountain granite lack late-stage dikes, reflecting crystallization of unfractionated magma (Figure 5.14).

The appearance of skeletal tourmaline in granite can be linked to Cartoons A and B. Cartoon A (Figure 5.18) illustrates the complex evolution of a PAD, and relates dike exposure to weathering of the Stone Mountain granite. Cartoon B (Figure 5.19) illustrates the evolution through time of an ED and it's associated skeletal tourmaline.

The appearance of tourmaline crystals in the Stone Mountain granite varies with exposure level as illustrated in Figure 5.20. PAD in the Stone Mountain granite all follow the same pattern of internal zonation. A pegmatitic core composed of euhedral tourmaline, enclosed by an outer aplitic zone of rare, small euhedral and abundant skeletal tourmaline, quartz, and feldspar. A halo zone of skeletal tourmaline crystals, enclosed in leucocratic quartz and feldspar surrounds PAD. Skeletal tourmaline in granite

appears to be unassociated with dikes on the surface. However, in three-dimensional space, these skeletal tourmaline crystals may be associated with a PAD not seen on the surface. At an erosional surface A (Figure 5.20), an exposure may show only skeletal tourmaline in granite, appearing disassociated with the dikes, when in fact is a part of a larger system. At an erosional surface B (Figure 5.21), skeletal tourmaline crystals in granite surrounded by an aplitic halo may be exposed with little to no euhedral crystals in the core. At a surface C (Figure 5.22), all zones of a PAD may be exposed; a euhedral tourmaline core, aplitic halo, skeletal tourmaline in halo and granite, all cut by a tourmaline vein.

It is unlikely that skeletal tourmaline crystals exist in open granite unassociated with any dike. Field studies indicate that every occurrence of PAD is linked to associated skeletal tourmaline crystals within halo and marginal granite. Areas of granite that lack PAD (or ED) also lack skeletal tourmaline.

Development of ED with associated skeletal tourmaline is illustrated in Figure 5.20. Starting at some time (y), magma propagates in two directions through a crack, pushing volatiles toward the ends of the dike (Rubin, 1993). The skeletal tourmaline "bloom" is shown at the dike ends represents final solidification (0) of the propagating dike.

Mineral Compositions

Tourmaline

The structural formula for tourmaline is very complex. In this study, boron, lithium, and hydrogen could not be analyzed with the microprobe. Although fluorine was analyzed, there was none above detectable limits. A normalization scheme was needed

because of an incomplete data set. Structural formulae were calculated using a spreadsheet made by Andy Tindle from his web address: http://www.open.ac.uk/earthresearch/tindle/AGTWebPages/AGTSoft.html Calculations were made for 31 anions, and assumed three atoms of B^{3+} *apfu*, and total Fe = Fe^{2+}.

Euhedral tourmaline crystals exhibit color zoning from brown rims to blue cores in plane-polarized light (Figure 5.17) with some sector zoning. Zoning patterns can also be complex in backscattered electron images (Figure 5.23) in euhedral tourmaline. Euhedral tourmaline from veins is homogeneous (Figure 5.24) and is enclosed in a mainly potassium feldspar matrix, with marginal quartz. Skeletal tourmaline crystals found in granite, viewed in thin section, consist of numerous optically continuous but disconnected skeletal limbs that are part of a single skeletal crystal. Occasionally euhedral terminations can be recognized on the tips of skeletal limbs. In plane-polarized light, the crystals appear light brown, with minimal light blue pleochroism. Skeletal tourmaline crystals in PAD dikes are coarser-grained (2 – 9mm) (Figure 5.24). They exhibit a euhedral outer shell with hollow interiors filled with quartz and feldspar. Slight brown to blue color zoning is visible in plane-polarized light. Just like the skeletal crystals in the granite, the tips of skeletal limbs are sometimes blue. The last zones of tourmaline to crystallize (limbs and interiors of skeletal crystals adjacent to an interior void) are low in Ti. This pattern mimics chemical zonation of euhedral crystals, where the core, being last to crystallize, is distinguished by a low Ti signature. (Figure 5.25).

Tourmaline mineralogy varies with it's x-site occupancy being Ca, or Na+K, and also with it's y-site occupancy being vacant, Li,Al, Fe_3, or Mg_3. All tourmaline from

PAD, vein, and skeletal crystals in granite plot into the schorl and alkali groups (Figure 5.26, 5.27). Tourmaline compositions show little to no variation between skeletal and euhedral within granite, pegmatites, and veins (Figure 5.28)(Table 5.2). The Stone Mountain tourmaline is a schorl variety with restricted range of FeO (10.5 – 13.4 wt. %) and low MgO (2.9 – 4.0 wt. %). Color zoning in euhedral and skeletal varieties is solely attributed to a shift in Ti. Low Ti (0.2 – 0.4 wt.% TiO_2) correlates with blue tourmaline in plane-polarized light, and higher Ti (1.0 – 1.4 wt. % TiO_2) with brown tourmaline (Figure 5.29). This pattern of optically complex zonation but a weak chemical variation is indicative of magmatic origin, a pattern recognized in other systems (Slack and Coad, 1989; Sinclair and Richardson, 1992).

Mica

Biotite and muscovite are common accessory phases in the Stone Mountain granite. Muscovite is also found within the white halos surrounding skeletal tourmaline crystals in the granite, tourmaline veins, and PAD. The aplitic portions of PAD also contain muscovite, but in lower amounts than the typical granite.

Mica compositions are uniform throughout the Stone Mountain granite and dikes. Biotite is Fe-rich (Fe/Fe+Mg = 0.72 to 0.79, (Tables 5.3 and 5.4) and does not contain any measurable F or Cl. The white mica is referred to as muscovite, but it contains a significant amount of Fe (3.0 to 3.9 wt. % total Fe as FeO) and MgO (1.0 to 1.9 wt. %) (Tables 5.3 and 5.4). A few grains of white mica included in plagioclase had even higher Fe and Mg contents (Figure 5.30). Elevated Fe and Mg is common in white mica found in granitic rocks (e.g. Zane and Rizzo, 1999).

Figure 5.1 Nearly parallel ED, East quarry, Stone Mountain, GA.

Figure 5.2 Nearly parallel ED, West trail, Stone Mountain, GA.

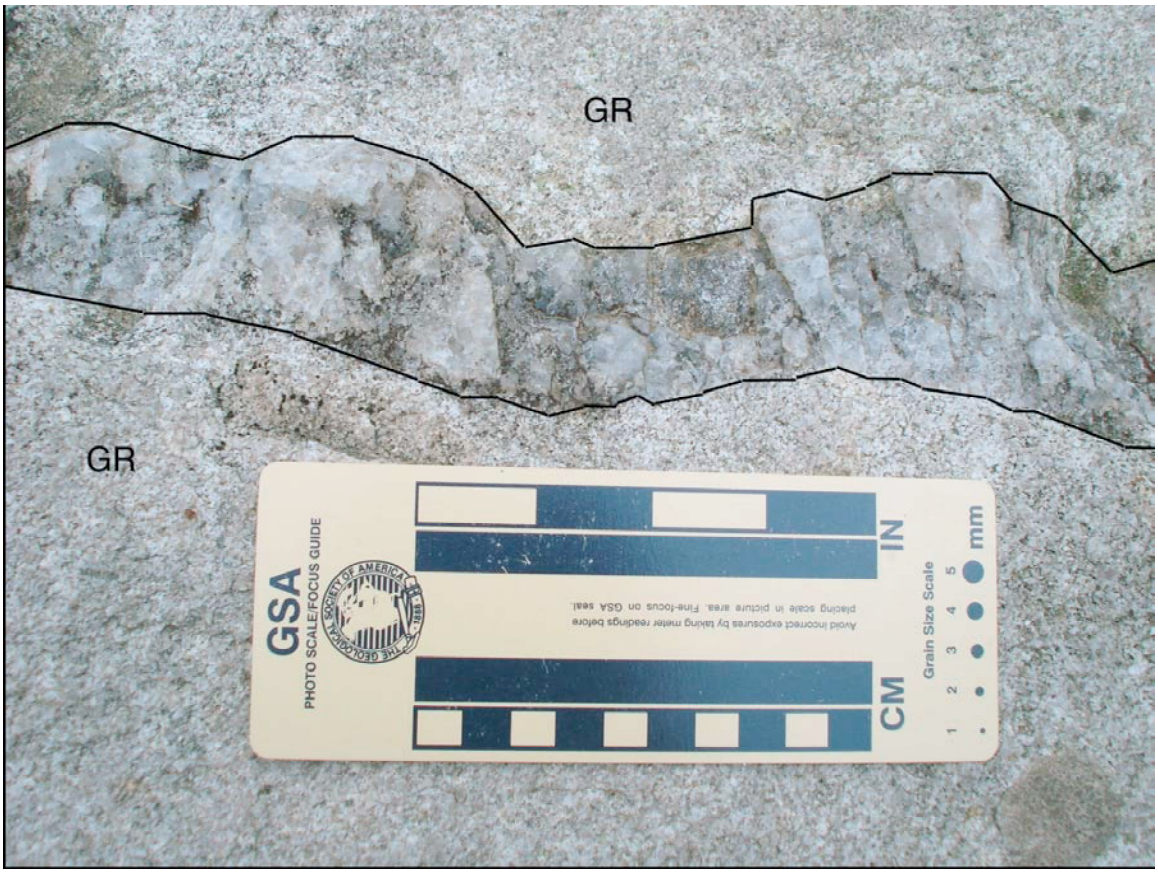

Figure 5.3 Coarse-grained ED, West trail, Stone Mountain, GA. ED with inward projecting K-spar ED in granite (GR).

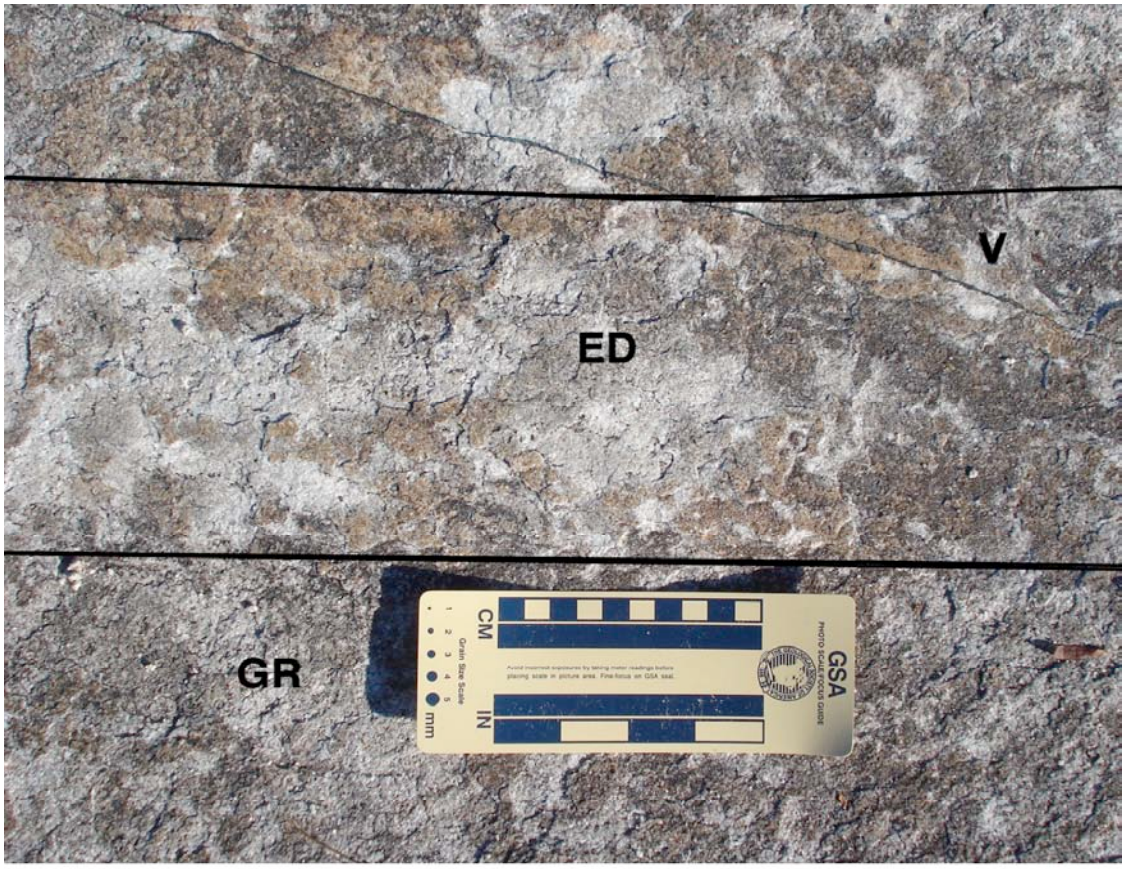

Figure 5.4 ED and granite (GR) are cross-cut by a quartz tourmaline vein (V), West trail, Stone Mountain, GA

Figure 5.5 ED, Summit, Stone Mountain, GA. A lone skeletal tourmaline crystal (T) in the bright white ED. ED on summit are highly weathered and have higher relief than the surrounding granite.

Figure 5.6 Skeletal tourmaline PAD, Summit, Stone Mountain, GA.

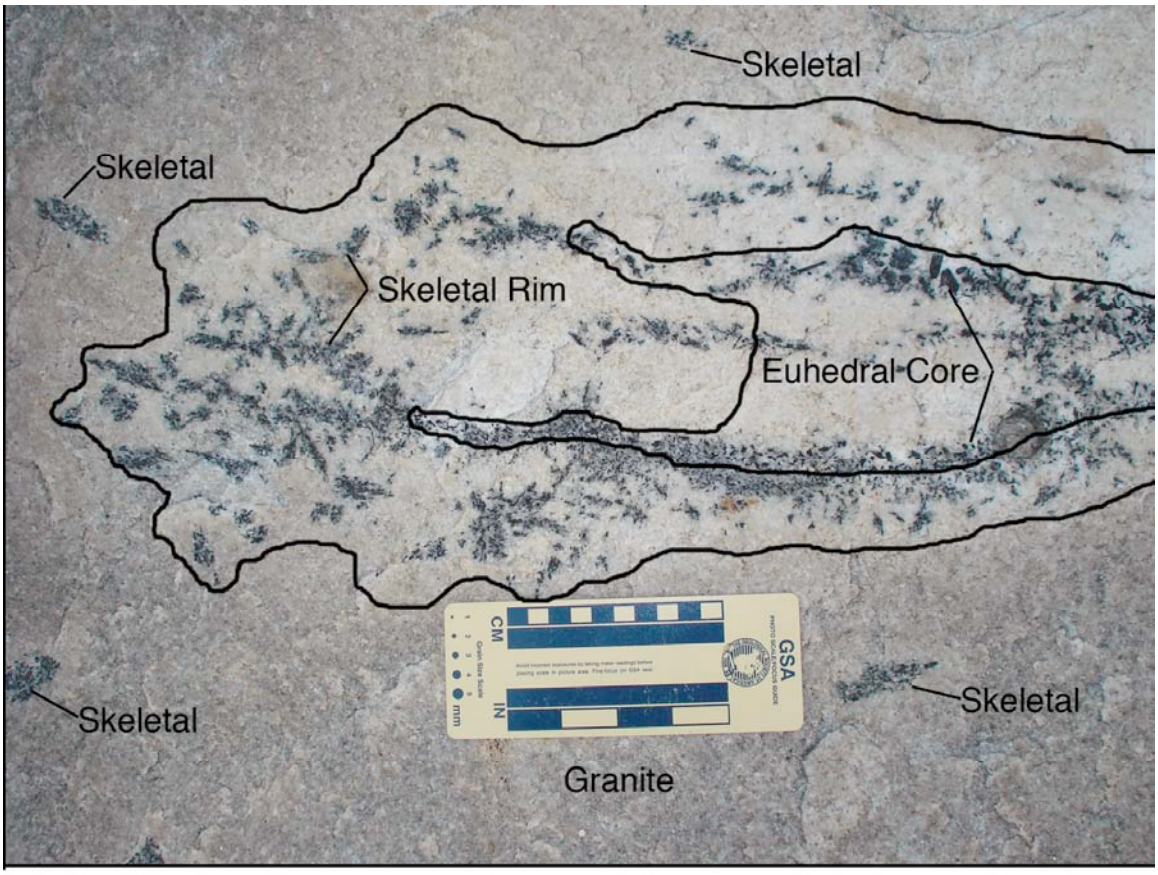

Figure 5.7 Mineralogical zoning of PAD in East quarry, Stone Mountain, GA. A euhedral tourmaline, quartz, and feldspar core is surrounded by an exclusively skeletal tourmaline rim, enclosed by a leucocratic quartz, feldspar, white mica halo. Skeletal tourmaline crystals with individual halos also occur in the enclosing granite.

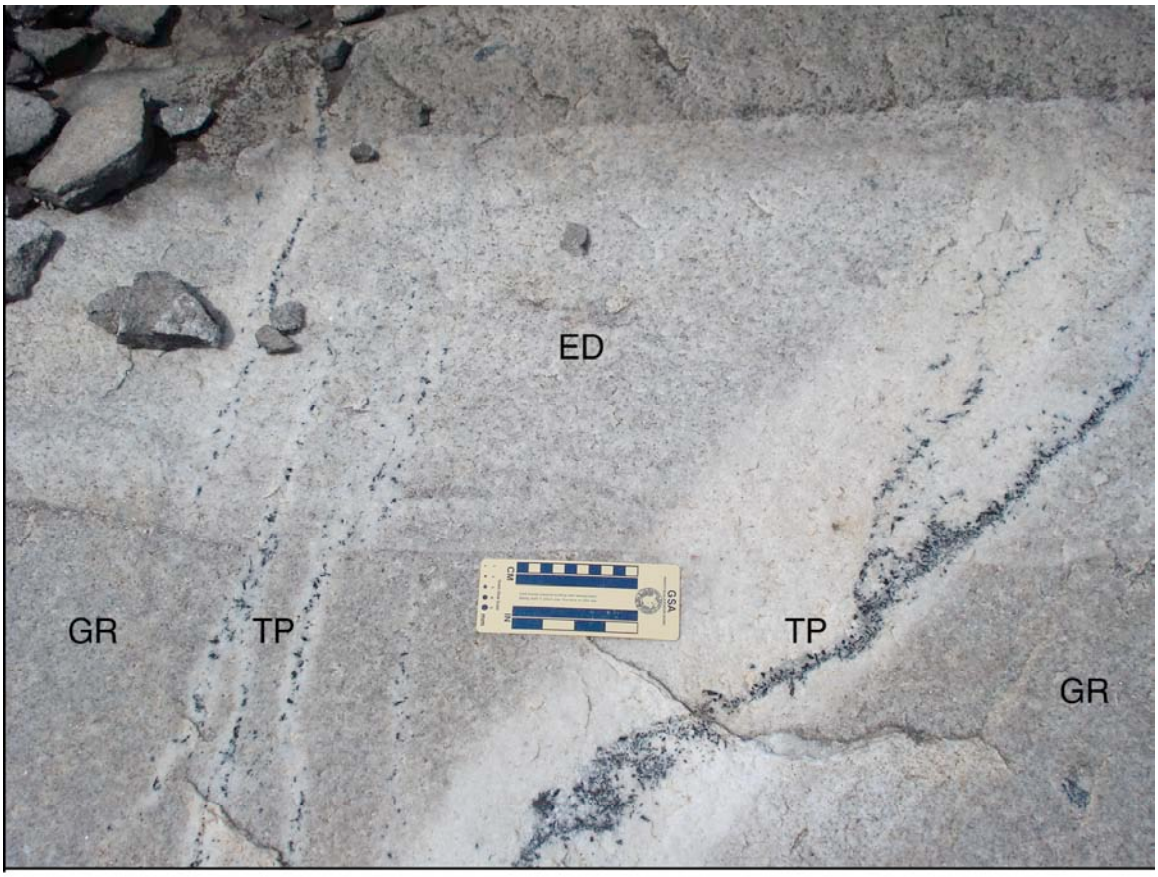

Figure 5.8 PAD cross cut ED, East quarry, Stone Mountain, GA. The early dike (ED) is being cross-cut by tourmaline-bearing pegmatite-aplite (TP) dikes.

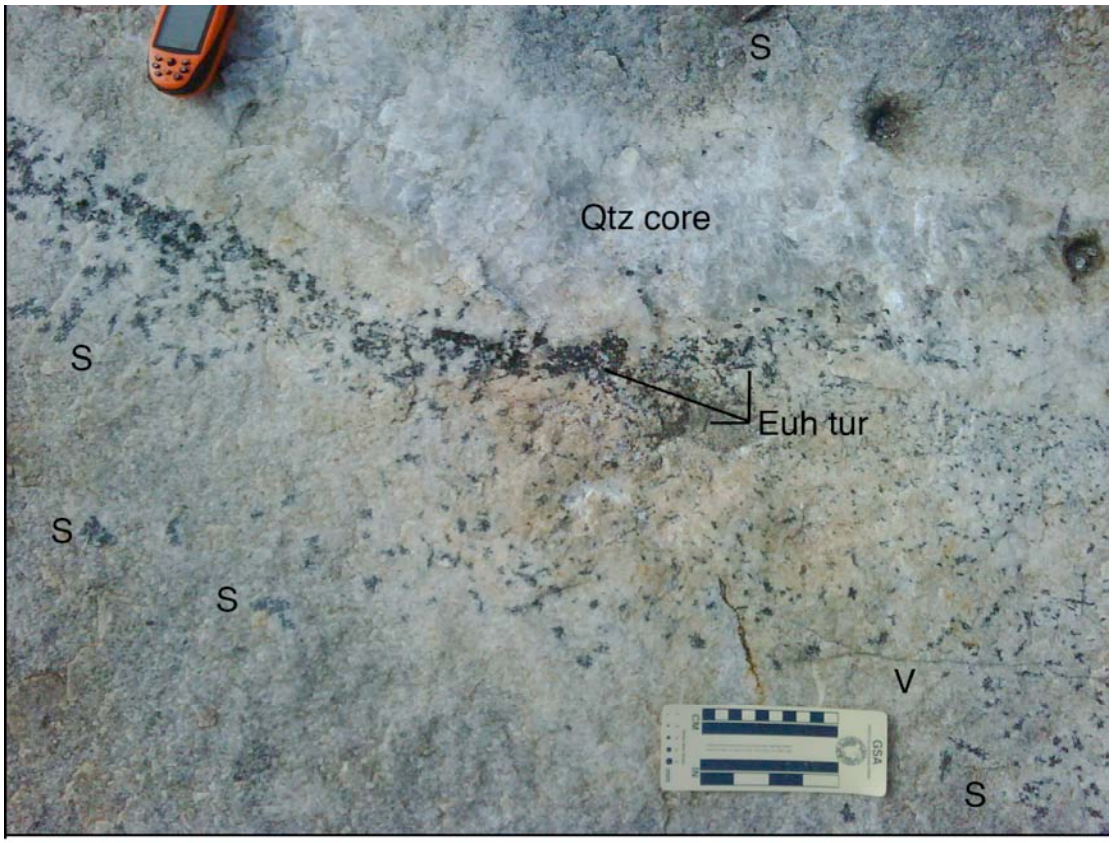

Figure 5.9 PAD, East quarry, Stone Mountain, GA. Very Pronounced quartz core (Qtz), euhedral (Euh) to skeletal (S) tourmaline (tur), and cross-cutting vein (V).

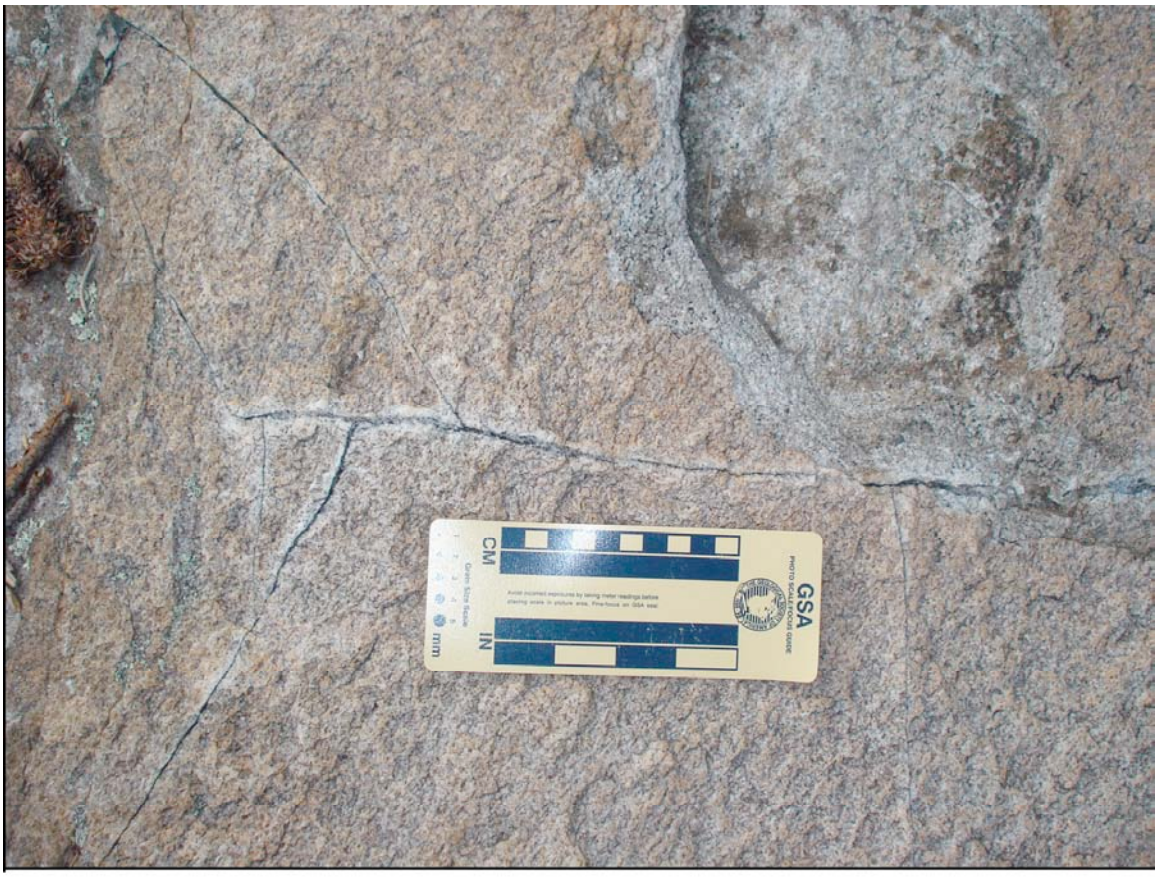

Figure 5.10 Quartz-tourmaline vein, West trail, Stone Mountain, GA. Field stop WTE4, sample WTA,B,C.

Figure 5.11 Skeletal tourmaline (S) "bloom" at end of ED, East quarry, Stone Mountain, GA

Figure 5.12 Elliptical and elongate skeletal tourmaline crystals, East quarry, Stone Mountain, GA

Figure 5.13 Long skeletal tourmaline (15 cm), East quarry, Stone Mountain, GA.

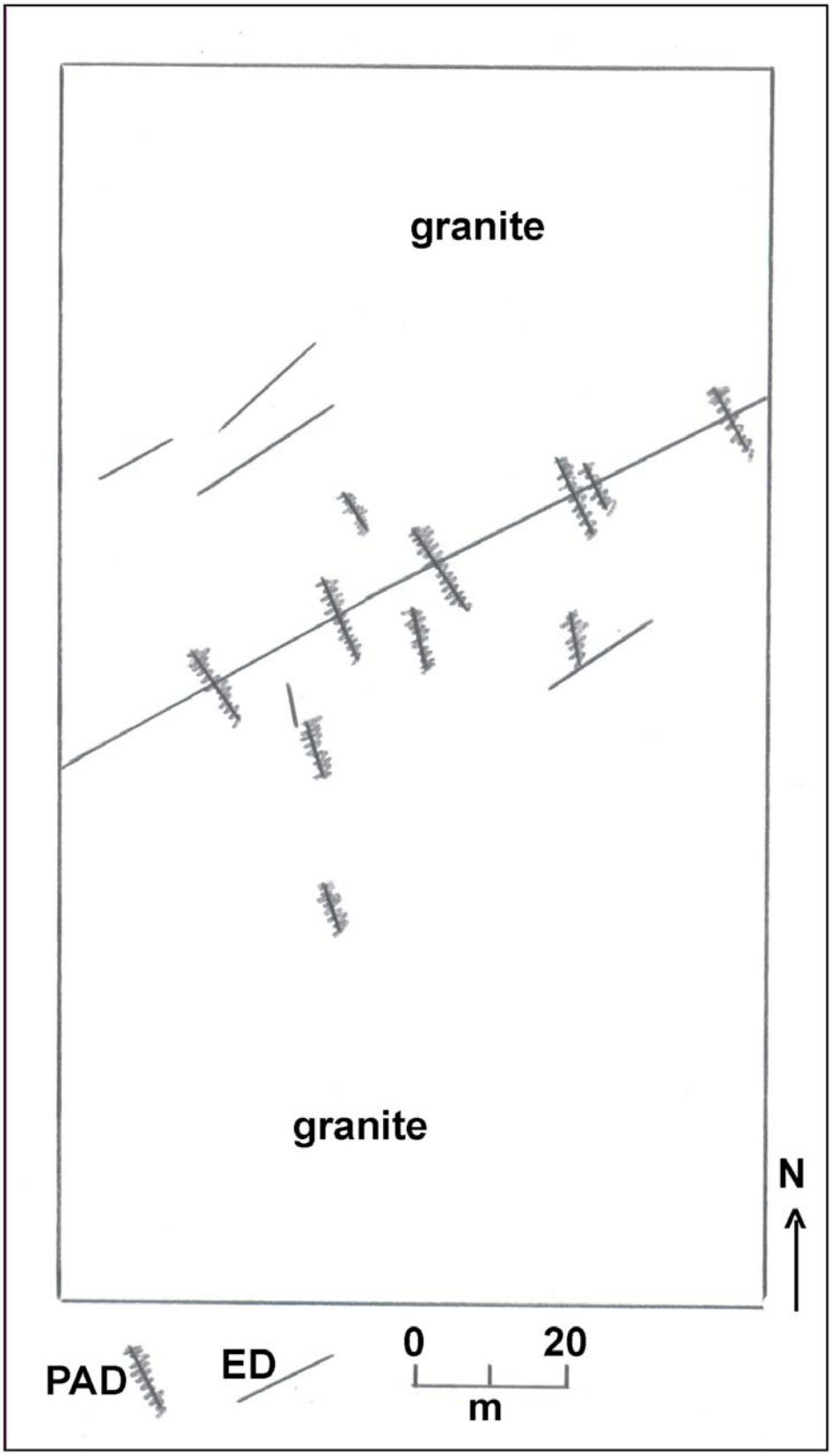

Figure 5.14 Map of dike distribution in the East quarry, Stone Mountain, GA

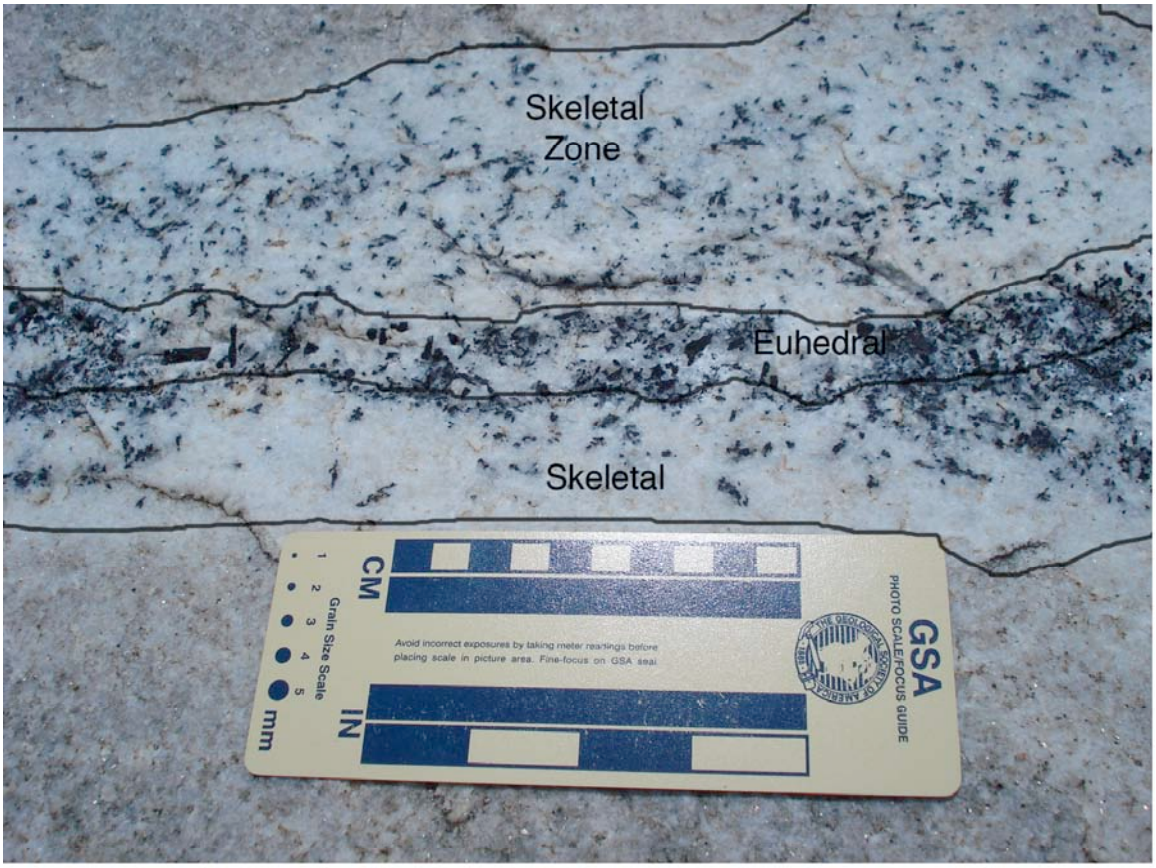

Figure 5.15 PAD displaying a core with euhedral tourmaline, and an aplitic margin with skeletal tourmaline, East Quarry, Stone Mountain, GA

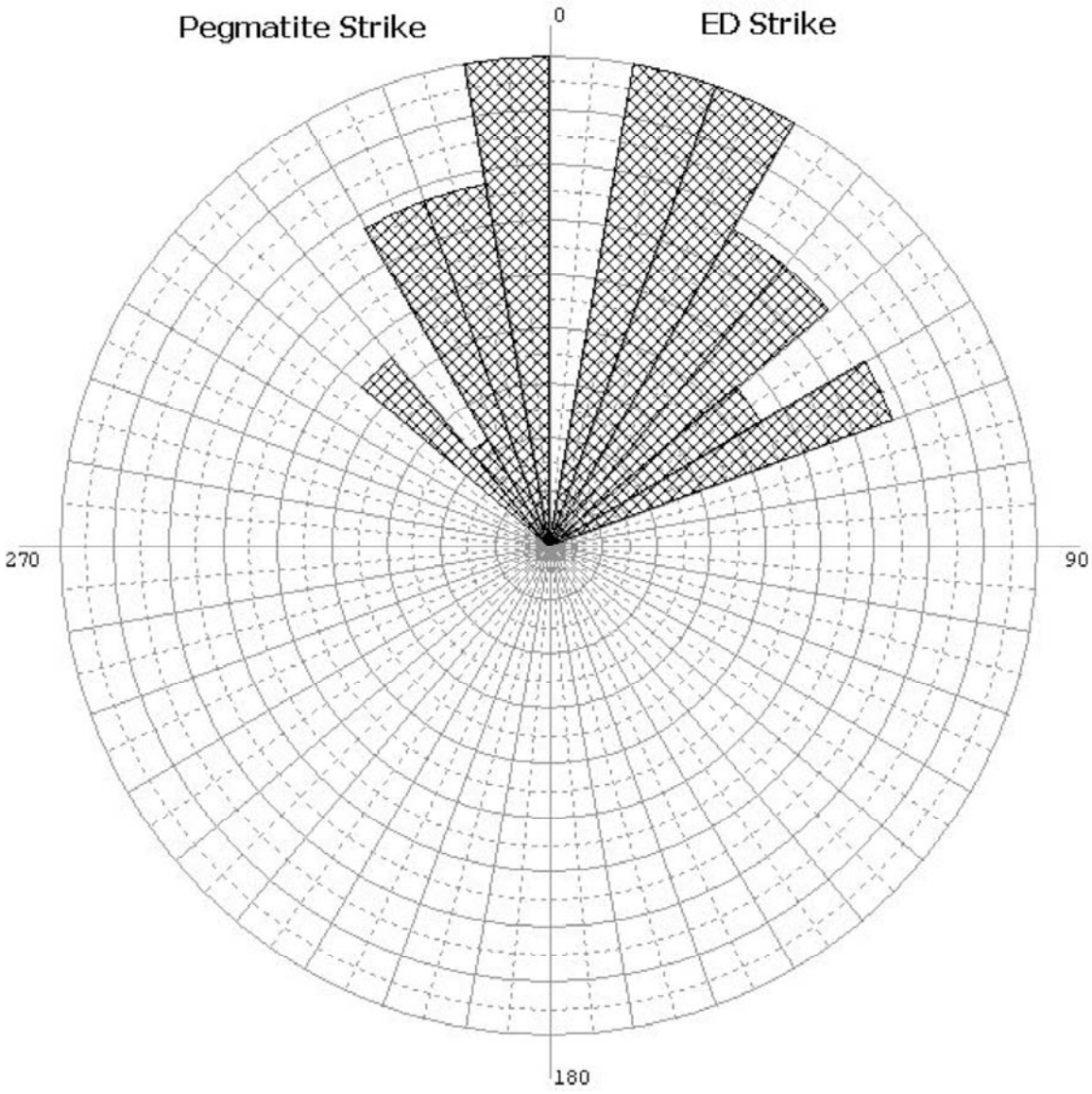

Figure 5.16 Rose diagram of dikes. ED trend NNE while PAD trend NNW.

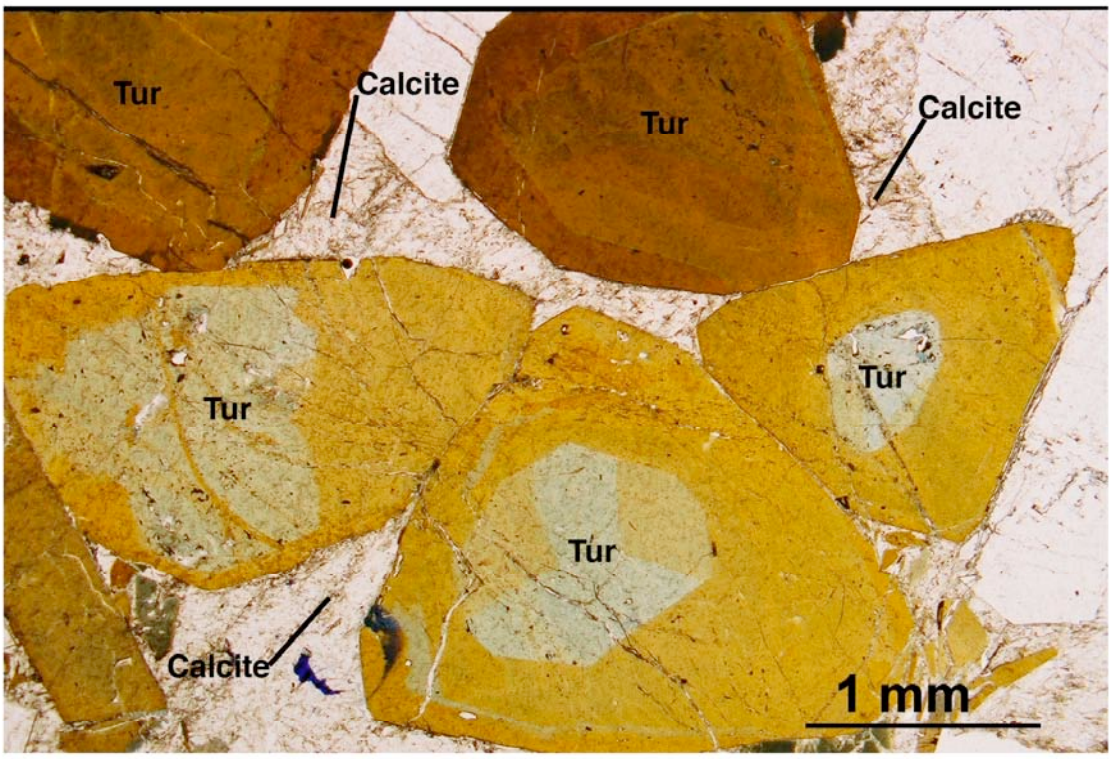

Figure 5.17 Euhedral tourmaline and calcite, East quarry, Stone Mountain, GA. In plane-polarized light, euhedral tourmaline exhibit brown to blue color zonation. This color change is due to a shift in Titanium. Blue cores represent higher Titanium while brown rims represent lower Titanium. Interstitial calcite is present.

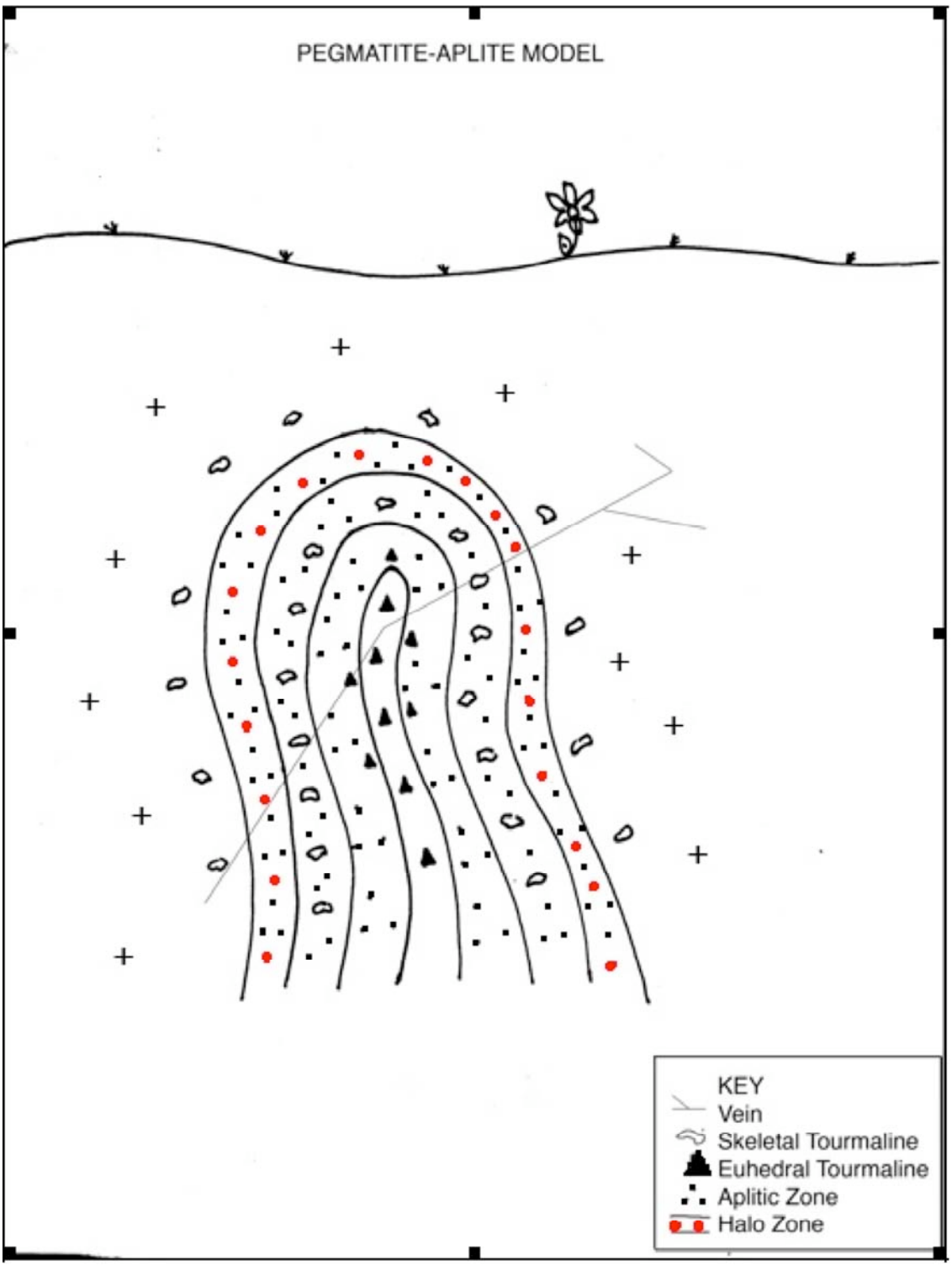

Figure 5.18 Cartoon A, complex evolution of PAD.

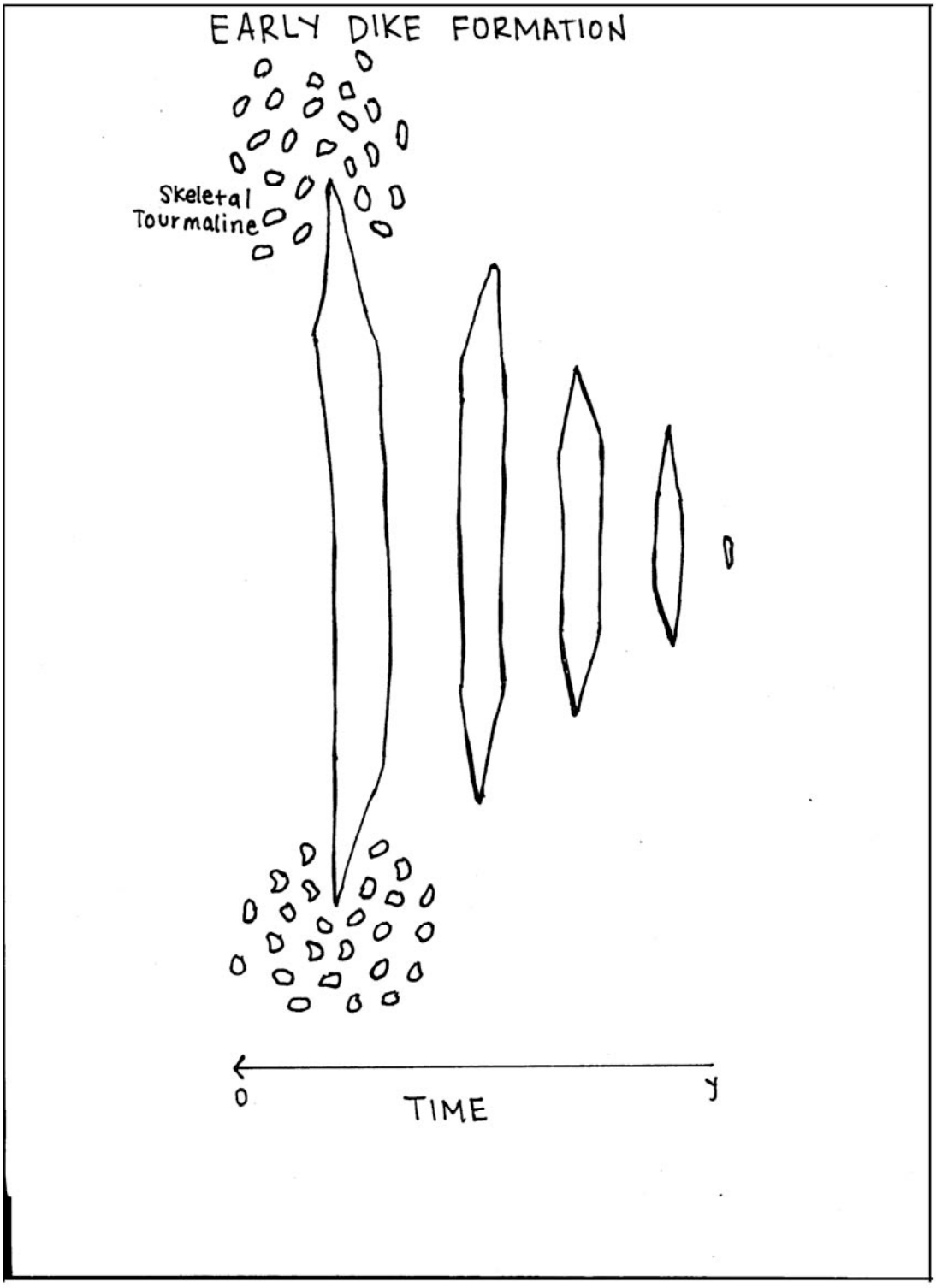

Figure 5.19 Model for Emplacement of ED. Time scale at bottom showing some time (y) to time of solidification (0). Skeletal tourmaline "bloom" extends from tips of ED.

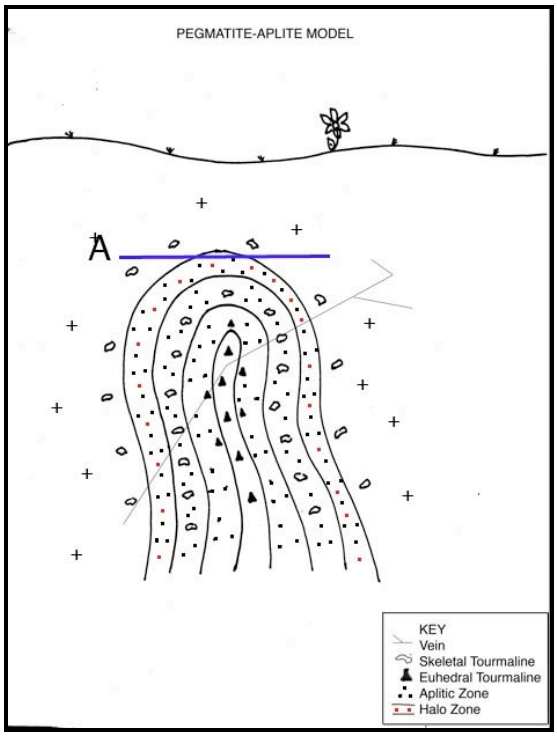

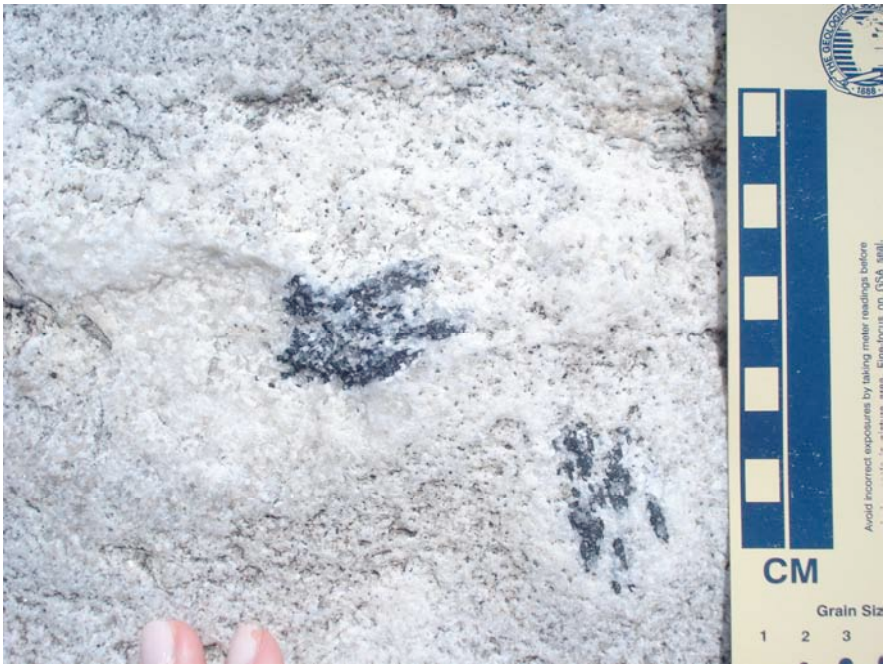

Figure 5.20 Erosional surface A correlates with a skeletal tourmaline exposure, Stone Mountain, GA. Skeletal tourmaline crystals surrounded by a leucocratic halo, in granite.

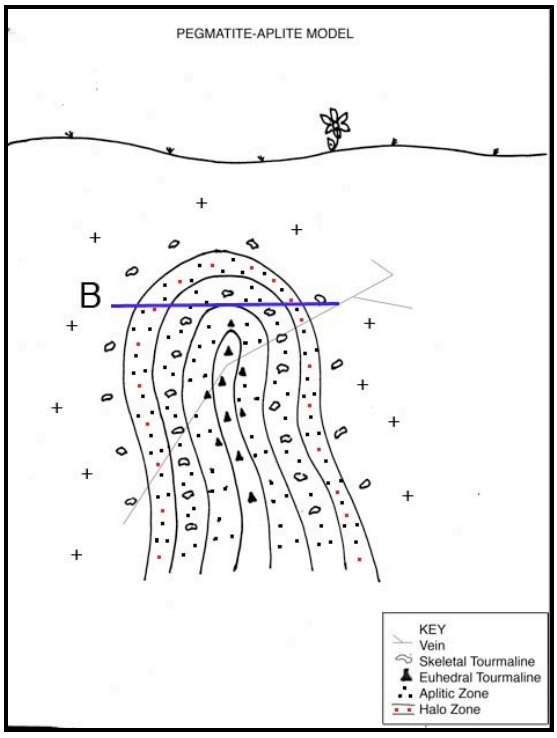

Figure 5.21 Erosional surface B correlates with a skeletal PAD exposure, Stone Mountain, GA. Skeletal tourmaline crystals are enclosed by a leucocratic halo, lacking a coarse-grained core, in granite.

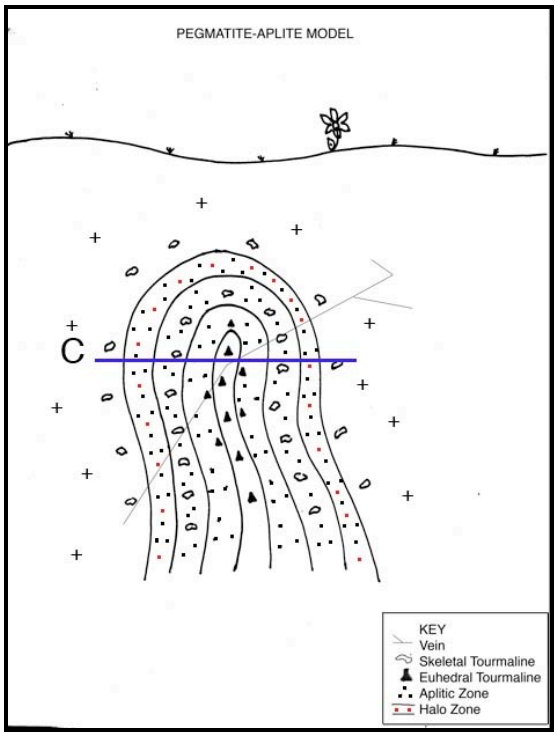

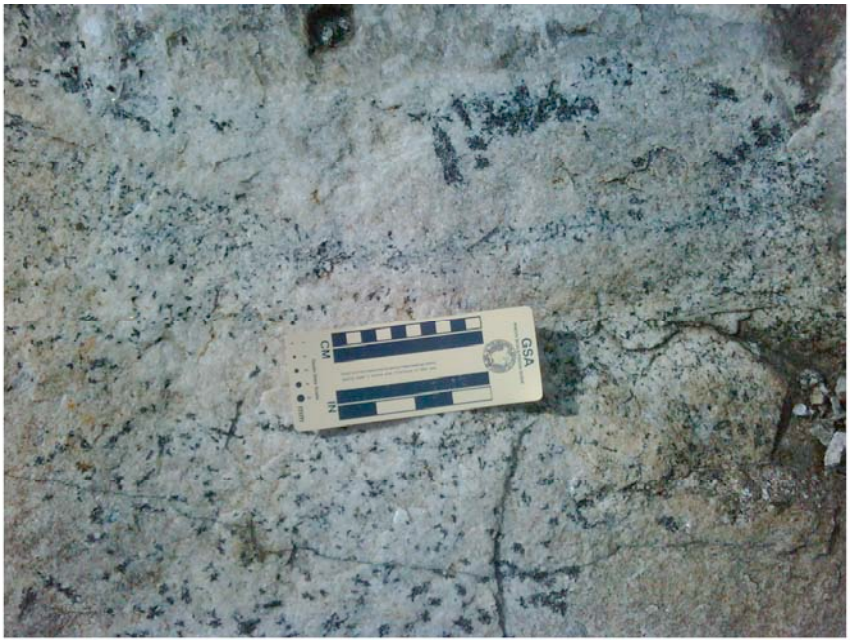

Figure 5.22 Erosional surface A correlates with a PAD exposure, Stone Mountain, GA. This PAD exhibits all tourmaline textures beginning with a euhedral tourmaline core, skeletal tourmaline in the halo, and skeletal tourmaline in granite, all cut by very fine-grained euhedral tourmaline vein.

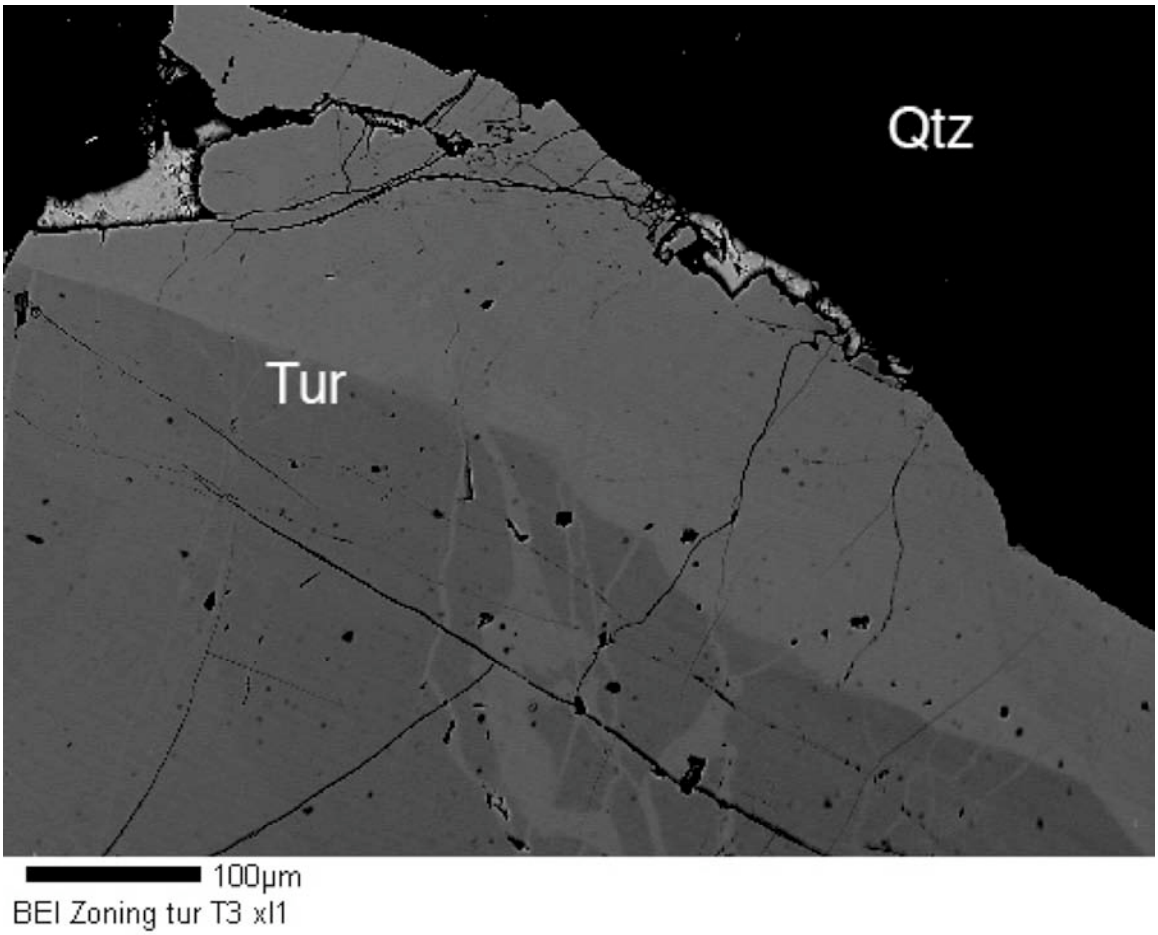

Figure 5.23 Backscattered electron image, euhedral tourmaline East quarry, Stone Mountain, GA. This euhedral crystal was taken from sample EQB. Light to dark color change indicates a shift in iron. This sample contains an iron rich rim and an iron poor core.

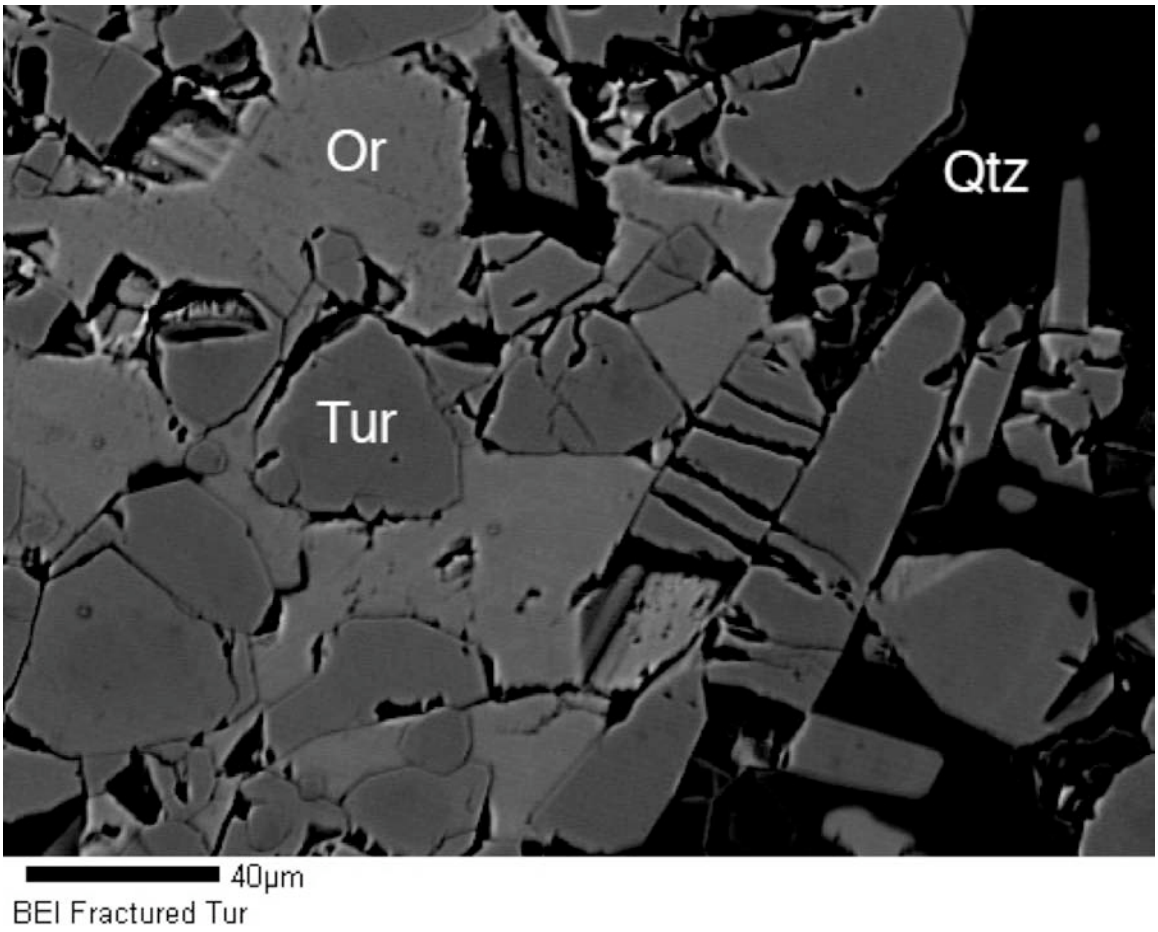

Figure 5.24 Backscattered electron image, tourmaline vein, West quarry, Stone Mountain, GA. This sample is labeled WTA. Euhedral tourmaline are enclosed in a matrix of potassium feldspar. There are no apparent zoning patterns in tourmaline.

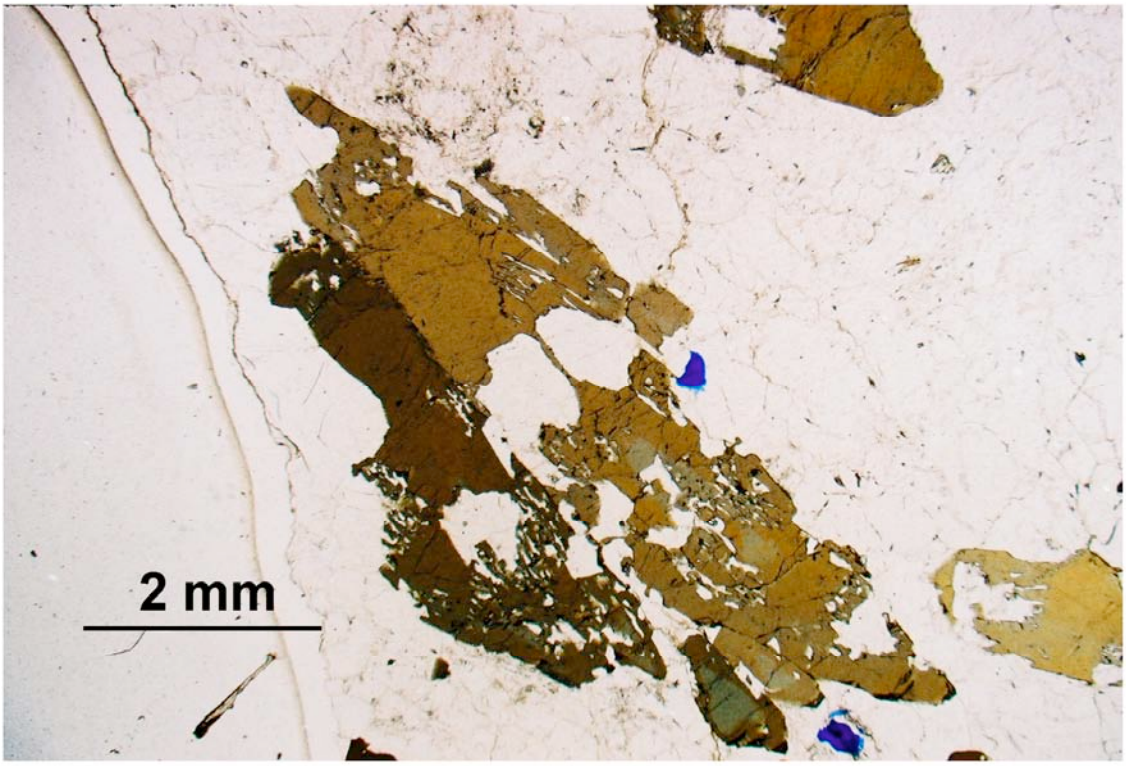

Figure 5.25 Plane-polarized light, skeletal tourmaline crystal in PA, East quarry, Stone Mountain, GA. This single skeletal tourmaline crystal is showing blue to brown pleochroism, most notable in lower extinction tips towards the bottom of the image.

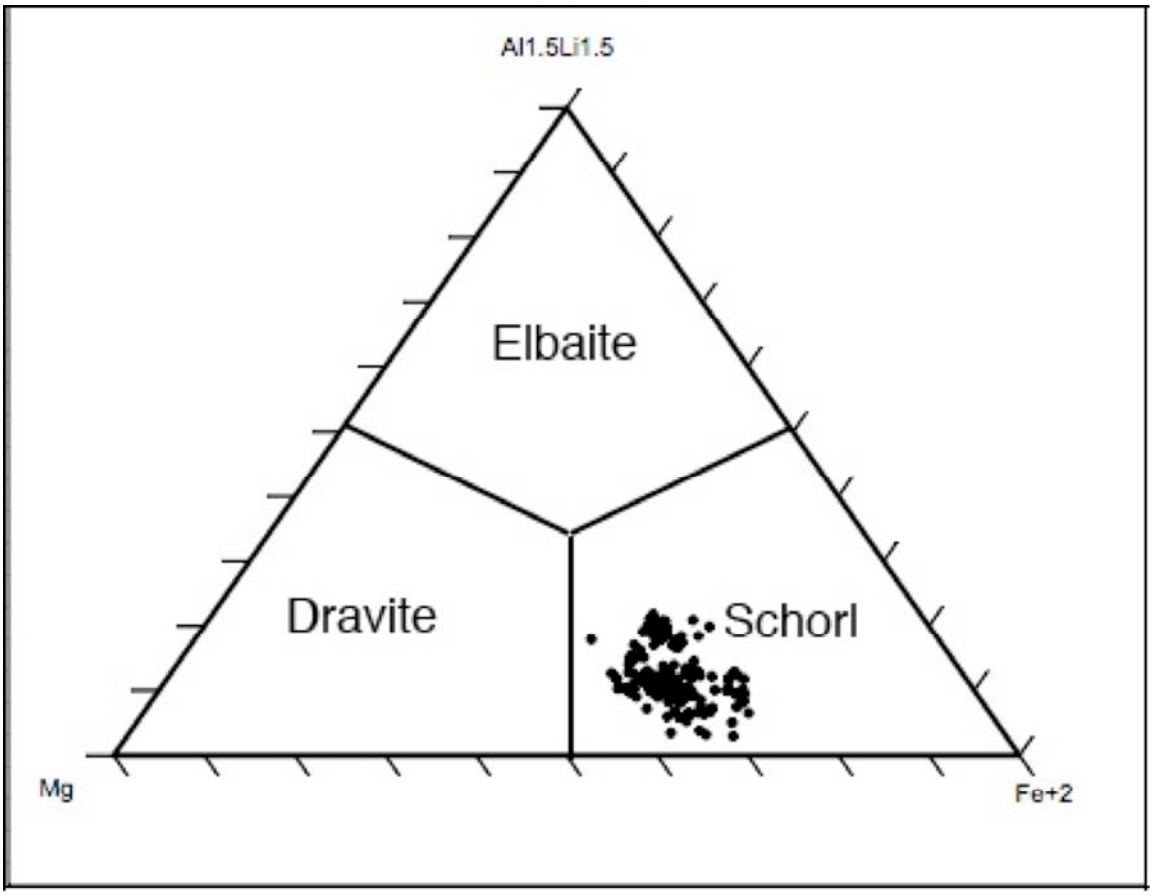

Figure 5.26 Y-Site occupancy plot of tourmaline, Stone Mountain granite, GA. The y-site plot shown represents 161 points from all tourmaline textures and locations in the Stone Mountain granite. All points plot in the Schorl category.

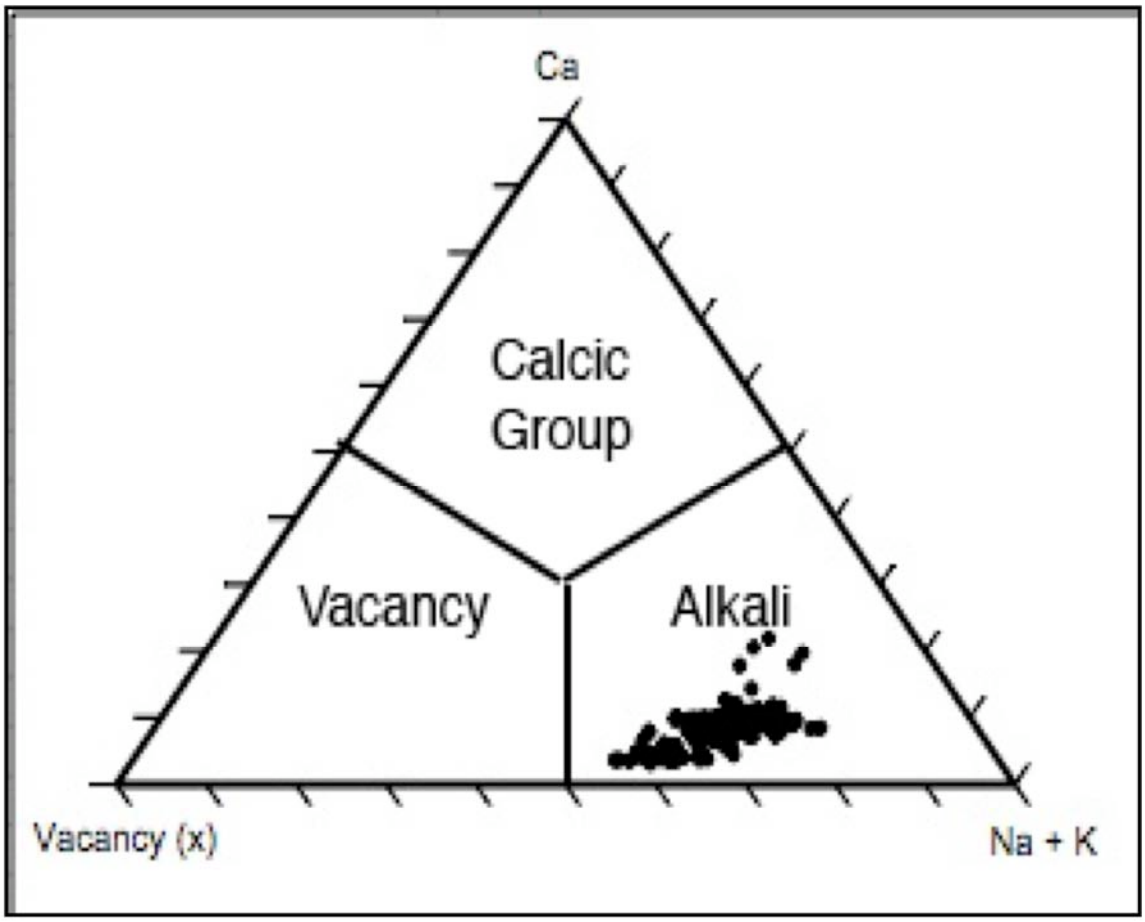

Figure 5.27 X-Site vacancy plot of tourmaline, Stone Mountain granite, GA. The x-site plot shown represents 161 points from all tourmaline textures and locations in the Stone Mountain granite. All points plot in the Alkali group.

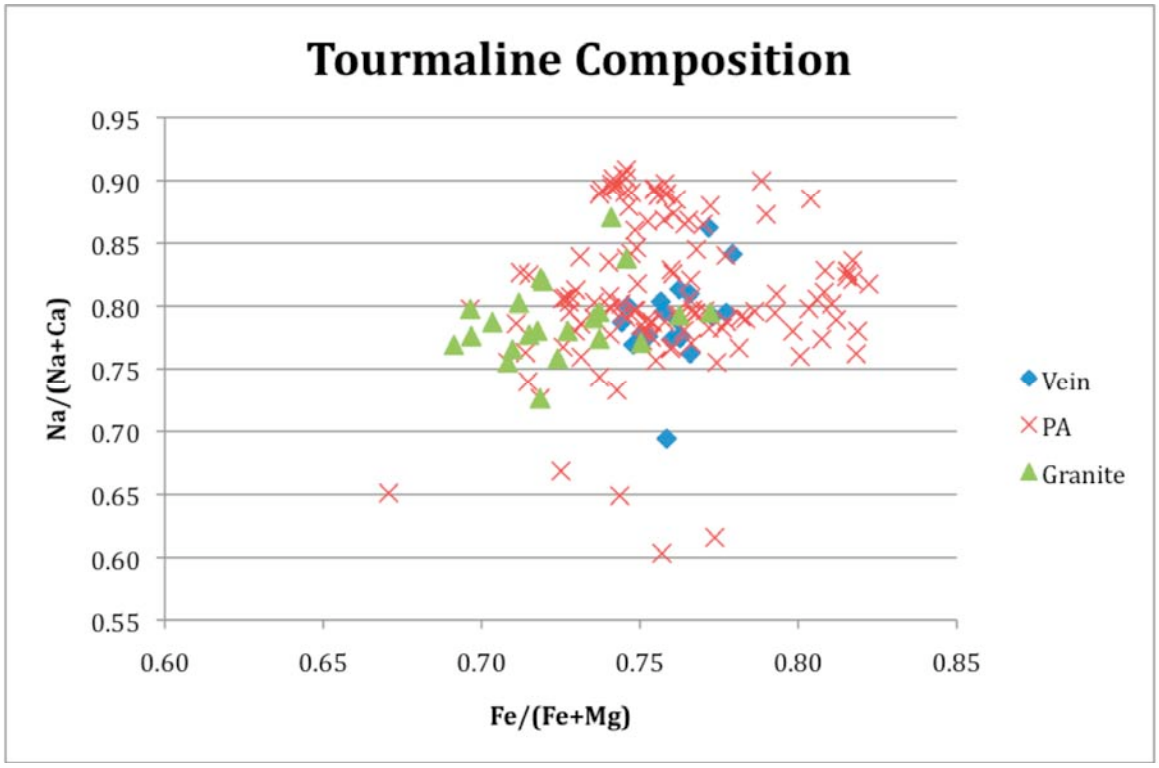

Figure 5.28 Nearly homogeneous tourmaline compositions.

A.

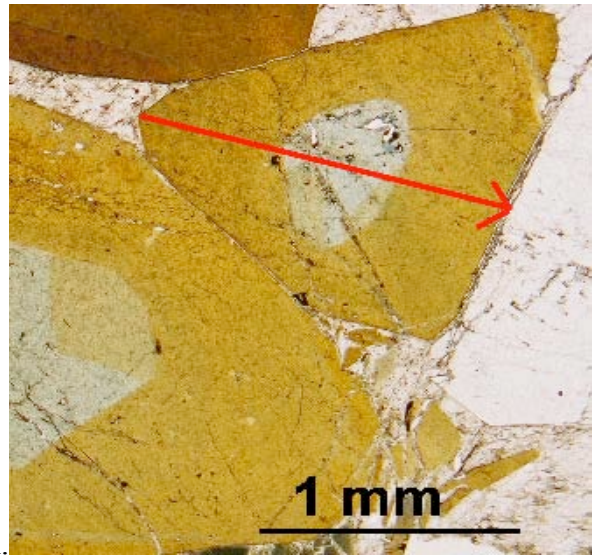

B.

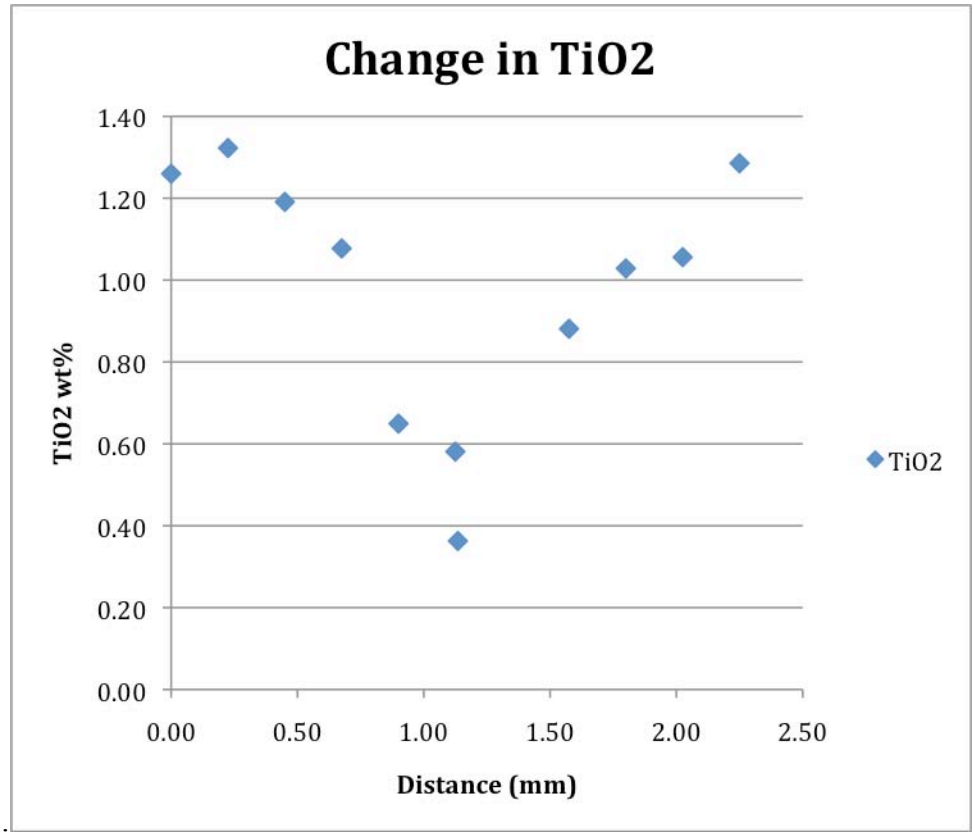

Figure 5.29 Change in TiO_2 with tourmaline crystals. This plot illustrates a drop in TiO_2 (B) as you move toward the core of a euhedral tourmaline crystal (A). Distance between points is approximately .225 mm.

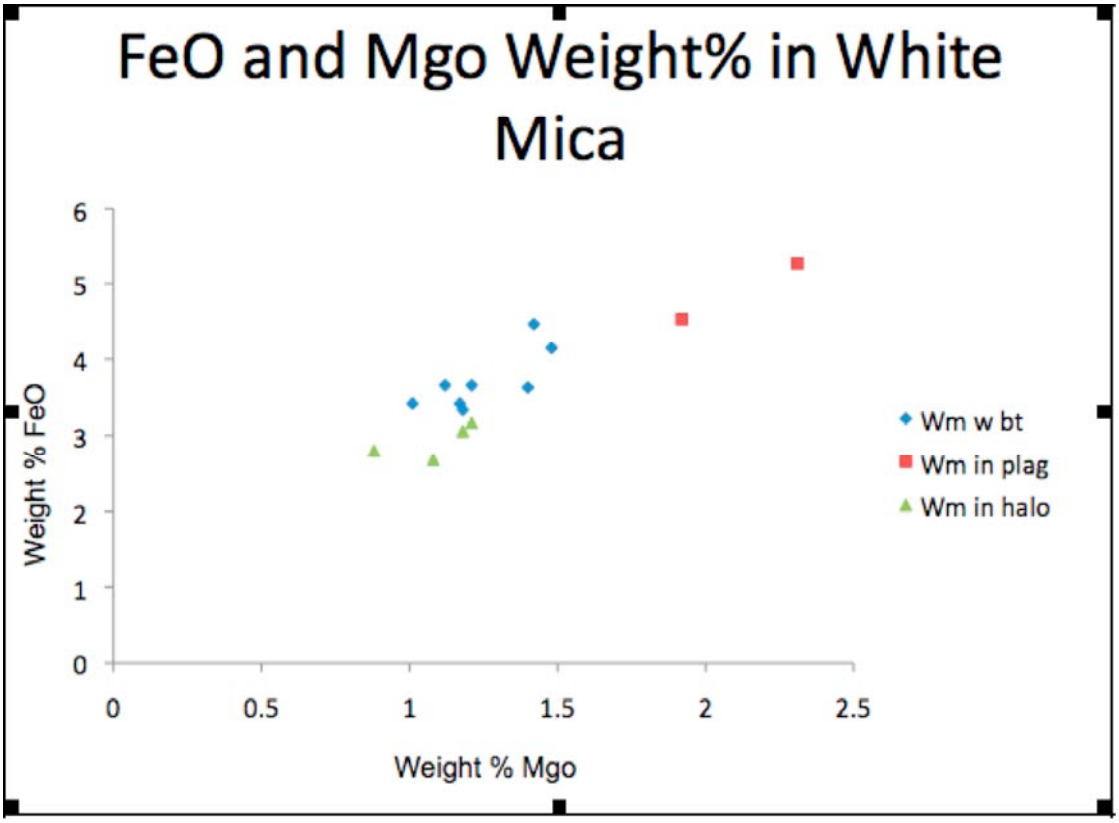

Figure 5.30 FeO and MgO in White Mica.

Table 5.1 Modal analyses of tourmaline and granite.

Sample	SM1	SM1	SM2	SM2	EQA-1	EQB-1	Gr-1	Gr-2	Gr-3
Tur Texture	Sk	Sk	Sk	Sk	Sk	Euh			
Location	halo in gr	tur in gr	halo in gr	tur in gr	PAD tur	PAD tur	gr	gr	gr
Quartz	40.6	50.4	42.3	43.3	47.2	34.1	31.5	32.6	30.8
Plagioclase	22.9	18.3	18.1	23.6	12.1	12.2	34.9	28.4	31.1
K-Feldspar	26.3	31.3	27.5	31.8	40.7	36.6	24.0	25.6	27.9
Muscovite	10.2	tr.	11.5	1.3	tr.	17.1	7.7	11.8	8.7
Biotite	tr.	0.0	0.6	0.0	0.0	0.0	1.4	1.3	1.4
Epidote	0.0	0.0	0.0	0.0	0.0	0.0	0.4	0.3	0.1
Apatite	0.0	0.0	0.0	0.0	0.0	0.0	0.1	tr.	tr.
Tourmaline	..	..	..	..	..	..	..	tr.	tr.
Number of pts	118	115	182	157	199	41			

Sk = Skeletal tourmaline, Euh = Euhedral tourmaline, halo in gr = halo of skeletal tourmaline in granite, tur in gr = within skeletal tourmaline crystal in granite, PAD tur = within a Pegmatite-aplite dike, gr = granite

Granite -1 is an average of 3 analyses from Whitney et al. (1976), Granite -2 is an average of 49 analyses from Wright (1966), Granite -3 is an averave of 6 analyses from Hermann (1954).

Table 5.2 Representative Microprobe Analyses of Tourmaline.

	Pegmatite				Vein		Granite	
grain	1c	1r	2c	2r	3c	4c	5c	5r
texture	Eu	Eu	Sk	Sk	Eu	Eu	Sk	Sk
color	blu	brn	blu	brn	nd	nd	brn	blu
SiO_2	36.63	33.73	35.79	34.61	35.45	35.17	35.53	36.25
TiO_2	0.15	1.35	0.35	1.15	1.05	1.20	1.16	0.29
Al_2O_3	32.94	31.63	33.66	32.02	31.33	31.31	32.74	33.97
FeO	11.72	13.14	11.81	11.73	11.90	11.57	12.07	10.53
MnO	bdl	0.26	0.24	0.23	bdl	0.26	bdl	0.20
MgO	3.58	3.32	2.88	3.57	3.81	3.40	3.76	3.59
CaO	0.38	0.57	0.23	0.51	0.52	0.54	0.45	0.35
Na_2O	1.73	2.01	1.78	2.01	2.04	2.05	1.71	1.80
K_2O	bdl	0.06	bdl	0.07	0.06	0.08	0.04	0.05
total	87.17	86.07	86.75	85.90	86.32	85.58	87.60	87.03

C = core, r = rim, Eu = euhedral, Sk = skeletal, blu = blue, brn = brown, bdl = below detection limit, MDL = silicon, 0.051; titanium, 0.068; aluminum, 0.042; iron, 0.129; manganese, 0.171; magnesium, 0.032; calcium, 0.035; sodium, 0.061; potassium, 0.030; fluorine, 0.124; and chlorine, 0.024

Table 5.3 Analysis of biotite and white mica within granite, Stone Mountain GA. Swanson et al., 2001.

Texture	1bt	3bt	2wm	4wm
Si02	35.19	34.87	47.60	47.95
Al2O3	17.27	17.96	33.63	34.16
TiO2	3.20	2.82	0.62	0.81
MgO	3.92	4.06	1.12	0.99
FeO	25.49	25.93	3.90	3.34
MnO	0.77	0.95	0.07	0.15
CaO	0.07	0.00	0.00	0.06
Na2O	0.14	0.22	0.24	0.36
K2O	7.89	7.94	8.28	7.93
F	0.00	0.00	0.00	0.00
Cl	0.02	0.02	0.00	0.01
Total	93.93	94.77	95.46	96.30
Oxy = 11				
Si	2.7898	2.7489	3.1530	3.1350
Al4				
Al6				
Sum Al	1.6135	1.6684	2.6253	2.6671
Ti	0.1906	0.1671	0.0304	0.0397
Mg	0.4613	0.4775	0.1106	0.0966
Fe	1.6903	1.7095	0.2162	0.1874
Mn	0.0514	0.0632	0.0037	0.0081
Ca	0.0057	0.0002	0.0000	0.0044
Na	0.0213	0.0341	0.0312	0.0457
K	0.7977	0.7987	0.7795	0.6615
F	0.0000	0.0000	0.0000	0.0000
Cl	0.0023	0.0028	0.0000	0.0016

Table 5.4 Analysis of white mica from bleached zone and biotite from proximal area, Stone Mountain GA. Swanson et al., 2001.

Texture	8bt	9bt	5wm	6wm	7wm
Si02	35.16	35.02	47.94	47.45	45.63
Al2O3	16.86	17.38	34.22	31.87	33.23
TiO2	2.68	3.07	0.83	0.14	0.82
MgO	5.05	4.09	1.16	1.90	1.07
FeO	23.26	25.70	3.00	3.54	3.45
MnO	0.86	0.75	0.07	0.39	0.11
CaO	0.43	0.04	0.04	0.51	0.09
Na2O	0.22	0.00	0.36	0.4	0.25
K2O	8.61	7.78	7.07	7.48	7.01
F	0.00	0.00	0.00	0.00	0.00
Cl	0.00	0.00	0.00	0.00	0.04
Total	93.13	93.84	94.69	93.68	91.68
Oxy = 11					
Si	2.8019	2.7787	3.1610	3.1970	3.1250
Al4					
Al6					
Sum Al	1.5833	1.6258	2.6591	2.5303	2.6832
Ti	0.1609	0.1830	0.0413	0.0071	0.0421
Mg	0.5995	0.4842	0.1148	0.1908	0.1088
Fe	1.5501	1.7056	0.1654	0.1995	0.1978
Mn	0.0580	0.0506	0.0037	0.0221	0.0062
Ca	0.0370	0.0037	0.0027	0.0365	0.0067
Na	0.0345	0.0000	0.0426	0.0524	0.0330
K	0.8752	0.7878	0.5944	0.6429	0.6126
F	0.0000	0.0000	0.0000	0.0000	0.0000
Cl	0.0000	0.0000	0.0000	0.0005	0.0044

CHAPTER 6

CONCLUSIONS

Textural variation of tourmaline was useful as guide to the crystallization history of the Stone Mountain granite. The transition from skeletal to euhedral tourmaline in pegmatite-aplites dikes is related to the "boron quench" model of Londol (1986a, 1986b) and displays the role of undercooling and boron in the system at time of crystallization. The Stone Mountain pluton evolved from early dikes with little boron to later crystallization of pegmatite-aplite dikes with extensive boron. The development of skeletal tourmaline "blooms" on ED and in aplite zone of PA show initial nucleation from an under saturated magma. Initial crystallization of skeletal tourmaline reflects delay in nucleation in a volatile-rich magma. Once skeletal tourmaline started to crystallize (and B was removed from the melt) the solidus temperature increased and feldspars and quartz crystallized, forming the aplitic zone. Continued crystallization of the magma at low undercoolings produced the euhedral tourmaline and coarse-grained quartz in the core zone.

Future work could involve bulk analyses of dikes, and stable isotope work to document fluid evolution. A study of fluid inclusions in various dikes would also help to determine fluid evolution. A refinement of the P-T estimates of intrusion using metamorphic xenoliths and country rock would be useful.

REFERENCES

Armstrong, J.T. (1988): Quantitative analysis of silicate and oxide materials: comparison of Monte Carlo, ZAF, and phi-rho-z procedures. *Microbeam Analysis*. 239-246.

Atkins, R. L. and Higgins, M. W. (1978): Relationship between superimposed folding and geologic history in the Georgia piedmont. *Geol. Soc. Am. Abstracts w programs.* **10**, 361.

Atkins, R. L., Higgins, M. W., and Gottfried, D. (1980): Geochemical Data Bearing on the Origin of Stone Mountain Granite, Panola Granite, and Lithonia Gneiss near Atlanta, Georgia. *Geol. Soc. Am. Abstracts w Programs.* **12,** 170.

Barenblatt, G. I. (1962): The Mathematical Theory of Equilibrium Cracks in Brittle Fracture. *Adv. Appl. Mech.* **7,** 55-129.

Brongniart, A. (1813): Essaid'une classification mineralogique des roches mélanges. *J. des Mines.* **34,** 32.

Brush, G. J. (1862): On amblygonite from Hebron in Maine. *Am. J. Sci.* **84**, 243-245.

Brush, G. J. (1863): Discovery of childrenite at Hebron in Maine. *Am. J. Sci.* **86**, 122-123, 257.

Buddington, A. F. (1959): Granite emplacement with special reference to North America. *Geol. Soc. Am. Bull.* **70,** 671-747.

Cameron, E. N., Jahns, R. H., McNair, A. H., and Page, L. R. (1949): Internal structure of granitic pegmatites. *Econ. Geol., Monogr.* **2**.

Dallmeyer, R. D. (1978): Ar^{40}/Ar^{39} incremental-release ages of hornblende and biotite across the Georgia Inner Piedmont: their bearing on late Paleozoic-early Mesozoic tectonothermal history. *Am. J. Sci*. **278**, 124-149.

Dingwell, D. B. (1997): The Brittle-Ductile Transition in High-Level Granitic Magmas: Material Constraints. *J. Petrol.* **38**, 1635-1644.

Donaldson, C. H. (1976): An experimental investigation of olivine morphology. *Contrib. Mineral. Pet.* **57,** 187-213.

Fenn, P. M. (1977): The nucleation and growth of alkali feldspar from hydrous melts. *Can. Mineral.* **62,** 135-171.

Fernandez, C. and Castro, A. (1999): Brittle Behaviour of Granitic Magma: the example of Puente del Congosto, Iberian Massif, Spain. *Geol. Soc. London Special Pubs.* **168,** 191-206.

Grant, W. H., Size, W. B., and O'Connor, B. J. (1980): Petrology and structure of the Stone Mountain Granite and Mount Arabia Migmatite, Lithonia, Georgia. *Geol. Soc. Am. 1980 Atlanta Field Trip no.3*. **17,** 41-57.

Grant, W. H. (1986): Structural and petrologic features of the Stone Mountain granite pluton, Georgia. *Geol. Soc. Am. Centennial Field Guide – Southeastern Section.* 285-290.

Haidinger, W. (1845): Handbuch der Bestimmenden Mineralogie. *Braumuller and Seidel, Wien, Austria.*

Hatcher, R. D., Jr., Thomas, W. A., Geiser, P. A., Snoke, A. W., Mosher, S. and Wiltschko, D. V. (1989): Alleghanian orogen *In* The Appalachian-Ouachita Orogen in the United States (R. D. Hatcher, Jr., W. A. Thomas, and G. W. Viele, eds.) *The geology of North America*. **F-2**, 233-318.

Hermann, L. A. (1954): Geology of the Stone Mountain-Lithonia District, Georgia. *Ga. Geol. Surv. Bull.* **61,** 139.

Jahns, R. H. (1955): The study of pegmatites. *Econ. Geol., 50th Anniv. Vol.* 1025-1130.

Jahns, R. H. and Burnham, C. W. (1969): Experimental studies of pegmatite genesis. **I**. A model for the derivation and crystallization of granitic pegmatites. *Econ. Geol.* **64,** 843-864.

Lister, J. R. (1990): Buoyancy-driven fluid fracture: the effects of material toughness and of low-viscosity precursors. *J. Fluid Mech.* **210**, 263-280.

Lofgren, G. E. (1974): An experimental study of plagioclase crystal morphology. *Am. J. Sci.* **274,** 243-273.

London, D. (1986a): The magmatic-hydrothermal transition in the Tanco rare-element pegmatite: evidence from fluid inclusions and phase equilibrium experiments. *Am. Mineral.* **71**, 376-395.

London, D. (1986b): Formation of tourmaline-rich gem pockets in miarolitic pegmatites. *Am. Mineral.* **71**, 396-405.

London, D. (2008): *Pegmatites*. The Canadian Mineralogist Special Publication **10**.

Manning, D. A. C. (1982): Chemical and morphological variation in tourmaline from the Hub Kapong batholith of peninsular Thiland. *Mineral. Mag.* **45,** 139-147.

Perugini, D, and Poli, G. (2007): Tourmaline nodules from Capo Bianco aplite (Elba Island, Italy): an example of diffusion limited aggregation growth in a magmatic system: *Contrib. Mineral. Petrol*. **153**, 493-508.

Rubin, A. M. (1993): Dikes vs. Diapirs in Viscoelastic Rock: *Earth Planet. Sci. Lett*. **117**, 653-670.

Rubin, A. M. (1995): Propagation of Magma-Filled Cracks. *Annu. Rev. Earth Planet. Sci.* **23**, 278-336.

Sinclair, W.D, and Richardson, J.M. (1992): Quartz-Tourmaline Orbicules in the Seagull Batholith, Yukon Territory. *Can. Mineral*. **30,** 923-935.

Size, W.B., and Khairallah, N. (1989): Geology of the Stone Mountain Granite and Mount Arabia Migmatite; Georgia: *"Excursions in Georgia Geology", Ga. Geol. Surv. Guidebook*. **9** no. 1, 159-169.

Slack, J. F. and Coad, P. R. (1989): Multiple hydrothermal and metamorphic events in the Kidd Creek volcanogenic massive sulfide deposit, Timmins, Ontario: evidence from tourmaline and chlorites. *Can. J. Earth Sci.* **26,** 694-715.

Sorby, H. C. (1858): On the microscopic structure of crystals, indicating the origin of minerals and rocks. *Geol. Soc. of London, Quarterly Journal*. **14**(I), 453-500.

Speer, A. J., McSween, H. Y. Jr., and Gates, A. E. (1994): Emplacement of Alleghanian Plutons in the Southern Appalachians. *J. Geol*. **102**, 249-267.

Swanson, S. E. (1977): Relation of nucleation and crystal growth rate to the development of granitic textures. *Am. Mineral.* **62,** 966-978.

Swanson, S. E. (1979): The Effect of CO_2 on Phase Equilibria and Crystal Growth in the System $KAlSi_3O_8$-$NaAlSi_3O_8$-$CaAl_2Si_2O_8$-SiO_2-H_2O-CO_2 To 8000 Bars. *Am. Journal of Sci.* **279**, 703-720.

Swanson, S. E. and Fenn, P. M. (1986): Quartz crystallization in igneous rocks. *Am. Mineral.* **71,** 331-342.

Swanson, S. E. and Fenn, P. M. (1992): The effect of F and Cl on the inetics of albite crystallization: a model for granitic pegmatites? *Can. Mineral.* **30,** 549-559.

Swanson, S.E., Mirante, D.C., Schrader, C.M., Tracy, B.J., Wolak, C.E., and Roden, M.F. (2001): Undercooling in granitoid systems: an example from Stone Mtn., GA. *Geol. Soc. Am. Abstracts w Programs*. **33,** A-29.

Watson, T.L. (1902): On the Occurrence of Aplite, Pegmatite, and Tourmaline Bunches in the Stone Mountain Granite of Georgia. *J. Geol*. **10**, 186-193.

Whitney, J. A., Jones, L.M., and Walker, R.L. (1976): Age and Origin of the Stone Mountain Granite, Lithonia district, Georgia. *Geol. Soc. Am*. *Bull.* **87**, 1067-1077.

Whitney, J. A., Dennison, J., and Gore, Pamela J. W. (1999): Geology and geomorphology of Stone Mountain, Georgia. *Geol. Soc. Am. Centennial Field Guide – Southeastern Section.*

APPENDIX A

FIELD PHOTOS

PA – West Trail

Field Site WTG

1 

2 

3 

PA – East Quarry

Field Site EQO

4

EQO

5

EQO

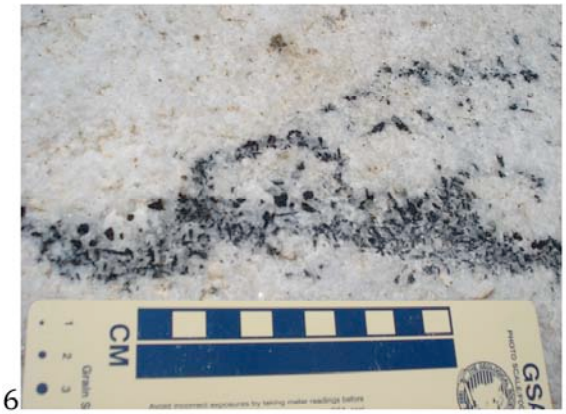

6

EQO

7

EQO

8

EQO

9

10 

11 

EQG

EQG

12 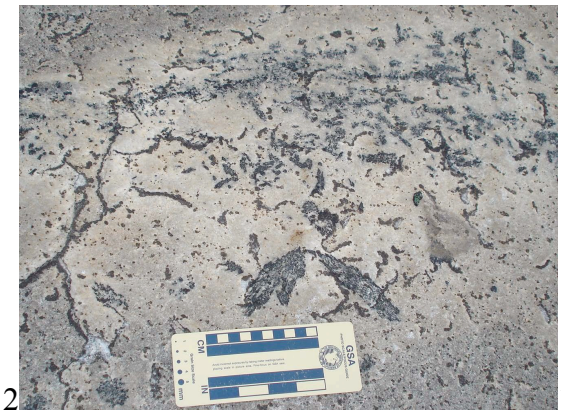

13 

EQH

EQH

14 

15 

EQI

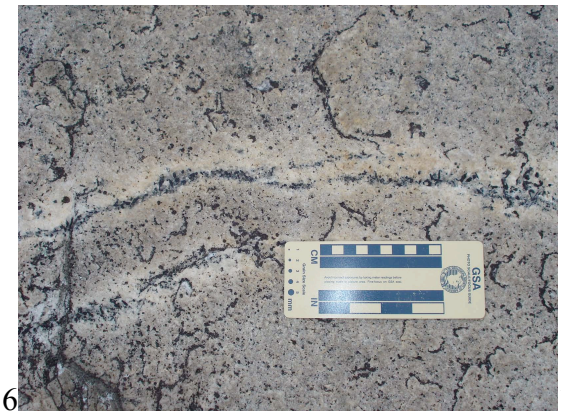

16

EQI

17

EQJ

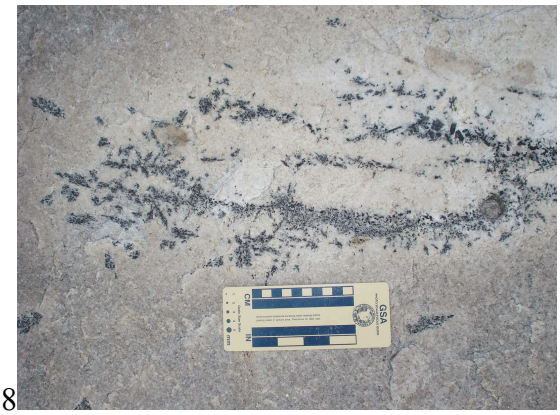

18

EQJ

19

20

21

EQO – Sample EQB taken here 22-25

22 

23 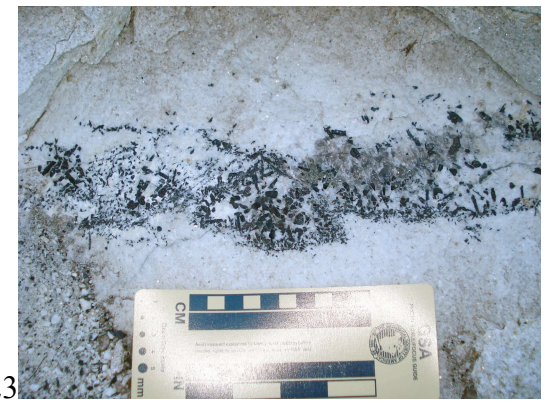

24 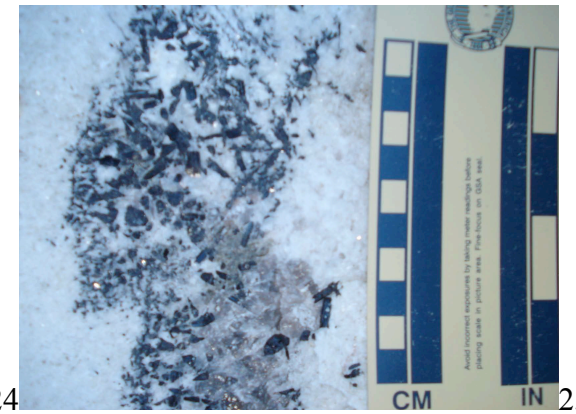

25 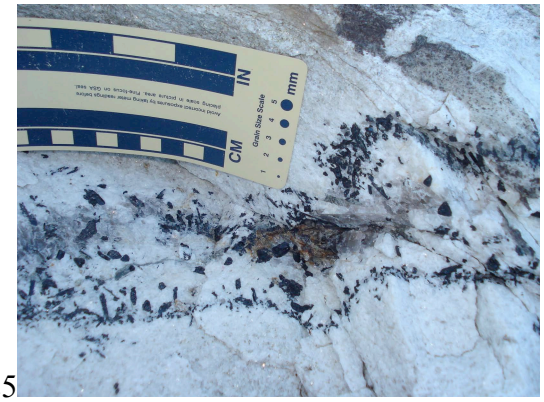

26 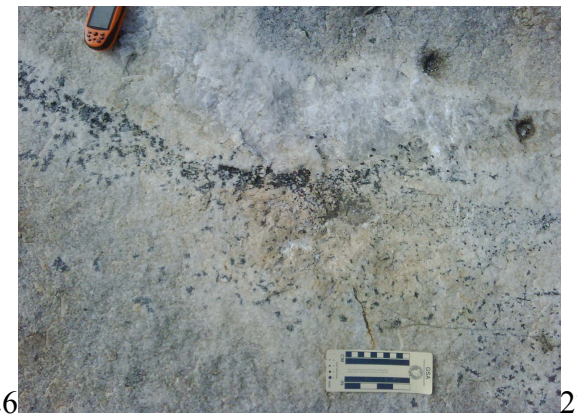

27 

28 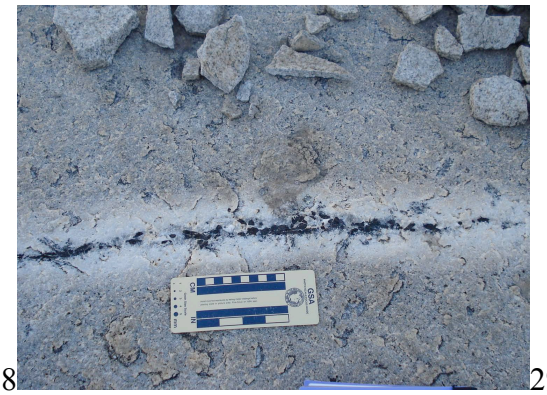

29 

30 

31 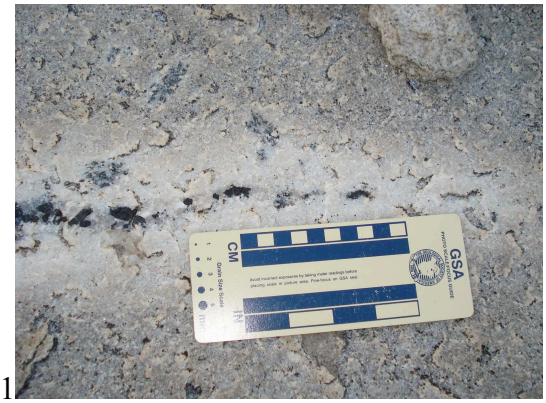

PA – Summit

S4

32

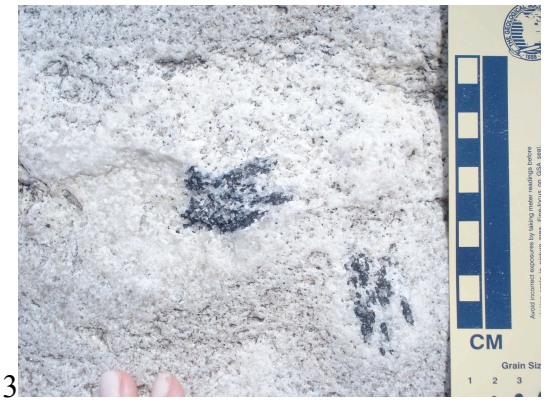

33

S4

S1

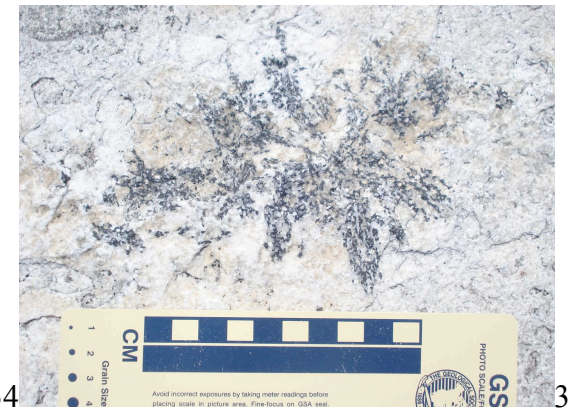

34

35

S5

S5

36

37

ED – West Trail

Field Site WTF

38

WTF

39

40

41

WT01

42

WT2

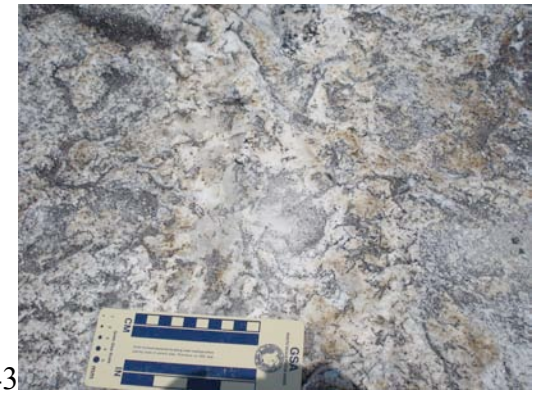

43

WT2

44

WT3

45

WT3

46

47

WTA

48

WTB

49

WTC

50

WTC

51

WTD

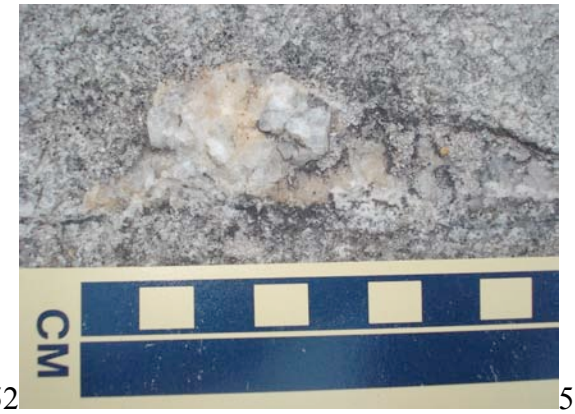

52

WTD

53

WTE1 & WTE2

54

WTE2

55

56 

57 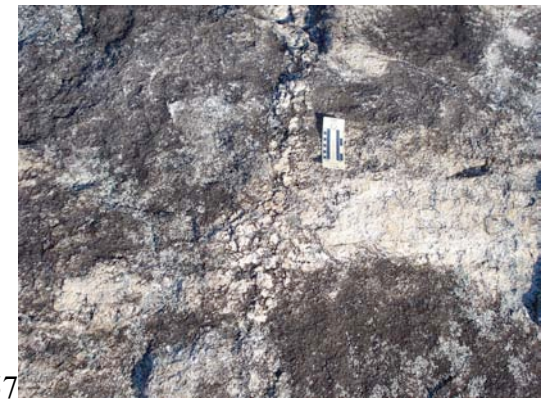

ED – East Quarry

EQ2A

58

EQ2A

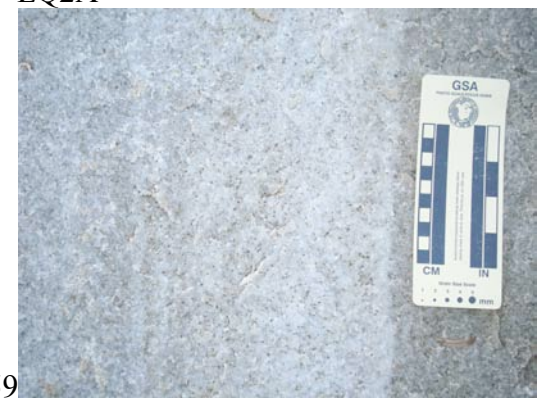

59

EQ01

60

EQ3

61

EQ2A

62

EQF

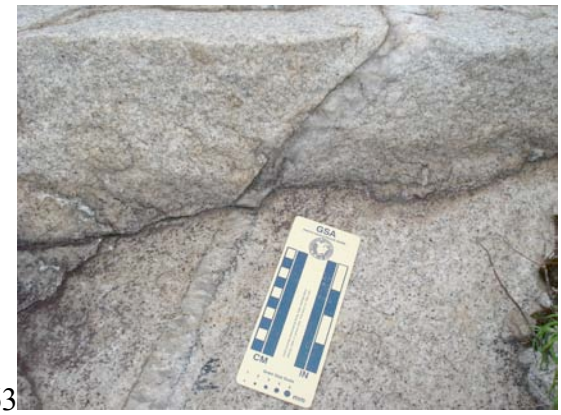

63

EQ2A

64

EQD

65

EQ2A

66

EQ2A & EQ3

67

ED – Summit

S3

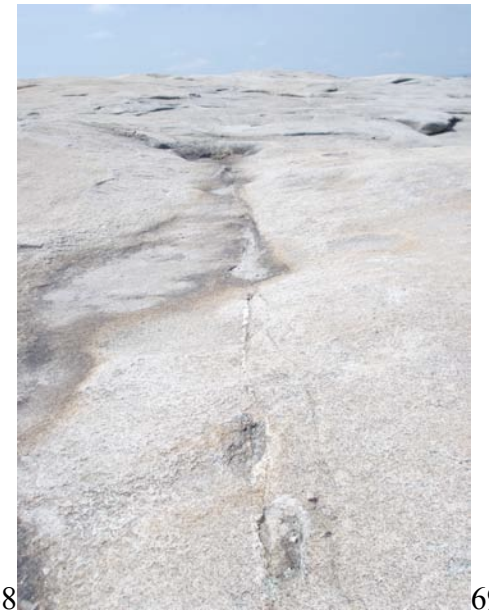

68

S3

69

SKELETAL TOURMALINE IN GRANITE – East Quarry

EQ2B

70

EQC

71

EQ2A

72

EQ2A

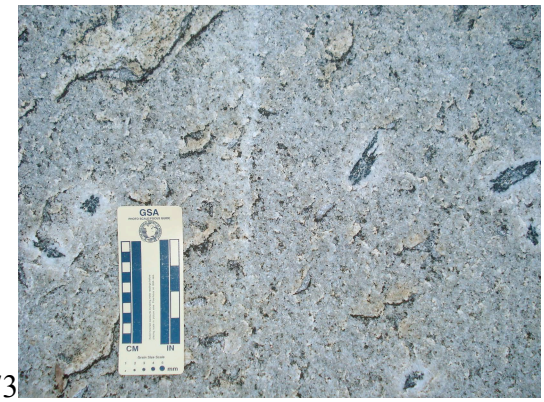

73

EQ2A

74

EQ2A

75

SKELETAL TOURMALINE GRANITE - Summit

S2

76

S6 – sample

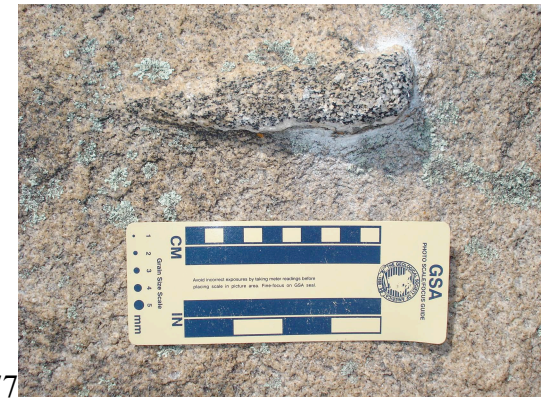

77

TOURMALINE VEINS – West Trail

WTE4 - Sample

78

WTE4

79

WTE4

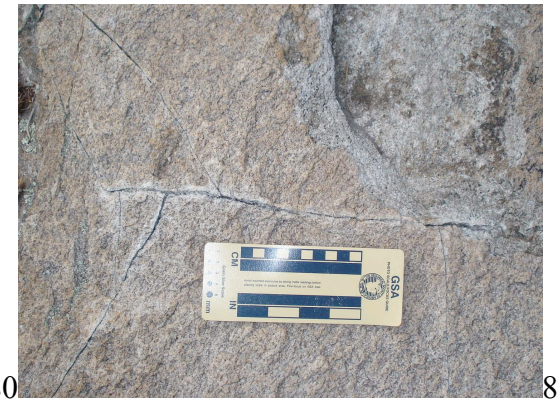

80

WTE4

81

EQP

82

83

APPENDIX B

FIELD NOTES

FIELD STUDY SITES

EAST QUARRY – ED

Stop	Date	Mineralogy	Dimensions	Strike/Dip	GPS – Lowest Point	Additional Notes
EQ01.	6/16/09	<6cm bt, ms, qtz, fsp	7cm x 6.3 m	60° ENE	n/a	Coarse inward micas w/ fsp + qtz. anastomosing
EQ2A.	6/16/09	>1mm qtz, fsp	48.3cm x >152m	49° ENE	16765078 E – 3744146 N	Cut by tur-bearing PA(EQO), skel. tur. bloom EQN at end SAMPLE TAKEN, ED2: early dike, silver vein cutting ED
EQ3.	6/16/09	>1mm qtz, fsp	3.5cm to 22.8cm x >152m	55° ENE	16765083 E – 3744122 N	6 m south, parallel to 2A. Also cut by tur. PA(EQO)
EQ4.	6/16/09	>1mm qtz, fsp	35.5cm x >152m	62° ENE	16765030 E – 3744081 N	Appears parallel to EQ2A & EQ3
EQD.	6/22/09	>1mm qtz, fsp	30cm x > 500m	61° ENE	16765116 E – 3744120 N	Qtz-tur vein runs on left margin of ED (<2cm x3.4m)
EQF.	6/22/09	2-4cm fsp, qtz	4cm x 15.2m	9° WNW/43° WSW	16765068 E – 3743937 N	Coarse-grained ED, rare. Euh. fsp xls. Anastomosing.
EQ2&3	6/22/09	>1mm qtz, fsp	82.5cm x > 150m	58° ENE	16764960 E – 3744055 N	EQ2 & EQ3 merge & extend, above 307m
EQK.	6/22/09	>1mm qtz, fsp	5cm x 50m	63° ENE	n/a	Long, thin ED, local skel.tur
EQL.	6/22/09	<6cm bt, ms, qtz, fsp	9cm x 6.5 m	65° ENE	n/a	Coarse inward micas w/ fsp + qtz, anastomosing
EQZ.	11/25/09	>1mm qtz, fsp	?	?	?	Cut by: Peg, PA, skel. tur., and another PA.

EAST QUARRY – Tourmaline

Stop	Date	Mineralogy	Dimensions	Strike/Dip	GPS – Lowest Point	Additional Notes
EQ2B.	6/16/09	srl, qtz, fsp	3 x 13cm	n/a	16765047 E – 3744105 N	Crossing skel tur next to EQ3, starburst shape, 286m ele.
EQC.	6/16/09	srl, qtz, fsp	1.5 x 15cm	n/a	16765101 E – 3744113 N	Longest skel. tur found, 277m ele. single skel tur xl
EQE.	6/16/09	srl, qtz, fsp	9cm x 2.75m	44° WNW	n/a	PA-Extremely anastomosing, variable strike.
EQG.	6/16/09	<1.5cm srl, qtz, fsp	33cm x 1.4m	26° WNW	16765054 E – 3743968 N	PA-Skel. tur 2 x 12cm, 2-9cm halo, <1.5cm euh tur in core
EQH.	6/16/09	<3cm srl, qtz, fsp	3 x 11cm	5° WNW	16764969 E – 3744059 N	PA-Euh. tur 2.7 x 0.3 cm in core, skel tur in halo
EQI.	6/16/09	<2.5cm srl, qtz, fsp	8cm x 2.7m	21° WNW	16765059 E – 3744025 N	PA-Thin (1cm) tur connect larger PA, skel. to euh. core
EQJ.	6/16/09	<2.5cm srl, qtz, fsp, grt	23cm x 2.3 m	14° WNW	16765024 E – 3744064 N	PA-<11cm halo, v.coarse-gr. core - skel tur in margin+halo
EQM.	6/16/09	srl, qtz, fsp	3 x 43.2cm	n/a	16765078 E – 3744146 N	PA-Cuts EQ2A, very short and thin, ele. 278.5m
EQN.	6/16/09	srl, qtz, fsp	2.4 x 3.41m	n/a	16765078 E – 3744146 N	Skel. tur "Bloom" at EQ2A end, random orientation, prominent halos
EQO.	6/16/09	srl, qtz, fsp, grt, zo, ap, brl	14cm x >30cm	53° WNW	16765016 E – 3744087 N	PA-Skel (<2cm) to euh tur gradation, connects/cuts EQ2A, SAMPLE TAKEN, EQB: euhedral tur, pink thulite, green beryl, qtz, fsp, ap, grt. 288m ele.
EQP	11/25/09	srl, qtz, fsp	2.25 x 5.9m	n/a	16765096 E – 3744107 N	PA-C. grain qtz core, euh. tur core below, grades outward t skel. tur, cut by vein

WEST TRAIL – ED

Stop	Date	Mineralogy	Dimensions	Strike/Dip	GPS – Lowest Point	Additional Notes
WT01.	6/22/09	>1mm qtz, fsp	9cm x >15m	42° ENE	n/a	At start of W. Trail, heavily weathered, foliation.
WT2.	6/22/09	>1mm qtz, fsp	20cm x 13.4 m	36° ENE	n/a	Just above WT01, heavily weathered, faint edges
WT3.	6/22/09	>1mm qtz, fsp	99cm x 13.7 m	17° ENE	n/a	3 bands, bleached white to gray in center, step-up
WTA.	7/12/09	<5cm qtz, fsp	8.5-35.2cm x 8.2m	28° ENE	16762989 E – 3744769 N	C. Grained ED w/ fine-grained margin. Heavily pitted/weathered, 293.5m ele
WTB.	7/12/09	<5cm qtz, fsp	34.5cm x 19.8m	26° ENE	16762982 E – 3744759 N	C. Grained ED margins w/ fine-grained core, margins weathered, 324.5 m ele
WTC.	7/12/09	>1mm qtz, fsp	0.8-1.8cm x 14.6m	28° ENE	16763079 E – 3744787 N	Very fine-grained with faint edges, ele. 337 m
WTD.	7/12/09	>1mm qtz, srl	0.8cm x 10.6 m	38° ENE	16763242 E – 3744710 N	Very thin, quartz vein w/ marginal srl. local qtz nodules (3x2cm), ele. 484 m
WTE1.	7/12/09	>1mm qtz, fsp	4cm x >54m	18° ENE	16763265 E – 3744655 N	Parallel to WTE2 ED off W. trail, ele. 54m, fine-grained, end covered by foliation
WTE2.	7/12/09	>1mm qtz, fsp	10.8-26.5cm x >54m	16° ENE	16763265 E – 3744655 N	Parallel to WTE1 & WTE3, fine-grained, end unknown, also covered by foliation
WTE3.	7/12/09	>1mm qtz, fsp	1.6-28cm x >55m	10° ENE	16763265 E – 3744655 N	Parallel to WTE2 & WTE1, fine-grained, end unknown, also covered by foliation
WTF.	7/12/09	<5.5cm qtz, fsp	2-5.5cm x >10m	7° ENE	16763258 E – 3744699 N	C. Grained inward projecting fsp + qtz, ele. 364.5m, anastomosing

WEST TRAIL – Tourmaline

Stop	Date	Mineralogy	Dimensions	Strike/Dip	GPS – Lowest Point	Additional Notes
WTE4.	7/12/09	>1mm srl, qtz, fsp	1.1cm x 28m	9.5° ENE	16763254 E - 3744612 N	Vein-w/in a fracture, tur core, qtz halo, cuts WTE2 & WTE3, ends at 354m ele.
WTG.	11/07/09	<2cm euh srl, qtz	11cm x 2m	4° WNW	16763285 E – 3744617 N	SAMPLES TAKEN, WTA, B, C- pieces of vein, tur + qtz PA- Only C. Grained PA on W. Trail, heaily eroded, euh tur in core, ele. 363

SUMMIT – ED

Stop	Date	Mineralogy	Dimensions	Strike/Dip	GPS – Lowest Point	Additional Notes
S3.	7/12/09	>1mm qtz, fsp, srl	1.8cm x >60m	2.5° ENE	n/a	ED- very thin, raised due to weathering, one 1cm skeletal tur inclusion

SUMMIT – Tourmaline

Stop	Date	Mineralogy	Dimensions	Strike/Dip	GPS – Lowest Point	Additional Notes
S1.	7/12/09	<1.5cm srl, qtz, fsp	14cm x 14.2m	5° ENE	n/a	PA-very defined halo 4.5cm, c. grained core, skel tur fine-grained margin
S2.	7/12/09	<1 cm srl, qtz, fsp	10cm x 3 m	9° ENE	n/a	PA- 8m east of S1. very defined halo, euh to skel tur
S3.	7/12/09	srl, qtz, fsp	1.8cm x 2m	2.5° ENE	n/a	PA- thin skel tur xls w/in a long leucocratic halo area
S4.	7/12/09	skel tur, qtz, fsp	15cm x 3.5m	10° ENE	16764201 E – 3744314 N	PA-skeletal tur overlapping each other in "starburst" pattern, >12cm skel. tur
S5.	9/6/09	skel tur, qtz	>10cm x 25cm	n/a	16763939 E – 3744369 N	PA-skeletal tur heavily weathered, tur and halo raised above granite, ele. 468.5m
S6.	9/6/09	skel tur, qtz	3.5cm x 14cm	n/a	16763933 E – 3744488 N	Skel tur heavily weathered, lone cluster of skel tur, ele. 466m SAMPLE TAKEN, S6- skel. tur

APPENDIX C

BEI IMAGES

SKELETAL TOURMALINE – In Granite

SM1

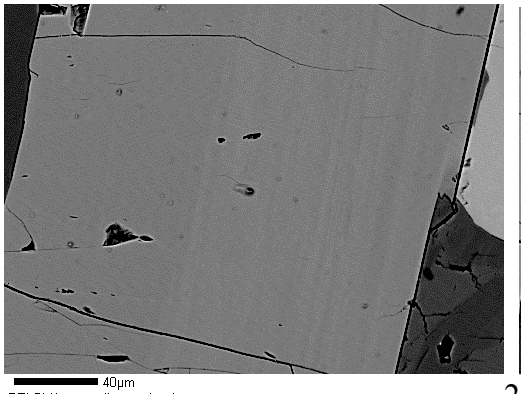

1 BEI SM1 tourmaline zoning 1

SM1

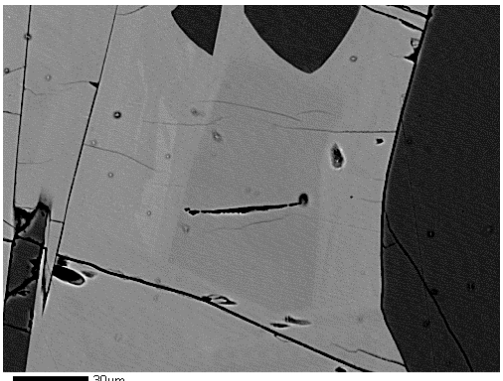

2 BEI SM1 tourmaline zoning 2

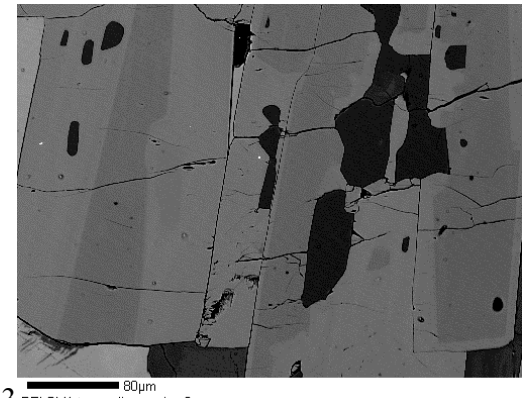

3 BEI SM1 tourmaline zoning 3

SKELETAL TOURMALINE – In PA

SM2

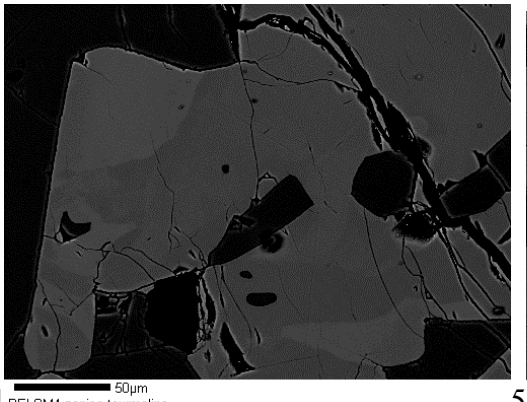

4 BEI SM4 zoning tourmaline

SM2

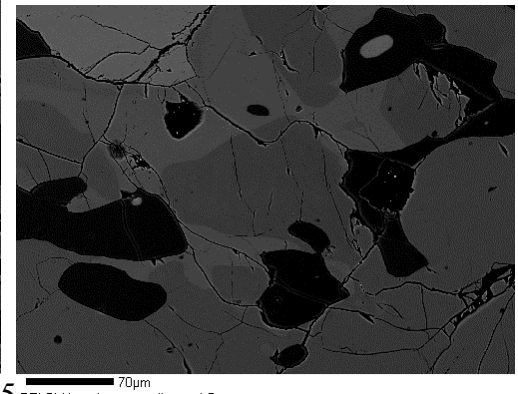

5 BEI SM4 zoning tourmaline pt 4,5

SM2

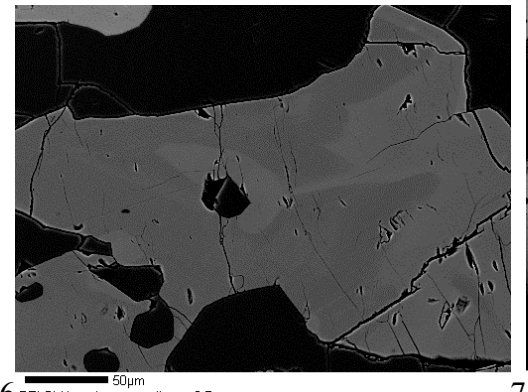

6 BEI SM4 zoning tourmaline pt 6,7

EQA-1

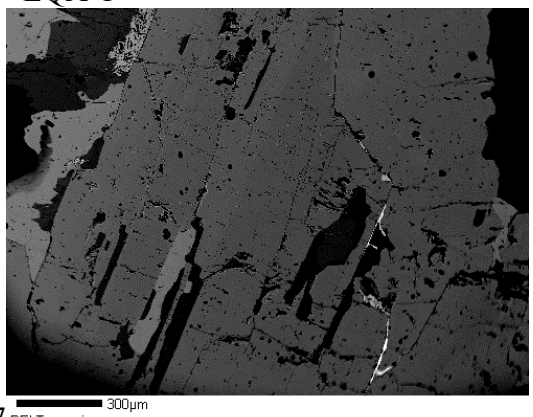

7 BEI Tur zoning

EQA-1

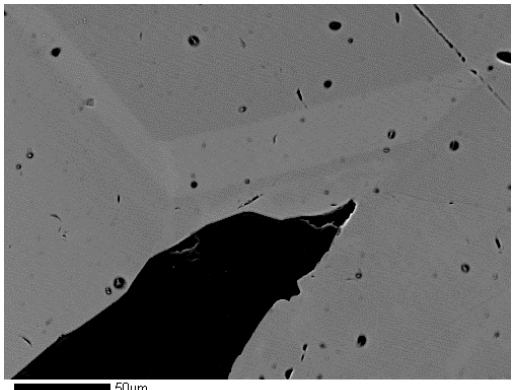

8 BEI Tur zoning

EQA-1

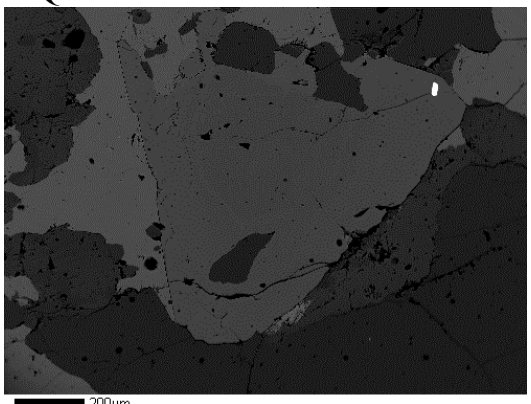

9 BEI Tur, pl, qtz, or, ap

EUHEDRAL TOURMALINE – In PA

T3

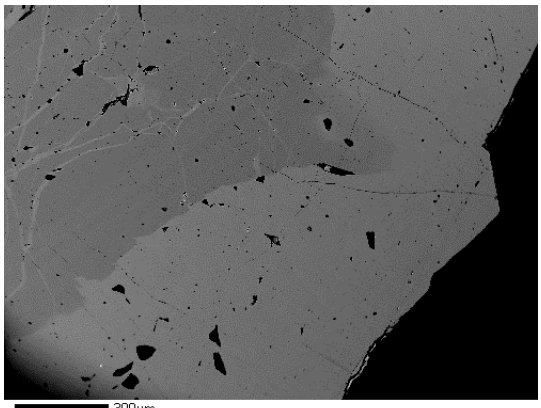

10 BEI Zoning tur T3

T3

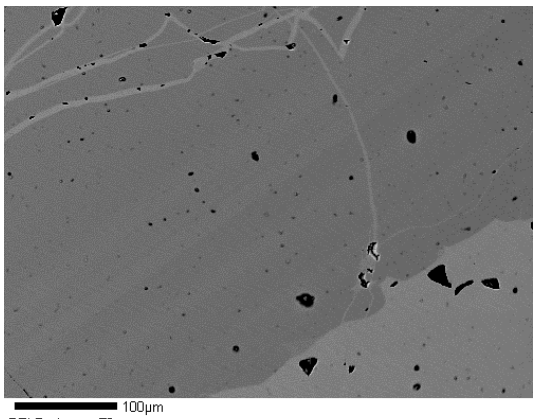

11 BEI Zoning tur T3

T3

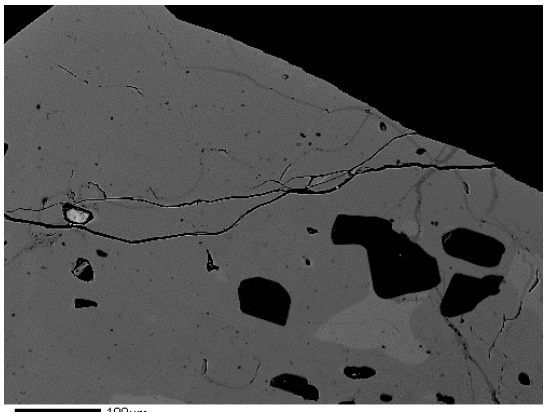

12 BEI Zoning tur T3 xl3

T3

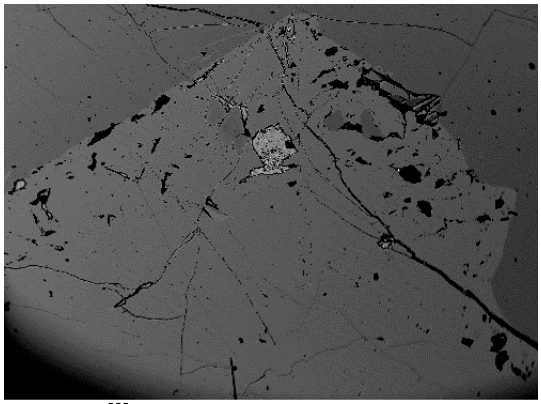

13 BEI Zoning tur T3 xl4

T2

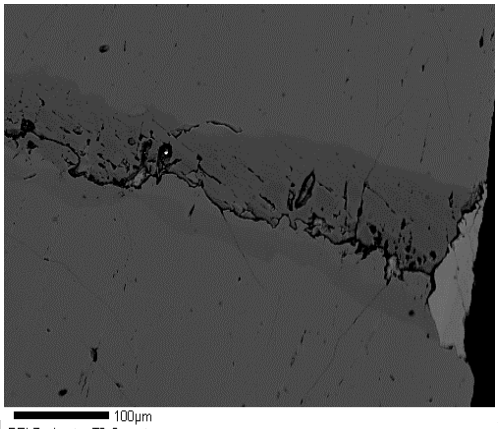

14 BEI Zoning tur T6 Garnet

EQB-1

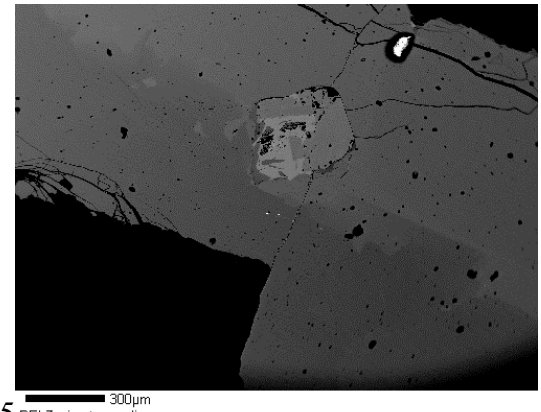

15 BEI Zoning tourmaline

EQB-1

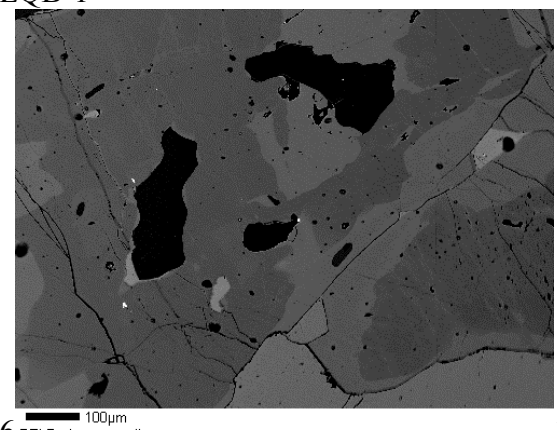

16 BEI Zoning tourmaline

EQB-1

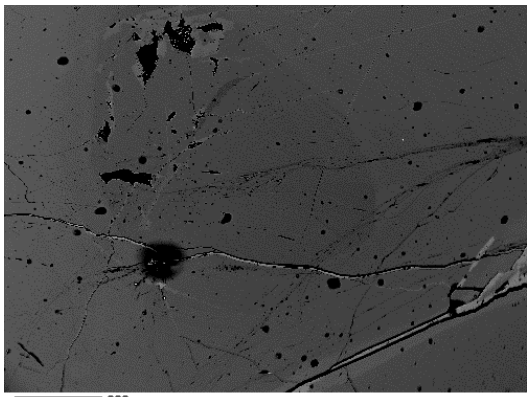

17 BEI Zoning tourmaline, grn core

EQB-1

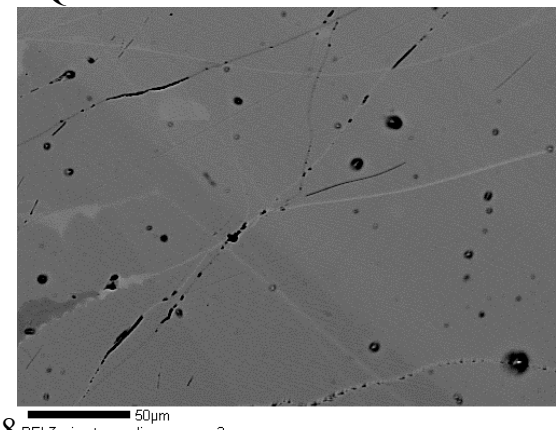

18 BEI Zoning tourmaline, grn core2

EUHEDRAL TOURMALINE – In Vein

T1

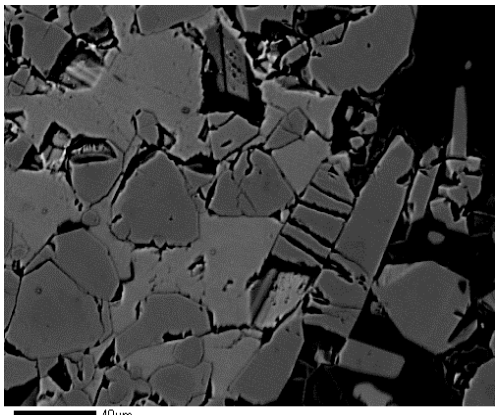

19 BEI Fractured Tur

T1

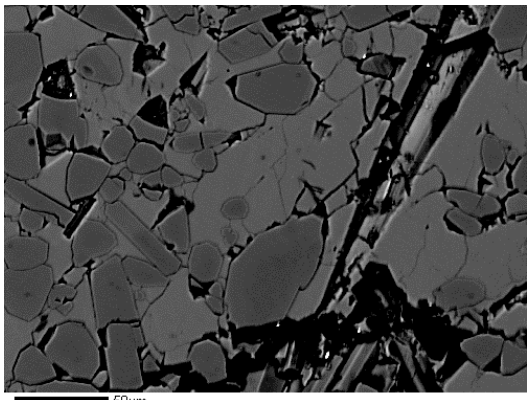

20 BEI Fine Grained Tour/Fspar

T1

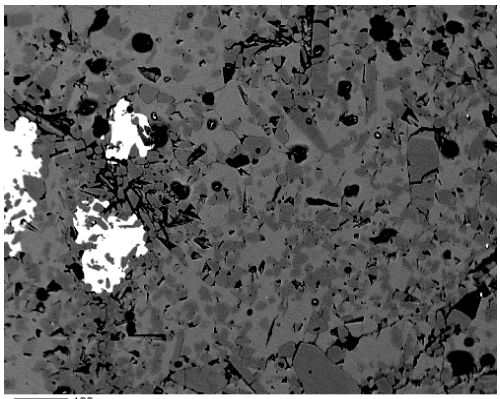

21 BEI Tour Vein w/ Garnet

T1

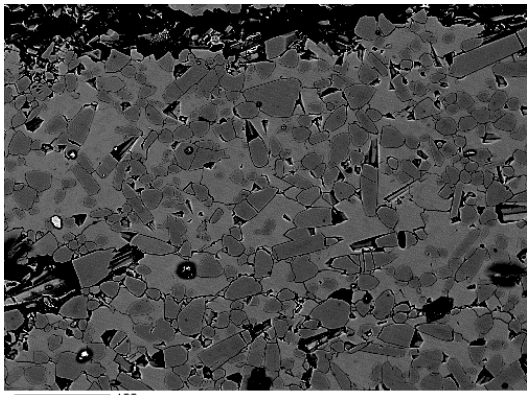

22 BEI Comp.Tourmaline 2

APPENDIX D

ELECTRON MICROPROBE ANALYSIS ROUTINE FOR TOURMALINE AND MICAS

Tourmaline and micas were analyzed for silicon, titanium, aluminum, iron, manganese, magnesium, calcium, sodium, potassium, fluorine, and chlorine. The element, standard, and crystals used are as follows: silicon, Diopside5A, Spectrometer 1; titanium, TiO_2, PET; aluminum, Spin (spinel), TAP; iron, Fayalite, LIF; manganese, Spes (spessartine), LIF; magnesium, Olivine, TAP; calcium, Sphene, PET; sodium, ABOX (amelia albite), TAP; potassium, Or10, PET; fluorine, FPHL (synthetic phalogopite glass), LDE1; chlorine, Sacpolite, PET. Precision of analysis was tested through the standard Lemhi Biotite at the beginning of each probing secession. Tourmaline samples were analysed used an accelerating voltage of 15 keV and 5 nA beam current. Counting time was 10 seconds on standard peaks and a 1 micron beam diameter was used. Peak positions for tourmaline elements are as follows: silicon, 77.522; titanium, 87.721; aluminum, 90.310; iron, 134.915; manganese, 146.427; magnesium, 107.240, calcium, 107.300; sodium, 129.275; potassium, 119.582; fluorine, 84.760; and chlorine, 151.154. Representative minimum detection limits for tourmaline elements (in oxide wt. %) are as followes: silicon, 0.051; titanium, 0.068; aluminum, 0.042; iron, 0.129; manganese, 0.171; magnesium, 0.032; calcium, 0.035; sodium, 0.061; potassium, 0.030; fluorine, 0.124; and chlorine, 0.024.

Muscovite and biotite were analyzed for the same elements as tourmaline. Mica samples were analysed used an accelerating voltage of 15 keV and 5 nA beam current. Counting time was 10 seconds on standard peaks and a 5 micron beam diameter was used. Precision of analysis was tested through the standard Lemhi Biotite at the beginning of each probing secession. Peak positions (Kfor mica elements are as follows: silicon, 77.542; titanium, 87.721; aluminum, 90.280; iron, 134.875; manganese, 146.397;

magnesium, 107.240, calcium, 107.310; sodium, 129.280; potassium, 119.592; fluorine, 84.834; and chlorine, 151.184. Representative minimum detection limits for mica elements (in oxide wt. %) are as followes: silicon, 0.083; titanium, 0.119; aluminum, 0.086; iron, 0.251; manganese, 0.294; magnesium, 0.057; calcium, 0.094; sodium, 0.137; potassium, 0.139; fluorine, 0.268; and chlorine, 0.124.

APPENDIX E

ELECTRON MICROPROBE ANALYSIS OF TOURMALINE IN VEINS

Label		Vein 1.2	Vein 1.3	Vein 1.4	Vein 1.5
Spot		rim	inter.	inter.	inter.
Texture		euh. f.g.	euh. f.g.	euh. f.g.	euh. f.g.
SiO2		35.270	35.070	34.970	35.080
TiO2		1.210	1.170	1.108	1.182
Al2O3		32.560	32.630	33.010	32.620
FeO		12.220	11.350	11.630	12.030
MnO		0.118	0.127	0.254	0.281
MgO		3.740	3.900	3.920	3.740
CaO		0.526	0.597	0.633	0.620
Na2O		2.240	2.208	2.111	2.156
K2O		0.081	0.103	0.094	0.082
F		0.000	0.000	0.000	0.000
Cl		0.000	0.002	0.003	0.002
Total		87.960	87.150	87.730	87.790
Structural formula based on 31 anions (O, OH, F)					
T:	Si	5.800	5.792	5.756	5.782
	Al	0.200	0.208	0.244	0.218
B		3.000	3.000	3.000	3.000
Z:	Al	6.000	6.000	6.000	6.000
	Mg	0.000	0.000	0.000	0.000
	Cr	0.000	0.000	0.000	0.000
	Fe3+	0.000	0.000	0.000	0.000
Y:	Al	0.110	0.143	0.159	0.118
	Ti	0.150	0.145	0.137	0.147
	V	0.000	0.000	0.000	0.000
	Cr	0.000	0.000	0.000	0.000
	Fe3+	0.000	0.000	0.000	0.000
	Mg	0.917	0.960	0.962	0.919
	Mn	0.016	0.018	0.035	0.039
	Fe2+	1.681	1.568	1.601	1.658
	Zn	0.000	0.000	0.000	0.000
	Li*	0.126	0.166	0.106	0.119
∑Y		3.000	3.000	3.000	3.000
X:	Ca	0.093	0.106	0.112	0.109
	Ba	0.000	0.000	0.000	0.000
	Na	0.714	0.707	0.674	0.689
	K	0.017	0.022	0.020	0.017
	Rb	0.000	0.000	0.000	0.000
	Cs	0.000	0.000	0.000	0.000
	❒	0.176	0.166	0.195	0.184
OH		4.000	4.000	3.999	4.000
F		0.000	0.000	0.000	0.000
Cl		0.000	0.000	0.001	0.000

Label		Vein 1.6	Vein 1.7	Vein 3.1	Vein 3.2
Spot		rim	rim	rim	core
Texture		euh. f.g.	euh. f.g.	euh. f.g.	euh. f.g.
SiO2		35.510	35.300	34.790	35.430
TiO2		1.032	1.206	1.336	1.149
Al2O3		32.740	32.770	32.770	33.030
FeO		11.570	11.830	11.590	11.870
MnO		0.236	0.290	0.118	0.164
MgO		3.850	3.700	3.810	4.040
CaO		0.624	0.549	0.623	0.557
Na2O		2.185	2.054	2.158	2.231
K2O		0.070	0.075	0.092	0.073
F		0.002	0.000	0.000	0.002
Cl		0.008	0.000	0.000	0.000
Total		87.820	87.770	87.290	88.540
Structural formula based on 31 anions (O, OH, F)					
T:	Si	5.824	5.804	5.749	5.779
	Al	0.176	0.196	0.251	0.221
B		3.000	3.000	3.000	3.000
Z:	Al	6.000	6.000	6.000	6.000
	Mg	0.000	0.000	0.000	0.000
	Cr	0.000	0.000	0.000	0.000
	Fe3+	0.000	0.000	0.000	0.000
Y:	Al	0.152	0.155	0.132	0.129
	Ti	0.127	0.149	0.166	0.141
	V	0.000	0.000	0.000	0.000
	Cr	0.000	0.000	0.000	0.000
	Fe3+	0.000	0.000	0.000	0.000
	Mg	0.941	0.907	0.939	0.982
	Mn	0.033	0.040	0.017	0.023
	Fe2+	1.587	1.627	1.602	1.619
	Zn	0.000	0.000	0.000	0.000
	Li*	0.159	0.122	0.145	0.106
∑Y		3.000	3.000	3.000	3.000
X:	Ca	0.110	0.097	0.110	0.097
	Ba	0.000	0.000	0.000	0.000
	Na	0.695	0.655	0.691	0.706
	K	0.015	0.016	0.019	0.015
	Rb	0.000	0.000	0.000	0.000
	Cs	0.000	0.000	0.000	0.000
	❐	0.181	0.233	0.179	0.182
OH		3.997	4.000	4.000	3.999
F		0.001	0.000	0.000	0.001
Cl		0.002	0.000	0.000	0.000

Label	Vein 3.3	Light area T1	Tour. at edge	Tour. at edge
Spot	rim	core	rim	rim
Texture	euh. f.g.	euh. f.g.	euh. f.g.	euh. f.g.
SiO2	32.690	35.450	35.410	30.750
TiO2	1.365	0.689	1.051	0.910
Al2O3	34.010	32.160	31.330	32.230
FeO	10.830	11.720	11.900	11.360
MnO	0.273	0.182	0.165	0.208
MgO	3.450	3.320	3.810	3.540
CaO	0.788	0.358	0.523	0.416
Na2O	1.788	1.896	2.037	1.815
K2O	0.230	0.078	0.063	0.062
F	0.000	0.000	0.000	0.000
Cl	0.025	0.000	0.002	0.011
Total	85.430	85.860	86.300	81.290

Structural formula based on 31 anions (O, OH, F)

T:	Si	5.524	5.933	5.920	5.497
	Al	0.476	0.067	0.080	0.503
B		3.000	3.000	3.000	3.000
Z:	Al	6.000	6.000	6.000	6.000
	Mg	0.000	0.000	0.000	0.000
	Cr	0.000	0.000	0.000	0.000
	Fe3+	0.000	0.000	0.000	0.000
Y:	Al	0.298	0.276	0.093	0.288
	Ti	0.174	0.087	0.132	0.122
	V	0.000	0.000	0.000	0.000
	Cr	0.000	0.000	0.000	0.000
	Fe3+	0.000	0.000	0.000	0.000
	Mg	0.869	0.828	0.950	0.943
	Mn	0.039	0.026	0.023	0.031
	Fe2+	1.531	1.640	1.664	1.698
	Zn	0.000	0.000	0.000	0.000
	Li*	0.090	0.143	0.138	0.000
ΣY		3.000	3.000	3.000	3.084
X:	Ca	0.143	0.064	0.094	0.080
	Ba	0.000	0.000	0.000	0.000
	Na	0.586	0.615	0.660	0.629
	K	0.049	0.017	0.013	0.014
	Rb	0.000	0.000	0.000	0.000
	Cs	0.000	0.000	0.000	0.000
	❐	0.222	0.304	0.232	0.277
OH		3.993	4.000	4.000	3.997
F		0.000	0.000	0.000	0.000
Cl		0.007	0.000	0.000	0.003

Label		Tour. at edge	Tour. at edge	Large tour. in center	Fractured Tur
Spot		rim	rim	core	core
Texture		euh. f.g.	euh. f.g.	euh. f.g.	euh. f.g.
SiO2		34.760	35.450	35.590	35.170
TiO2		1.295	1.228	0.982	1.198
Al2O3		31.620	31.260	31.970	31.310
FeO		12.350	12.300	11.500	11.570
MnO		0.303	0.130	0.174	0.260
MgO		3.540	3.760	3.700	3.400
CaO		0.518	0.617	0.458	0.540
Na2O		2.005	1.981	1.873	2.052
K2O		0.046	0.057	0.073	0.077
F		0.000	0.000	0.000	0.000
Cl		0.011	0.005	0.000	0.011
Total		86.450	86.790	86.310	85.590
Structural formula based on 31 anions (O, OH, F)					
T:	Si	5.832	5.907	5.922	5.913
	Al	0.168	0.093	0.078	0.087
B		3.000	3.000	3.000	3.000
Z:	Al	6.000	6.000	6.000	6.000
	Mg	0.000	0.000	0.000	0.000
	Cr	0.000	0.000	0.000	0.000
	Fe3+	0.000	0.000	0.000	0.000
Y:	Al	0.084	0.046	0.192	0.118
	Ti	0.163	0.154	0.123	0.151
	V	0.000	0.000	0.000	0.000
	Cr	0.000	0.000	0.000	0.000
	Fe3+	0.000	0.000	0.000	0.000
	Mg	0.885	0.934	0.918	0.852
	Mn	0.043	0.018	0.024	0.037
	Fe2+	1.733	1.714	1.600	1.627
	Zn	0.000	0.000	0.000	0.000
	Li*	0.091	0.133	0.143	0.214
ΣY		3.000	3.000	3.000	3.000
X:	Ca	0.093	0.110	0.082	0.097
	Ba	0.000	0.000	0.000	0.000
	Na	0.652	0.640	0.604	0.669
	K	0.010	0.012	0.015	0.017
	Rb	0.000	0.000	0.000	0.000
	Cs	0.000	0.000	0.000	0.000
	❒	0.245	0.238	0.299	0.217
OH		3.997	3.999	4.000	3.997
F		0.000	0.000	0.000	0.000
Cl		0.003	0.001	0.000	0.003

Label	Fractured Tur	Tur in Qtz	Tur in Qtz
Spot	core	rim	core
Texture	euh. f.g.	euh. f.g.	euh. f.g.
SiO2	34.930	35.750	35.920
TiO2	1.157	1.049	0.552
Al2O3	31.670	31.700	32.260
FeO	12.250	12.340	11.290
MnO	0.182	0.243	0.156
MgO	3.870	3.840	3.340
CaO	0.550	0.567	0.313
Na2O	1.878	1.950	1.959
K2O	0.084	0.089	0.079
F	0.000	0.000	0.000
Cl	0.002	0.019	0.000
Total	86.570	87.550	85.870

Structural formula based on 31 anions (O, OH, F)

T:	Si	5.846	5.909	5.982
	Al	0.154	0.091	0.018
B		3.000	3.000	3.000
Z:	Al	6.000	6.000	6.000
	Mg	0.000	0.000	0.000
	Cr	0.000	0.000	0.000
	Fe3+	0.000	0.000	0.000
Y:	Al	0.093	0.085	0.313
	Ti	0.146	0.130	0.069
	V	0.000	0.000	0.000
	Cr	0.000	0.000	0.000
	Fe3+	0.000	0.000	0.000
	Mg	0.966	0.946	0.829
	Mn	0.026	0.034	0.022
	Fe2+	1.715	1.706	1.572
	Zn	0.000	0.000	0.000
	Li*	0.055	0.099	0.194
ΣY		3.000	3.000	3.000
X:	Ca	0.099	0.100	0.056
	Ba	0.000	0.000	0.000
	Na	0.609	0.625	0.633
	K	0.018	0.019	0.017
	Rb	0.000	0.000	0.000
	Cs	0.000	0.000	0.000
	❒	0.274	0.256	0.295
OH		4.000	3.995	4.000
F		0.000	0.000	0.000
Cl		0.000	0.005	0.000

APPENDIX F

ELECTRON MICROPROBE ANALYSIS OF TOURMALINE IN PEGMATITE-APLITES

Label		EQB A1	EQB A2	EQB A3	EQB A4
Spot		rim	rim	rim	inter.
Texture		ehu. c.g.	ehu. c.g.	ehu. c.g.	ehu. c.g.
SiO2		35.240	34.830	34.600	35.610
TiO2		1.253	1.161	1.435	1.085
Al2O3		31.530	31.220	30.610	30.810
FeO		12.980	12.760	12.210	11.780
MnO		0.273	0.218	0.291	0.155
MgO		2.873	2.954	2.941	4.080
CaO		0.501	0.478	0.470	0.636
Na2O		1.779	1.790	1.945	1.745
K2O		0.046	0.070	0.109	0.040
F		0.000	0.055	0.000	0.000
Cl		0.000	0.002	0.006	0.005
Total		86.470	85.510	84.610	85.950
Structural formula based on 31 anions (O, OH, F)					
T:	Si	5.908	5.905	5.913	5.971
	Al	0.092	0.095	0.087	0.029
B		3.000	3.000	3.000	3.000
Z:	Al	6.000	6.000	6.000	6.000
	Mg	0.000	0.000	0.000	0.000
	Cr	0.000	0.000	0.000	0.000
	Fe3+	0.000	0.000	0.000	0.000
Y:	Al	0.137	0.143	0.078	0.060
	Ti	0.158	0.148	0.184	0.137
	V	0.000	0.000	0.000	0.000
	Cr	0.000	0.000	0.000	0.000
	Fe3+	0.000	0.000	0.000	0.000
	Mg	0.718	0.747	0.749	1.020
	Mn	0.039	0.031	0.042	0.022
	Fe2+	1.820	1.809	1.745	1.652
	Zn	0.000	0.000	0.000	0.000
	Li*	0.128	0.122	0.201	0.109
ΣY		3.000	3.000	3.000	3.000
X:	Ca	0.090	0.087	0.086	0.114
	Ba	0.000	0.000	0.000	0.000
	Na	0.578	0.588	0.645	0.567
	K	0.010	0.015	0.024	0.008
	Rb	0.000	0.000	0.000	0.000
	Cs	0.000	0.000	0.000	0.000
	❒	0.322	0.310	0.246	0.310
OH		4.000	3.970	3.998	3.999
F		0.000	0.029	0.000	0.000
Cl		0.000	0.000	0.002	0.001

Label		EQB A5	EQB A6	EQB A7	EQB A8
Spot		core	core	inter.	inter.
Texture		ehu. c.g.	ehu. c.g.	ehu. c.g.	ehu. c.g.
SiO2		35.370	35.280	34.790	34.770
TiO2		1.035	1.194	1.223	1.127
Al2O3		30.440	30.670	31.160	31.880
FeO		11.000	11.960	10.840	11.620
MnO		0.219	0.100	0.146	0.119
MgO		3.920	3.910	3.980	3.840
CaO		0.627	0.561	0.604	0.537
Na2O		1.815	1.936	1.907	1.895
K2O		0.056	0.044	0.060	0.070
F		0.088	0.000	0.000	0.000
Cl		0.000	0.000	0.002	0.003
Total		84.530	85.650	84.710	85.860
Structural formula based on 31 anions (O, OH, F)					
T:	Si	6.002	5.945	5.892	5.839
	Al	0.000	0.055	0.108	0.161
B		3.000	3.000	3.000	3.000
Z:	Al	6.000	6.000	6.000	6.000
	Mg	0.000	0.000	0.000	0.000
	Cr	0.000	0.000	0.000	0.000
	Fe3+	0.000	0.000	0.000	0.000
Y:	Al	0.088	0.037	0.111	0.149
	Ti	0.132	0.151	0.156	0.142
	V	0.000	0.000	0.000	0.000
	Cr	0.000	0.000	0.000	0.000
	Fe3+	0.000	0.000	0.000	0.000
	Mg	0.992	0.982	1.005	0.961
	Mn	0.031	0.014	0.021	0.017
	Fe2+	1.561	1.686	1.535	1.632
	Zn	0.000	0.000	0.000	0.000
	Li*	0.196	0.130	0.172	0.098
ΣY		3.000	3.000	3.000	3.000
X:	Ca	0.114	0.101	0.110	0.097
	Ba	0.000	0.000	0.000	0.000
	Na	0.597	0.633	0.626	0.617
	K	0.012	0.010	0.013	0.015
	Rb	0.000	0.000	0.000	0.000
	Cs	0.000	0.000	0.000	0.000
	❒	0.277	0.257	0.251	0.272
OH		3.953	4.000	4.000	3.999
F		0.047	0.000	0.000	0.000
Cl		0.000	0.000	0.000	0.001

Label		EQB A9	EQB A10	EQB B1	EQB B2
Spot		rim	rim	rim	inter.
Texture		ehu. c.g.	ehu. c.g.	ehu. c.g.	ehu. c.g.
SiO2		34.640	34.590	35.060	34.980
TiO2		1.321	1.223	1.260	1.323
Al2O3		31.000	31.230	30.870	31.330
FeO		12.770	12.190	13.130	12.790
MnO		0.300	0.392	0.237	0.182
MgO		3.030	2.907	3.270	2.840
CaO		0.449	0.578	0.642	0.534
Na2O		1.926	1.978	2.034	1.713
K2O		0.058	0.036	0.087	0.060
F		0.000	0.013	0.085	0.117
Cl		0.000	0.000	0.000	0.000
Total		85.490	85.130	86.640	85.820
Structural formula based on 31 anions (O, OH, F)					
T:	Si	5.883	5.877	5.893	5.905
	Al	0.117	0.123	0.107	0.095
B		3.000	3.000	3.000	3.000
Z:	Al	6.000	6.000	6.000	6.000
	Mg	0.000	0.000	0.000	0.000
	Cr	0.000	0.000	0.000	0.000
	Fe3+	0.000	0.000	0.000	0.000
Y:	Al	0.088	0.130	0.009	0.139
	Ti	0.169	0.156	0.159	0.168
	V	0.000	0.000	0.000	0.000
	Cr	0.000	0.000	0.000	0.000
	Fe3+	0.000	0.000	0.000	0.000
	Mg	0.767	0.736	0.819	0.715
	Mn	0.043	0.056	0.034	0.026
	Fe2+	1.814	1.732	1.846	1.806
	Zn	0.000	0.000	0.000	0.000
	Li*	0.119	0.189	0.133	0.147
ΣY		3.000	3.000	3.000	3.000
X:	Ca	0.082	0.105	0.116	0.097
	Ba	0.000	0.000	0.000	0.000
	Na	0.634	0.651	0.663	0.561
	K	0.012	0.008	0.019	0.013
	Rb	0.000	0.000	0.000	0.000
	Cs	0.000	0.000	0.000	0.000
	❒	0.272	0.236	0.203	0.330
OH		4.000	3.993	3.955	3.937
F		0.000	0.007	0.045	0.063
Cl		0.000	0.000	0.000	0.000

Label		EQB B3	EQB B4	EQB B5	EQB B6
Spot		inter.	inter.	inter.	core
Texture		ehu. c.g.	ehu. c.g.	ehu. c.g.	ehu. c.g.
SiO2		34.890	35.350	35.460	35.610
TiO2		1.191	1.077	0.649	0.581
Al2O3		30.750	31.650	32.040	32.230
FeO		12.180	10.770	10.980	10.710
MnO		0.191	0.173	0.064	0.055
MgO		3.600	4.070	3.440	3.590
CaO		0.552	0.566	0.246	0.324
Na2O		1.985	1.869	1.892	1.785
K2O		0.067	0.044	0.042	0.035
F		0.149	0.004	0.000	0.015
Cl		0.002	0.000	0.009	0.000
Total		85.490	85.570	84.810	84.930
Structural formula based on 31 anions (O, OH, F)					
T:	Si	5.911	5.915	5.969	5.974
	Al	0.089	0.085	0.031	0.026
B		3.000	3.000	3.000	3.000
Z:	Al	6.000	6.000	6.000	6.000
	Mg	0.000	0.000	0.000	0.000
	Cr	0.000	0.000	0.000	0.000
	Fe3+	0.000	0.000	0.000	0.000
Y:	Al	0.052	0.156	0.325	0.347
	Ti	0.152	0.136	0.082	0.073
	V	0.000	0.000	0.000	0.000
	Cr	0.000	0.000	0.000	0.000
	Fe3+	0.000	0.000	0.000	0.000
	Mg	0.909	1.015	0.863	0.898
	Mn	0.027	0.025	0.009	0.008
	Fe2+	1.726	1.507	1.546	1.503
	Zn	0.000	0.000	0.000	0.000
	Li*	0.134	0.161	0.174	0.172
ΣY		3.000	3.000	3.000	3.000
X:	Ca	0.100	0.102	0.044	0.058
	Ba	0.000	0.000	0.000	0.000
	Na	0.652	0.606	0.617	0.581
	K	0.015	0.009	0.009	0.007
	Rb	0.000	0.000	0.000	0.000
	Cs	0.000	0.000	0.000	0.000
	❒	0.233	0.283	0.329	0.354
OH		3.920	3.998	3.997	3.992
F		0.080	0.002	0.000	0.008
Cl		0.000	0.000	0.003	0.000

Label		EQB B7	EQB B8	EQB B9	EQB B10
Spot		core	core	inter.	rim
Texture		ehu. c.g.	ehu. c.g.	ehu. c.g.	ehu. c.g.
SiO2		35.600	35.380	35.830	35.420
TiO2		0.363	0.881	1.029	1.056
Al2O3		32.870	31.680	31.850	31.260
FeO		10.720	10.470	10.750	11.620
MnO		0.119	0.037	0.128	0.164
MgO		3.420	3.910	4.020	3.900
CaO		0.206	0.490	0.483	0.533
Na2O		1.643	2.056	1.878	2.085
K2O		0.037	0.037	0.049	0.037
F		0.000	0.000	0.000	0.000
Cl		0.000	0.000	0.003	0.005
Total		84.980	84.950	86.020	86.080
Structural formula based on 31 anions (O, OH, F)					
T:	Si	5.964	5.940	5.951	5.926
	Al	0.036	0.060	0.049	0.074
B		3.000	3.000	3.000	3.000
Z:	Al	6.000	6.000	6.000	6.000
	Mg	0.000	0.000	0.000	0.000
	Cr	0.000	0.000	0.000	0.000
	Fe3+	0.000	0.000	0.000	0.000
Y:	Al	0.455	0.209	0.185	0.089
	Ti	0.046	0.111	0.128	0.133
	V	0.000	0.000	0.000	0.000
	Cr	0.000	0.000	0.000	0.000
	Fe3+	0.000	0.000	0.000	0.000
	Mg	0.854	0.979	0.995	0.973
	Mn	0.017	0.005	0.018	0.023
	Fe2+	1.502	1.470	1.493	1.626
	Zn	0.000	0.000	0.000	0.000
	Li*	0.126	0.226	0.180	0.156
ΣY		3.000	3.000	3.000	3.000
X:	Ca	0.037	0.088	0.086	0.095
	Ba	0.000	0.000	0.000	0.000
	Na	0.534	0.669	0.605	0.676
	K	0.008	0.008	0.010	0.008
	Rb	0.000	0.000	0.000	0.000
	Cs	0.000	0.000	0.000	0.000
	❒	0.421	0.235	0.299	0.220
OH		4.000	4.000	3.999	3.999
F		0.000	0.000	0.000	0.000
Cl		0.000	0.000	0.001	0.001

Label		EQB B11	EQA A1	EQA A2	EQA A3
Spot		rim	rim	rim	inter.
Texture		ehu. c.g.	skel. c.g.	skel. c.g.	skel. c.g.
SiO2		34.740	35.200	35.400	35.310
TiO2		1.285	1.090	1.293	1.146
Al2O3		30.760	31.830	31.220	31.090
FeO		12.540	12.330	11.760	11.520
MnO		0.328	0.109	0.091	0.110
MgO		2.930	3.810	3.280	3.760
CaO		0.514	0.545	0.477	0.508
Na2O		2.078	1.942	1.812	1.880
K2O		0.046	0.034	0.026	0.035
F		0.100	0.000	0.000	0.000
Cl		0.000	0.000	0.000	0.008
Total		85.290	86.890	85.370	85.360
Structural formula based on 31 anions (O, OH, F)					
T:	Si	5.907	5.862	5.956	5.946
	Al	0.093	0.138	0.044	0.054
B		3.000	3.000	3.000	3.000
Z:	Al	6.000	6.000	6.000	6.000
	Mg	0.000	0.000	0.000	0.000
	Cr	0.000	0.000	0.000	0.000
	Fe3+	0.000	0.000	0.000	0.000
Y:	Al	0.072	0.110	0.147	0.116
	Ti	0.164	0.136	0.164	0.145
	V	0.000	0.000	0.000	0.000
	Cr	0.000	0.000	0.000	0.000
	Fe3+	0.000	0.000	0.000	0.000
	Mg	0.743	0.946	0.823	0.944
	Mn	0.047	0.015	0.013	0.016
	Fe2+	1.783	1.717	1.655	1.622
	Zn	0.000	0.000	0.000	0.000
	Li*	0.190	0.075	0.199	0.157
ΣY		3.000	3.000	3.000	3.000
X:	Ca	0.094	0.097	0.086	0.092
	Ba	0.000	0.000	0.000	0.000
	Na	0.685	0.627	0.591	0.614
	K	0.010	0.007	0.006	0.007
	Rb	0.000	0.000	0.000	0.000
	Cs	0.000	0.000	0.000	0.000
	❒	0.211	0.268	0.317	0.287
OH		3.946	4.000	4.000	3.998
F		0.054	0.000	0.000	0.000
Cl		0.000	0.000	0.000	0.002

Label		EQA A4	EQA A5	EQA A6	EQA A7
Spot		core	core	core	inter.
Texture		skel. c.g.	skel. c.g.	skel. c.g.	skel. c.g.
SiO2		35.130	34.780	34.800	35.170
TiO2		0.449	1.222	1.107	0.993
Al2O3		32.280	31.060	31.650	31.730
FeO		11.390	11.700	11.690	11.630
MnO		0.164	0.137	0.182	0.155
MgO		3.030	3.570	3.540	3.680
CaO		0.243	0.532	0.513	0.540
Na2O		1.670	1.788	1.986	1.771
K2O		0.060	0.053	0.037	0.058
F		0.000	0.000	0.000	0.000
Cl		0.000	0.000	0.000	0.000
Total		84.410	84.850	85.500	85.720
Structural formula based on 31 anions (O, OH, F)					
T:	Si	5.957	5.907	5.866	5.904
	Al	0.043	0.093	0.134	0.096
B		3.000	3.000	3.000	3.000
Z:	Al	6.000	6.000	6.000	6.000
	Mg	0.000	0.000	0.000	0.000
	Cr	0.000	0.000	0.000	0.000
	Fe3+	0.000	0.000	0.000	0.000
Y:	Al	0.408	0.123	0.154	0.181
	Ti	0.057	0.156	0.140	0.125
	V	0.000	0.000	0.000	0.000
	Cr	0.000	0.000	0.000	0.000
	Fe3+	0.000	0.000	0.000	0.000
	Mg	0.766	0.904	0.890	0.921
	Mn	0.024	0.020	0.026	0.022
	Fe2+	1.615	1.662	1.648	1.633
	Zn	0.000	0.000	0.000	0.000
	Li*	0.130	0.136	0.143	0.118
ΣY		3.000	3.000	3.000	3.000
X:	Ca	0.044	0.097	0.093	0.097
	Ba	0.000	0.000	0.000	0.000
	Na	0.549	0.589	0.649	0.577
	K	0.013	0.011	0.008	0.012
	Rb	0.000	0.000	0.000	0.000
	Cs	0.000	0.000	0.000	0.000
	❒	0.394	0.303	0.250	0.314
OH		4.000	4.000	4.000	4.000
F		0.000	0.000	0.000	0.000
Cl		0.000	0.000	0.000	0.000

Label		EQA A8	TH 1.1	TH 1.2	TH 1.3
Spot		rim	rim	rim	inter.
Texture		skel. c.g.	euh. c.g.	euh. c.g.	euh. c.g.
SiO2		35.180	34.960	35.150	35.120
TiO2		1.287	1.233	1.119	0.938
Al2O3		31.330	33.990	35.430	35.250
FeO		11.610	11.920	11.130	11.420
MnO		0.173	0.136	0.173	0.082
MgO		3.250	3.990	4.460	4.330
CaO		0.556	0.485	0.636	1.050
Na2O		1.825	2.176	2.049	2.118
K2O		0.038	0.052	0.041	0.047
F		0.000	0.000	0.000	0.000
Cl		0.002	0.000	0.000	0.015
Total		85.260	88.940	90.190	90.370
Structural formula based on 31 anions (O, OH, F)					
T:	Si	5.928	5.684	5.611	5.605
	Al	0.072	0.316	0.389	0.395
B		3.000	3.000	3.000	3.000
Z:	Al	6.000	6.000	6.000	6.000
	Mg	0.000	0.000	0.000	0.000
	Cr	0.000	0.000	0.000	0.000
	Fe3+	0.000	0.000	0.000	0.000
Y:	Al	0.150	0.196	0.277	0.234
	Ti	0.163	0.151	0.134	0.113
	V	0.000	0.000	0.000	0.000
	Cr	0.000	0.000	0.000	0.000
	Fe3+	0.000	0.000	0.000	0.000
	Mg	0.816	0.967	1.061	1.030
	Mn	0.025	0.019	0.023	0.011
	Fe2+	1.636	1.621	1.486	1.524
	Zn	0.000	0.000	0.000	0.000
	Li*	0.210	0.047	0.018	0.088
ΣY		3.000	3.000	3.000	3.000
X:	Ca	0.100	0.084	0.109	0.179
	Ba	0.000	0.000	0.000	0.000
	Na	0.596	0.686	0.634	0.655
	K	0.008	0.011	0.008	0.010
	Rb	0.000	0.000	0.000	0.000
	Cs	0.000	0.000	0.000	0.000
	❒	0.295	0.219	0.249	0.156
OH		4.000	4.000	4.000	3.996
F		0.000	0.000	0.000	0.000
Cl		0.000	0.000	0.000	0.004

Label		TH 1.4	TH 1.5	TH 1.6	TH 1.7
Spot		inter.	core	core	core
Texture		euh. c.g.	euh. c.g.	euh. c.g.	euh. c.g.
SiO2		35.850	35.740	35.670	36.000
TiO2		0.358	0.335	0.317	0.360
Al2O3		37.140	36.850	37.410	37.470
FeO		11.380	10.970	10.970	11.070
MnO		0.173	0.146	0.200	0.209
MgO		3.700	3.710	3.750	3.930
CaO		0.243	0.263	0.236	0.230
Na2O		2.038	2.133	1.920	1.901
K2O		0.030	0.043	0.046	0.036
F		0.000	0.000	0.000	0.000
Cl		0.009	0.000	0.000	0.000
Total		90.930	90.190	90.520	91.220
Structural formula based on 31 anions (O, OH, F)					
T:	Si	5.654	5.667	5.637	5.647
	Al	0.346	0.333	0.363	0.353
B		3.000	3.000	3.000	3.000
Z:	Al	6.000	6.000	6.000	6.000
	Mg	0.000	0.000	0.000	0.000
	Cr	0.000	0.000	0.000	0.000
	Fe3+	0.000	0.000	0.000	0.000
Y:	Al	0.557	0.554	0.605	0.574
	Ti	0.042	0.040	0.038	0.042
	V	0.000	0.000	0.000	0.000
	Cr	0.000	0.000	0.000	0.000
	Fe3+	0.000	0.000	0.000	0.000
	Mg	0.870	0.877	0.883	0.919
	Mn	0.023	0.020	0.027	0.028
	Fe2+	1.501	1.455	1.450	1.452
	Zn	0.000	0.000	0.000	0.000
	Li*	0.007	0.055	0.000	0.000
ΣY		3.000	3.000	3.003	3.016
X:	Ca	0.041	0.045	0.040	0.039
	Ba	0.000	0.000	0.000	0.000
	Na	0.623	0.656	0.588	0.578
	K	0.006	0.009	0.009	0.007
	Rb	0.000	0.000	0.000	0.000
	Cs	0.000	0.000	0.000	0.000
	❒	0.330	0.291	0.362	0.376
OH		3.998	4.000	4.000	4.000
F		0.000	0.000	0.000	0.000
Cl		0.002	0.000	0.000	0.000

Label		TH 1.8	TH 1.9	TH 1.10	TH 1.11
Spot		inter.	inter.	rim	rim
Texture		euh. c.g.	euh. c.g.	euh. c.g.	euh. c.g.
SiO2		35.720	35.730	35.240	35.380
TiO2		0.972	1.062	1.095	1.211
Al2O3		36.000	36.220	36.060	35.550
FeO		11.060	10.820	10.750	12.310
MnO		0.182	0.027	0.073	0.164
MgO		4.410	4.370	4.370	3.880
CaO		0.444	0.502	0.590	0.492
Na2O		2.090	2.392	2.170	2.329
K2O		0.056	0.063	0.033	0.076
F		0.000	0.000	0.000	0.000
Cl		0.000	0.002	0.000	0.006
Total		90.940	91.190	90.370	91.400
Structural formula based on 31 anions (O, OH, F)					
T:	Si	5.642	5.615	5.592	5.607
	Al	0.358	0.385	0.408	0.393
B		3.000	3.000	3.000	3.000
Z:	Al	6.000	6.000	6.000	6.000
	Mg	0.000	0.000	0.000	0.000
	Cr	0.000	0.000	0.000	0.000
	Fe3+	0.000	0.000	0.000	0.000
Y:	Al	0.343	0.324	0.336	0.246
	Ti	0.115	0.126	0.131	0.144
	V	0.000	0.000	0.000	0.000
	Cr	0.000	0.000	0.000	0.000
	Fe3+	0.000	0.000	0.000	0.000
	Mg	1.038	1.024	1.034	0.917
	Mn	0.024	0.004	0.010	0.022
	Fe2+	1.461	1.422	1.427	1.631
	Zn	0.000	0.000	0.000	0.000
	Li*	0.018	0.101	0.064	0.039
ΣY		3.000	3.000	3.000	3.000
X:	Ca	0.075	0.084	0.100	0.083
	Ba	0.000	0.000	0.000	0.000
	Na	0.640	0.729	0.668	0.716
	K	0.011	0.013	0.007	0.015
	Rb	0.000	0.000	0.000	0.000
	Cs	0.000	0.000	0.000	0.000
	❒	0.274	0.174	0.226	0.186
OH		4.000	4.000	4.000	3.998
F		0.000	0.000	0.000	0.000
Cl		0.000	0.000	0.000	0.002

Label		TH fracture	TH 2.1	TH 2.2	TH 2.3
Spot		core	core	core	core
Texture		euh. c.g.	euh. c.g.	euh. c.g.	euh. c.g.
SiO2		34.750	35.760	35.860	35.780
TiO2		0.737	0.282	0.327	0.317
Al2O3		33.810	37.730	37.320	37.780
FeO		12.820	11.140	10.880	10.850
MnO		0.091	0.055	0.146	0.218
MgO		4.420	3.800	3.730	3.700
CaO		1.133	0.221	0.202	0.188
Na2O		2.095	2.030	1.905	1.866
K2O		0.031	0.060	0.073	0.045
F		0.381	0.000	0.000	0.000
Cl		0.000	0.000	0.000	0.000
Total		90.110	91.080	90.440	90.750
Structural formula based on 31 anions (O, OH, F)					
T:	Si	5.637	5.619	5.663	5.632
	Al	0.363	0.381	0.337	0.368
B		3.000	3.000	3.000	3.000
Z:	Al	6.000	6.000	6.000	6.000
	Mg	0.000	0.000	0.000	0.000
	Cr	0.000	0.000	0.000	0.000
	Fe3+	0.000	0.000	0.000	0.000
Y:	Al	0.101	0.607	0.610	0.641
	Ti	0.090	0.033	0.039	0.038
	V	0.000	0.000	0.000	0.000
	Cr	0.000	0.000	0.000	0.000
	Fe3+	0.000	0.000	0.000	0.000
	Mg	1.069	0.890	0.878	0.868
	Mn	0.012	0.007	0.019	0.029
	Fe2+	1.739	1.464	1.437	1.428
	Zn	0.000	0.000	0.000	0.000
	Li*	0.000	0.000	0.017	0.000
ΣY		3.012	3.001	3.000	3.005
X:	Ca	0.197	0.037	0.034	0.032
	Ba	0.000	0.000	0.000	0.000
	Na	0.659	0.618	0.583	0.569
	K	0.006	0.012	0.015	0.009
	Rb	0.000	0.000	0.000	0.000
	Cs	0.000	0.000	0.000	0.000
	❒	0.138	0.333	0.368	0.390
OH		3.805	4.000	4.000	4.000
F		0.195	0.000	0.000	0.000
Cl		0.000	0.000	0.000	0.000

Label		TH 2.4	TH 2.5	TH 2.6	TH 2.7
Spot		core	core	core	core
Texture		euh. c.g.	euh. c.g.	euh. c.g.	euh. c.g.
SiO2		35.910	35.570	35.570	36.050
TiO2		0.259	0.385	0.386	0.345
Al2O3		37.670	37.390	37.490	36.940
FeO		11.320	11.620	10.990	11.180
MnO		0.146	0.127	0.109	0.164
MgO		3.660	3.780	3.830	3.880
CaO		0.232	0.240	0.226	0.238
Na2O		1.837	1.995	2.066	2.028
K2O		0.044	0.011	0.030	0.067
F		0.000	0.000	0.000	0.000
Cl		0.012	0.006	0.000	0.000
Total		91.090	91.140	90.700	90.890
Structural formula based on 31 anions (O, OH, F)					
T:	Si	5.643	5.605	5.613	5.680
	Al	0.357	0.395	0.387	0.320
B		3.000	3.000	3.000	3.000
Z:	Al	6.000	6.000	6.000	6.000
	Mg	0.000	0.000	0.000	0.000
	Cr	0.000	0.000	0.000	0.000
	Fe3+	0.000	0.000	0.000	0.000
Y:	Al	0.620	0.549	0.585	0.539
	Ti	0.031	0.046	0.046	0.041
	V	0.000	0.000	0.000	0.000
	Cr	0.000	0.000	0.000	0.000
	Fe3+	0.000	0.000	0.000	0.000
	Mg	0.857	0.888	0.901	0.911
	Mn	0.019	0.017	0.015	0.022
	Fe2+	1.488	1.531	1.450	1.473
	Zn	0.000	0.000	0.000	0.000
	Li*	0.000	0.000	0.004	0.014
ΣY		3.015	3.031	3.000	3.000
X:	Ca	0.039	0.041	0.038	0.040
	Ba	0.000	0.000	0.000	0.000
	Na	0.560	0.609	0.632	0.620
	K	0.009	0.002	0.006	0.013
	Rb	0.000	0.000	0.000	0.000
	Cs	0.000	0.000	0.000	0.000
	❒	0.393	0.348	0.323	0.327
OH		3.997	3.998	4.000	4.000
F		0.000	0.000	0.000	0.000
Cl		0.003	0.002	0.000	0.000

Label		TH 2.8	TH 2.9	TH 2.10	TH 2.11
Spot		core	core	core	core
Texture		euh. c.g.	euh. c.g.	euh. c.g.	euh. c.g.
SiO2		35.700	35.810	35.910	35.770
TiO2		0.596	0.315	0.297	0.377
Al2O3		37.040	37.720	37.770	37.470
FeO		10.850	11.140	11.220	10.820
MnO		0.000	0.109	0.055	0.136
MgO		3.990	3.970	3.920	3.780
CaO		0.380	0.233	0.224	0.231
Na2O		1.984	1.868	1.953	1.943
K2O		0.053	0.046	0.051	0.056
F		0.000	0.000	0.000	0.000
Cl		0.000	0.009	0.000	0.011
Total		90.600	91.220	91.400	90.590
Structural formula based on 31 anions (O, OH, F)					
T:	Si	5.632	5.620	5.622	5.641
	Al	0.368	0.380	0.378	0.359
B		3.000	3.000	3.000	3.000
Z:	Al	6.000	6.000	6.000	6.000
	Mg	0.000	0.000	0.000	0.000
	Cr	0.000	0.000	0.000	0.000
	Fe3+	0.000	0.000	0.000	0.000
Y:	Al	0.520	0.598	0.592	0.604
	Ti	0.071	0.037	0.035	0.045
	V	0.000	0.000	0.000	0.000
	Cr	0.000	0.000	0.000	0.000
	Fe3+	0.000	0.000	0.000	0.000
	Mg	0.938	0.929	0.915	0.889
	Mn	0.000	0.000	0.007	0.018
	Fe2+	1.432	1.462	1.469	1.427
	Zn	0.000	0.000	0.000	0.000
	Li*	0.040	0.000	0.000	0.017
ΣY		3.000	3.026	3.019	3.000
X:	Ca	0.064	0.039	0.038	0.039
	Ba	0.000	0.000	0.000	0.000
	Na	0.607	0.568	0.593	0.594
	K	0.011	0.009	0.010	0.011
	Rb	0.000	0.000	0.000	0.000
	Cs	0.000	0.000	0.000	0.000
	❒	0.318	0.383	0.359	0.356
OH		4.000	3.998	4.000	3.997
F		0.000	0.000	0.000	0.000
Cl		0.000	0.002	0.000	0.003

Label		TH 2.12	TH 2.13	EQB 2	EQB 3
Spot		core	core	rim	rim
Texture		euh. c.g.	euh. c.g.	euh. c.g.	euh. c.g.
SiO2		35.850	35.360	34.840	34.730
TiO2		0.390	0.392	0.563	1.215
Al2O3		36.850	37.380	32.600	31.940
FeO		11.110	11.220	11.820	12.320
MnO		0.109	0.000	0.201	0.315
MgO		3.900	3.810	3.390	2.785
CaO		0.390	0.263	0.354	0.387
Na2O		1.970	1.908	1.861	1.861
K2O		0.030	0.046	0.044	0.060
F		0.000	0.000	0.000	0.000
Cl		0.000	0.000	0.000	0.005
Total		90.610	90.380	85.680	85.610
Structural formula based on 31 anions (O, OH, F)					
T:	Si	5.665	5.603	5.859	5.861
	Al	0.335	0.397	0.141	0.139
B		3.000	3.000	3.000	3.000
Z:	Al	6.000	6.000	6.000	6.000
	Mg	0.000	0.000	0.000	0.000
	Cr	0.000	0.000	0.000	0.000
	Fe3+	0.000	0.000	0.000	0.000
Y:	Al	0.527	0.584	0.321	0.215
	Ti	0.046	0.047	0.071	0.154
	V	0.000	0.000	0.000	0.000
	Cr	0.000	0.000	0.000	0.000
	Fe3+	0.000	0.000	0.000	0.000
	Mg	0.919	0.900	0.850	0.701
	Mn	0.015	0.000	0.029	0.045
	Fe2+	1.468	1.487	1.662	1.739
	Zn	0.000	0.000	0.000	0.000
	Li*	0.026	0.000	0.067	0.147
ΣY		3.000	3.018	3.000	3.000
X:	Ca	0.066	0.045	0.064	0.070
	Ba	0.000	0.000	0.000	0.000
	Na	0.604	0.586	0.607	0.609
	K	0.006	0.009	0.009	0.013
	Rb	0.000	0.000	0.000	0.000
	Cs	0.000	0.000	0.000	0.000
	❒	0.324	0.360	0.320	0.308
OH		4.000	4.000	4.000	3.999
F		0.000	0.000	0.000	0.000
Cl		0.000	0.000	0.000	0.001

Label		EQB 4	EQB 6	EQB 7	EQB 8
Spot		core	rim	inter.	rim
Texture		euh. c.g.	euh. c.g.	euh. c.g.	euh. c.g.
SiO2		35.530	35.110	34.780	34.530
TiO2		0.739	1.291	0.704	1.237
Al2O3		33.090	31.680	32.950	32.350
FeO		10.470	12.270	10.220	13.130
MnO		0.123	0.280	0.176	0.271
MgO		3.960	3.210	4.080	2.975
CaO		0.466	0.525	0.674	0.449
Na2O		1.932	2.032	1.916	2.092
K2O		0.064	0.059	0.045	0.047
F		0.000	0.000	0.000	0.000
Cl		0.000	0.000	0.000	0.000
Total		86.370	86.460	85.540	87.080
Structural formula based on 31 anions (O, OH, F)					
T:	Si	5.869	5.871	5.808	5.773
	Al	0.131	0.129	0.192	0.227
B		3.000	3.000	3.000	3.000
Z:	Al	6.000	6.000	6.000	6.000
	Mg	0.000	0.000	0.000	0.000
	Cr	0.000	0.000	0.000	0.000
	Fe3+	0.000	0.000	0.000	0.000
Y:	Al	0.310	0.114	0.294	0.148
	Ti	0.092	0.162	0.088	0.155
	V	0.000	0.000	0.000	0.000
	Cr	0.000	0.000	0.000	0.000
	Fe3+	0.000	0.000	0.000	0.000
	Mg	0.975	0.800	1.016	0.741
	Mn	0.017	0.040	0.025	0.038
	Fe2+	1.446	1.716	1.427	1.836
	Zn	0.000	0.000	0.000	0.000
	Li*	0.159	0.168	0.150	0.081
ΣY		3.000	3.000	3.000	3.000
X:	Ca	0.082	0.094	0.121	0.080
	Ba	0.000	0.000	0.000	0.000
	Na	0.619	0.659	0.620	0.678
	K	0.014	0.013	0.010	0.010
	Rb	0.000	0.000	0.000	0.000
	Cs	0.000	0.000	0.000	0.000
	❒	0.285	0.235	0.249	0.231
OH		4.000	4.000	4.000	4.000
F		0.000	0.000	0.000	0.000
Cl		0.000	0.000	0.000	0.000

Label		EQB 9	EQB 10	EQB 11	EQB 12
Spot		core	core	core	inter.
Texture		euh. c.g.	euh. c.g.	euh. c.g.	euh. c.g.
SiO2		34.840	35.730	35.460	35.010
TiO2		0.430	0.410	0.418	0.929
Al2O3		32.720	32.390	32.720	33.020
FeO		11.270	11.170	11.210	11.520
MnO		0.132	0.061	0.158	0.123
MgO		4.140	4.180	4.220	4.140
CaO		0.558	0.504	0.477	0.516
Na2O		2.048	2.055	1.986	2.102
K2O		0.061	0.045	0.060	0.061
F		0.000	0.000	0.000	0.000
Cl		0.000	0.005	0.000	0.000
Total		86.200	86.560	86.720	87.430
Structural formula based on 31 anions (O, OH, F)					
T:	Si	5.819	5.920	5.876	5.775
	Al	0.181	0.080	0.124	0.225
B		3.000	3.000	3.000	3.000
Z:	Al	6.000	6.000	6.000	6.000
	Mg	0.000	0.000	0.000	0.000
	Cr	0.000	0.000	0.000	0.000
	Fe3+	0.000	0.000	0.000	0.000
Y:	Al	0.260	0.245	0.265	0.194
	Ti	0.054	0.051	0.052	0.115
	V	0.000	0.000	0.000	0.000
	Cr	0.000	0.000	0.000	0.000
	Fe3+	0.000	0.000	0.000	0.000
	Mg	1.031	1.032	1.042	1.018
	Mn	0.019	0.009	0.022	0.017
	Fe2+	1.574	1.548	1.553	1.589
	Zn	0.000	0.000	0.000	0.000
	Li*	0.063	0.115	0.065	0.066
ΣY		3.000	3.000	3.000	3.000
X:	Ca	0.100	0.089	0.085	0.091
	Ba	0.000	0.000	0.000	0.000
	Na	0.663	0.660	0.638	0.672
	K	0.013	0.009	0.013	0.013
	Rb	0.000	0.000	0.000	0.000
	Cs	0.000	0.000	0.000	0.000
	❒	0.224	0.241	0.265	0.224
OH		4.000	3.999	4.000	4.000
F		0.000	0.000	0.000	0.000
Cl		0.000	0.001	0.000	0.000

Label		EQB 13	EQB 14	EQB 15	EQB 16
Spot		inter.	core	core	core
Texture		euh. c.g.	euh. c.g.	euh. c.g.	euh. c.g.
SiO2		34.630	35.020	35.460	35.360
TiO2		1.163	0.517	0.419	0.549
Al2O3		31.830	32.600	32.630	31.940
FeO		12.540	11.590	11.100	11.910
MnO		0.184	0.096	0.061	0.166
MgO		2.805	4.060	4.110	3.920
CaO		0.394	0.561	0.504	0.557
Na2O		2.012	1.960	2.186	2.091
K2O		0.063	0.044	0.029	0.034
F		0.000	0.000	0.000	0.000
Cl		0.000	0.000	0.000	0.000
Total		85.620	86.460	86.500	86.520
Structural formula based on 31 anions (O, OH, F)					
T:	Si	5.852	5.838	5.880	5.898
	Al	0.148	0.162	0.120	0.102
B		3.000	3.000	3.000	3.000
Z:	Al	6.000	6.000	6.000	6.000
	Mg	0.000	0.000	0.000	0.000
	Cr	0.000	0.000	0.000	0.000
	Fe3+	0.000	0.000	0.000	0.000
Y:	Al	0.192	0.243	0.256	0.177
	Ti	0.148	0.065	0.052	0.069
	V	0.000	0.000	0.000	0.000
	Cr	0.000	0.000	0.000	0.000
	Fe3+	0.000	0.000	0.000	0.000
	Mg	0.707	1.009	1.016	0.975
	Mn	0.026	0.014	0.009	0.024
	Fe2+	1.772	1.616	1.539	1.661
	Zn	0.000	0.000	0.000	0.000
	Li*	0.155	0.054	0.128	0.095
ΣY		3.000	3.000	3.000	3.000
X:	Ca	0.071	0.100	0.089	0.100
	Ba	0.000	0.000	0.000	0.000
	Na	0.659	0.634	0.703	0.676
	K	0.014	0.009	0.006	0.007
	Rb	0.000	0.000	0.000	0.000
	Cs	0.000	0.000	0.000	0.000
	❒	0.256	0.257	0.202	0.217
OH		4.000	4.000	4.000	4.000
F		0.000	0.000	0.000	0.000
Cl		0.000	0.000	0.000	0.000

Label		EQB 17	EQB 18	EQB 19	EQB 20
Spot		rim	core	core	rim
Texture		euh. c.g.	euh. c.g.	euh. c.g.	euh. c.g.
SiO2		34.560	35.810	35.920	35.590
TiO2		1.343	0.191	0.243	1.106
Al2O3		32.090	34.410	33.940	32.350
FeO		12.690	11.560	10.800	11.170
MnO		0.210	0.149	0.175	0.184
MgO		2.742	3.410	3.440	3.760
CaO		0.463	0.252	0.207	0.513
Na2O		2.073	1.848	1.665	2.007
K2O		0.045	0.038	0.021	0.065
F		0.000	0.000	0.000	0.000
Cl		0.009	0.014	0.005	0.000
Total		86.220	87.690	86.420	86.740
Structural formula based on 31 anions (O, OH, F)					
T:	Si	5.808	5.853	5.919	5.883
	Al	0.192	0.147	0.081	0.117
B		3.000	3.000	3.000	3.000
Z:	Al	6.000	6.000	6.000	6.000
	Mg	0.000	0.000	0.000	0.000
	Cr	0.000	0.000	0.000	0.000
	Fe3+	0.000	0.000	0.000	0.000
Y:	Al	0.165	0.481	0.511	0.185
	Ti	0.170	0.024	0.030	0.137
	V	0.000	0.000	0.000	0.000
	Cr	0.000	0.000	0.000	0.000
	Fe3+	0.000	0.000	0.000	0.000
	Mg	0.687	0.831	0.845	0.927
	Mn	0.030	0.021	0.024	0.026
	Fe2+	1.784	1.580	1.488	1.544
	Zn	0.000	0.000	0.000	0.000
	Li*	0.165	0.063	0.100	0.181
ΣY		3.000	3.000	3.000	3.000
X:	Ca	0.083	0.044	0.036	0.091
	Ba	0.000	0.000	0.000	0.000
	Na	0.676	0.586	0.532	0.643
	K	0.010	0.008	0.004	0.014
	Rb	0.000	0.000	0.000	0.000
	Cs	0.000	0.000	0.000	0.000
	❒	0.231	0.362	0.427	0.252
OH		3.997	3.996	3.999	4.000
F		0.000	0.000	0.000	0.000
Cl		0.003	0.004	0.001	0.000

Label		EQA 21	EQA 22	EQA 23	EQA 24
Spot		core	inter.	rim	rim
Texture		skel C. to f.g.	skel C. to f.g.	skel C. to f.g.	skel C. to f.g.
SiO2		35.790	34.610	35.160	35.470
TiO2		0.348	1.153	1.109	0.969
Al2O3		33.660	32.030	32.480	32.290
FeO		11.810	11.730	11.280	12.270
MnO		0.237	0.228	0.123	0.254
MgO		2.880	3.570	3.790	3.200
CaO		0.230	0.512	0.538	0.440
Na2O		1.780	2.014	2.102	1.870
K2O		0.012	0.073	0.047	0.046
F		0.000	0.000	0.000	0.000
Cl		0.000	0.002	0.006	0.014
Total		86.760	85.920	86.630	86.820
Structural formula based on 31 anions (O, OH, F)					
T:	Si	5.912	5.815	5.831	5.895
	Al	0.088	0.185	0.169	0.105
B		3.000	3.000	3.000	3.000
Z:	Al	6.000	6.000	6.000	6.000
	Mg	0.000	0.000	0.000	0.000
	Cr	0.000	0.000	0.000	0.000
	Fe3+	0.000	0.000	0.000	0.000
Y:	Al	0.465	0.158	0.179	0.220
	Ti	0.043	0.146	0.138	0.121
	V	0.000	0.000	0.000	0.000
	Cr	0.000	0.000	0.000	0.000
	Fe3+	0.000	0.000	0.000	0.000
	Mg	0.709	0.894	0.937	0.793
	Mn	0.033	0.032	0.017	0.036
	Fe2+	1.631	1.648	1.564	1.705
	Zn	0.000	0.000	0.000	0.000
	Li*	0.118	0.121	0.164	0.125
∑Y		3.000	3.000	3.000	3.000
X:	Ca	0.041	0.092	0.096	0.078
	Ba	0.000	0.000	0.000	0.000
	Na	0.570	0.656	0.676	0.602
	K	0.003	0.016	0.010	0.010
	Rb	0.000	0.000	0.000	0.000
	Cs	0.000	0.000	0.000	0.000
	❒	0.387	0.236	0.219	0.310
OH		4.000	4.000	3.998	3.996
F		0.000	0.000	0.000	0.000
Cl		0.000	0.000	0.002	0.004

Label		EQA 25	EQA 26	EQA 27	EQA 28
Spot		inter. skel C. to	core skel C. to	inter. skel C. to	rim skel C. to
Texture		f.g.	f.g.	f.g.	f.g.
SiO2		35.270	36.220	35.070	35.170
TiO2		1.123	0.447	1.285	0.916
Al2O3		32.700	33.440	32.050	32.390
FeO		11.640	11.330	11.920	11.770
MnO		0.202	0.228	0.149	0.158
MgO		3.530	3.040	3.550	3.760
CaO		0.517	0.209	0.542	0.524
Na2O		1.986	1.871	2.120	1.944
K2O		0.051	0.038	0.064	0.042
F		0.000	0.000	0.000	0.000
Cl		0.000	0.011	0.000	0.009
Total		87.020	86.830	86.760	86.680
Structural formula based on 31 anions (O, OH, F)					
T:	Si	5.832	5.955	5.834	5.849
	Al	0.168	0.045	0.166	0.151
B		3.000	3.000	3.000	3.000
Z:	Al	6.000	6.000	6.000	6.000
	Mg	0.000	0.000	0.000	0.000
	Cr	0.000	0.000	0.000	0.000
	Fe3+	0.000	0.000	0.000	0.000
Y:	Al	0.205	0.434	0.117	0.197
	Ti	0.140	0.055	0.161	0.115
	V	0.000	0.000	0.000	0.000
	Cr	0.000	0.000	0.000	0.000
	Fe3+	0.000	0.000	0.000	0.000
	Mg	0.870	0.745	0.880	0.932
	Mn	0.028	0.032	0.021	0.022
	Fe2+	1.610	1.558	1.658	1.637
	Zn	0.000	0.000	0.000	0.000
	Li*	0.147	0.177	0.163	0.097
∑Y		3.000	3.000	3.000	3.000
X:	Ca	0.092	0.037	0.097	0.093
	Ba	0.000	0.000	0.000	0.000
	Na	0.637	0.597	0.684	0.627
	K	0.011	0.008	0.014	0.009
	Rb	0.000	0.000	0.000	0.000
	Cs	0.000	0.000	0.000	0.000
	❒	0.261	0.359	0.206	0.271
OH		4.000	3.997	4.000	3.997
F		0.000	0.000	0.000	0.000
Cl		0.000	0.003	0.000	0.003

Label		EQA 29	EQA 30	EQA 31	EQA 32
Spot		inter. skel C. to f.g.	core skel C. to f.g.	core skel C. to f.g.	inter. skel C. to f.g.
Texture					
SiO2		35.450	35.830	35.070	35.270
TiO2		1.077	0.444	0.403	1.339
Al2O3		31.540	32.700	32.850	32.410
FeO		12.180	11.960	11.290	11.790
MnO		0.368	0.210	0.149	0.175
MgO		3.840	3.780	3.820	3.610
CaO		0.616	0.447	0.403	0.452
Na2O		2.034	2.163	2.140	1.871
K2O		0.058	0.047	0.027	0.065
F		0.000	0.000	0.000	0.000
Cl		0.000	0.000	0.000	0.000
Total		87.170	87.580	86.150	86.990
Structural formula based on 31 anions (O, OH, F)					
T:	Si	5.889	5.897	5.849	5.841
	Al	0.111	0.103	0.151	0.159
B		3.000	3.000	3.000	3.000
Z:	Al	6.000	6.000	6.000	6.000
	Mg	0.000	0.000	0.000	0.000
	Cr	0.000	0.000	0.000	0.000
	Fe3+	0.000	0.000	0.000	0.000
Y:	Al	0.063	0.239	0.306	0.167
	Ti	0.134	0.055	0.051	0.167
	V	0.000	0.000	0.000	0.000
	Cr	0.000	0.000	0.000	0.000
	Fe3+	0.000	0.000	0.000	0.000
	Mg	0.951	0.927	0.950	0.891
	Mn	0.052	0.029	0.021	0.025
	Fe2+	1.692	1.646	1.575	1.633
	Zn	0.000	0.000	0.000	0.000
	Li*	0.107	0.103	0.098	0.117
∑Y		3.000	3.000	3.000	3.000
X:	Ca	0.110	0.079	0.072	0.080
	Ba	0.000	0.000	0.000	0.000
	Na	0.655	0.690	0.692	0.601
	K	0.012	0.010	0.006	0.014
	Rb	0.000	0.000	0.000	0.000
	Cs	0.000	0.000	0.000	0.000
	❒	0.223	0.221	0.230	0.305
OH		4.000	4.000	4.000	4.000
F		0.000	0.000	0.000	0.000
Cl		0.000	0.000	0.000	0.000

Label		T2 xl	T2 xl	T2 xl	T2 xl
Spot		rim	inter.	core	inter.
Texture		euh. c.g.	euh. c.g.	euh. c.g.	euh. c.g.
SiO2		35.650	35.930	35.960	36.170
TiO2		0.997	0.690	0.348	0.641
Al2O3		32.510	33.380	33.790	33.510
FeO		11.380	10.670	11.350	11.440
MnO		0.156	0.156	0.182	0.096
MgO		3.740	3.510	3.480	3.530
CaO		0.502	0.268	0.261	0.289
Na2O		1.839	1.750	1.722	1.854
K2O		0.041	0.034	0.036	0.035
F		0.000	0.000	0.000	0.000
Cl		0.000	0.000	0.000	0.000
Total		86.820	86.400	87.130	87.570
		9/29/09			
Structural formula based on 31 anions (O, OH, F)					
T:	Si	5.891	5.921	5.904	5.909
	Al	0.109	0.079	0.096	0.091
B		3.000	3.000	3.000	3.000
Z:	Al	6.000	6.000	6.000	6.000
	Mg	0.000	0.000	0.000	0.000
	Cr	0.000	0.000	0.000	0.000
	Fe3+	0.000	0.000	0.000	0.000
Y:	Al	0.223	0.404	0.442	0.361
	Ti	0.124	0.085	0.043	0.079
	V	0.000	0.000	0.000	0.000
	Cr	0.000	0.000	0.000	0.000
	Fe3+	0.000	0.000	0.000	0.000
	Mg	0.921	0.862	0.852	0.860
	Mn	0.022	0.022	0.025	0.013
	Fe2+	1.573	1.470	1.558	1.563
	Zn	0.000	0.000	0.000	0.000
	Li*	0.137	0.156	0.079	0.124
ΣY		3.000	3.000	3.000	3.000
X:	Ca	0.089	0.047	0.046	0.051
	Ba	0.000	0.000	0.000	0.000
	Na	0.589	0.559	0.548	0.587
	K	0.009	0.007	0.008	0.007
	Rb	0.000	0.000	0.000	0.000
	Cs	0.000	0.000	0.000	0.000
	❒	0.313	0.387	0.398	0.355
OH		4.000	4.000	4.000	4.000
F		0.000	0.000	0.000	0.000
Cl		0.000	0.000	0.000	0.000

Label		T2 xl	T2 xl	T2 xl6	T2 xl6
Spot		rim	core	rim	rim
Texture		euh. c.g.	euh. c.g.	euh. c.g.	euh. c.g.
SiO2		34.670	34.190	34.590	35.430
TiO2		1.259	0.300	1.044	1.032
Al2O3		32.370	33.870	32.290	32.120
FeO		11.370	11.180	11.670	11.190
MnO		0.139	0.000	0.173	0.165
MgO		3.880	3.520	3.650	3.850
CaO		0.527	0.255	0.542	0.484
Na2O		1.995	1.758	2.055	1.959
K2O		0.063	0.049	0.064	0.063
F		0.000	0.000	0.000	0.000
Cl		0.003	0.000	0.000	0.000
Total		86.280	85.120	86.070	86.290
Structural formula based on 31 anions (O, OH, F)					
T:	Si	5.789	5.763	5.799	5.891
	Al	0.211	0.237	0.201	0.109
B		3.000	3.000	3.000	3.000
Z:	Al	6.000	6.000	6.000	6.000
	Mg	0.000	0.000	0.000	0.000
	Cr	0.000	0.000	0.000	0.000
	Fe3+	0.000	0.000	0.000	0.000
Y:	Al	0.158	0.492	0.179	0.185
	Ti	0.158	0.038	0.132	0.129
	V	0.000	0.000	0.000	0.000
	Cr	0.000	0.000	0.000	0.000
	Fe3+	0.000	0.000	0.000	0.000
	Mg	0.966	0.885	0.912	0.954
	Mn	0.020	0.000	0.025	0.023
	Fe2+	1.588	1.576	1.636	1.556
	Zn	0.000	0.000	0.000	0.000
	Li*	0.111	0.009	0.117	0.152
ΣY		3.000	3.000	3.000	3.000
X:	Ca	0.094	0.046	0.097	0.086
	Ba	0.000	0.000	0.000	0.000
	Na	0.646	0.575	0.668	0.632
	K	0.013	0.011	0.014	0.013
	Rb	0.000	0.000	0.000	0.000
	Cs	0.000	0.000	0.000	0.000
	❒	0.246	0.369	0.221	0.269
OH		3.999	4.000	4.000	4.000
F		0.000	0.000	0.000	0.000
Cl		0.001	0.000	0.000	0.000

Label		T2 xl6	T2 xl6	T2 xl6	T2 xl6
Spot		inter.	core	core	inter.
Texture		euh. c.g.	euh. c.g.	euh. c.g.	euh. c.g.
SiO2		35.760	36.170	26.240	35.640
TiO2		0.648	0.311	0.404	0.805
Al2O3		33.430	34.060	29.510	30.240
FeO		10.500	11.020	10.310	12.610
MnO		0.130	0.139	0.035	0.173
MgO		3.530	3.520	3.080	3.690
CaO		0.276	0.197	0.256	1.140
Na2O		1.700	1.732	1.639	1.828
K2O		0.046	0.021	0.039	0.049
F		0.000	0.000	0.000	0.006
Cl		0.002	0.000	0.000	0.000
Total		86.020	87.170	71.510	86.170
Structural formula based on 31 anions (O, OH, F)					
T:	Si	5.912	5.916	5.340	5.991
	Al	0.088	0.084	0.660	0.009
B		3.000	3.000	3.000	3.000
Z:	Al	6.000	6.000	6.000	5.982
	Mg	0.000	0.000	0.000	0.018
	Cr	0.000	0.000	0.000	0.000
	Fe3+	0.000	0.000	0.000	0.000
Y:	Al	0.427	0.481	0.418	0.000
	Ti	0.081	0.038	0.062	0.102
	V	0.000	0.000	0.000	0.000
	Cr	0.000	0.000	0.000	0.000
	Fe3+	0.000	0.000	0.000	0.000
	Mg	0.870	0.858	0.934	0.907
	Mn	0.018	0.019	0.006	0.025
	Fe2+	1.452	1.507	1.755	1.773
	Zn	0.000	0.000	0.000	0.000
	Li*	0.153	0.096	0.000	0.194
ΣY		3.000	3.000	3.175	3.000
X:	Ca	0.049	0.035	0.056	0.205
	Ba	0.000	0.000	0.000	0.000
	Na	0.545	0.549	0.647	0.596
	K	0.010	0.004	0.010	0.010
	Rb	0.000	0.000	0.000	0.000
	Cs	0.000	0.000	0.000	0.000
	❒	0.396	0.412	0.288	0.188
OH		4.000	4.000	4.000	3.997
F		0.000	0.000	0.000	0.003
Cl		0.000	0.000	0.000	0.000

Label		T2 xl6	T2 xl6 zone int.	T3 euhedral grains	T3 euhedral grains
Spot		rim	n/a	rim	inter.
Texture		euh. c.g.	euh. c.g.	euh. c.g.	euh. c.g.
SiO2		34.820	36.630	34.970	35.420
TiO2		0.933	0.151	1.138	0.928
Al2O3		32.290	32.940	32.280	32.670
FeO		8.980	11.720	11.560	11.500
MnO		0.009	0.043	0.198	0.155
MgO		4.410	3.580	3.750	4.030
CaO		0.988	0.377	0.609	0.467
Na2O		1.844	1.726	1.895	1.963
K2O		0.021	0.018	0.073	0.053
F		0.201	0.000	0.000	0.000
Cl		0.008	0.000	0.004	0.000
Total		84.410	87.180	86.470	87.180
Structural formula based on 31 anions (O, OH, F)					
T:	Si	5.847	6.008	5.827	5.846
	Al	0.153	0.000	0.173	0.154
B		3.000	3.000	3.000	3.000
Z:	Al	6.000	6.000	6.000	6.000
	Mg	0.000	0.000	0.000	0.000
	Cr	0.000	0.000	0.000	0.000
	Fe3+	0.000	0.000	0.000	0.000
Y:	Al	0.237	0.368	0.165	0.201
	Ti	0.118	0.019	0.143	0.115
	V	0.000	0.000	0.000	0.000
	Cr	0.000	0.000	0.000	0.000
	Fe3+	0.000	0.000	0.000	0.000
	Mg	1.104	0.875	0.931	0.992
	Mn	0.001	0.006	0.028	0.022
	Fe2+	1.261	1.608	1.611	1.587
	Zn	0.000	0.000	0.000	0.000
	Li*	0.280	0.124	0.122	0.083
∑Y		3.000	3.000	3.000	3.000
X:	Ca	0.178	0.066	0.109	0.083
	Ba	0.000	0.000	0.000	0.000
	Na	0.600	0.549	0.612	0.628
	K	0.005	0.004	0.016	0.011
	Rb	0.000	0.000	0.000	0.000
	Cs	0.000	0.000	0.000	0.000
	❒	0.217	0.381	0.264	0.278
OH		3.891	4.000	3.999	4.000
F		0.106	0.000	0.000	0.000
Cl		0.002	0.000	0.001	0.000

Label		T3 euhedral grains	T3 euhedral grains	T3 euhedral grains	T3 euhedral grains
Spot		inter.	rim	rim	rim
Texture		euh. c.g.	euh. c.g.	euh. c.g.	euh. c.g.
SiO2		34.300	34.460	35.100	33.730
TiO2		1.333	1.315	1.082	1.346
Al2O3		31.990	32.020	32.410	31.630
FeO		12.420	13.020	10.980	13.140
MnO		0.249	0.206	0.267	0.258
MgO		3.040	2.945	3.840	3.320
CaO		0.519	0.435	0.498	0.566
Na2O		2.050	2.082	1.971	2.010
K2O		0.060	0.085	0.072	0.059
F		0.000	0.000	0.000	0.000
Cl		0.003	0.000	0.000	0.018
Total		85.970	86.570	86.230	86.060
Structural formula based on 31 anions (O, OH, F)					
T:	Si	5.785	5.790	5.843	5.731
	Al	0.215	0.210	0.157	0.269
B		3.000	3.000	3.000	3.000
Z:	Al	6.000	6.000	6.000	6.000
	Mg	0.000	0.000	0.000	0.000
	Cr	0.000	0.000	0.000	0.000
	Fe3+	0.000	0.000	0.000	0.000
Y:	Al	0.143	0.131	0.201	0.064
	Ti	0.169	0.166	0.135	0.172
	V	0.000	0.000	0.000	0.000
	Cr	0.000	0.000	0.000	0.000
	Fe3+	0.000	0.000	0.000	0.000
	Mg	0.764	0.738	0.953	0.841
	Mn	0.036	0.029	0.038	0.037
	Fe2+	1.752	1.830	1.529	1.867
	Zn	0.000	0.000	0.000	0.000
	Li*	0.136	0.106	0.144	0.019
∑Y		3.000	3.000	3.000	3.000
X:	Ca	0.094	0.078	0.089	0.103
	Ba	0.000	0.000	0.000	0.000
	Na	0.670	0.678	0.636	0.662
	K	0.013	0.018	0.015	0.013
	Rb	0.000	0.000	0.000	0.000
	Cs	0.000	0.000	0.000	0.000
	❒	0.223	0.225	0.260	0.222
OH		3.999	4.000	4.000	3.995
F		0.000	0.000	0.000	0.000
Cl		0.001	0.000	0.000	0.005

Label		T3 euhedral grains	T3 euhedral grains	T3 ?	T3 zoning
Spot		rim	rim	core	inter.
Texture		euh. c.g.	euh. c.g.	euh. c.g.	euh. c.g.
SiO2		34.730	34.900	35.840	35.220
TiO2		1.190	1.297	0.390	1.211
Al2O3		31.570	31.380	33.350	31.260
FeO		12.510	12.110	10.940	12.370
MnO		0.215	0.155	0.172	0.077
MgO		3.400	3.470	3.500	3.570
CaO		0.516	0.541	0.264	0.575
Na2O		2.011	2.010	1.746	2.070
K2O		0.079	0.058	0.056	0.081
F		0.000	0.000	0.000	0.000
Cl		0.009	0.000	0.000	0.004
Total		86.230	85.930	86.260	86.430
Structural formula based on 31 anions (O, OH, F)					
T:	Si	5.842	5.870	5.928	5.894
	Al	0.158	0.130	0.072	0.106
B		3.000	3.000	3.000	3.000
Z:	Al	6.000	6.000	6.000	6.000
	Mg	0.000	0.000	0.000	0.000
	Cr	0.000	0.000	0.000	0.000
	Fe3+	0.000	0.000	0.000	0.000
Y:	Al	0.102	0.090	0.430	0.060
	Ti	0.151	0.164	0.049	0.152
	V	0.000	0.000	0.000	0.000
	Cr	0.000	0.000	0.000	0.000
	Fe3+	0.000	0.000	0.000	0.000
	Mg	0.853	0.870	0.863	0.891
	Mn	0.031	0.022	0.024	0.011
	Fe2+	1.760	1.703	1.513	1.731
	Zn	0.000	0.000	0.000	0.000
	Li*	0.104	0.151	0.121	0.154
∑Y		3.000	3.000	3.000	3.000
X:	Ca	0.093	0.097	0.047	0.103
	Ba	0.000	0.000	0.000	0.000
	Na	0.656	0.655	0.560	0.672
	K	0.017	0.012	0.012	0.017
	Rb	0.000	0.000	0.000	0.000
	Cs	0.000	0.000	0.000	0.000
	❒	0.234	0.235	0.382	0.208
OH		3.998	4.000	4.000	3.999
F		0.000	0.000	0.000	0.000
Cl		0.002	0.000	0.000	0.001

Label		T3 xl3 ?	T3 xl3 ?	T3 xl3	T3 xl4 bright core
Spot		rim	rim	inter.	rim
Texture		euh. c.g.	euh. c.g.	euh. c.g.	euh. c.g.
SiO2		34.910	35.000	34.420	34.950
TiO2		1.313	1.141	1.129	1.365
Al2O3		32.070	31.840	32.550	31.220
FeO		13.410	11.340	11.910	12.830
MnO		0.266	0.189	0.129	0.112
MgO		3.000	3.890	3.960	3.740
CaO		0.420	0.532	0.567	0.659
Na2O		1.926	2.054	2.069	2.034
K2O		0.061	0.071	0.066	0.055
F		0.000	0.000	0.000	0.000
Cl		0.000	0.004	0.009	0.000
Total		87.370	86.060	86.810	86.960
Structural formula based on 31 anions (O, OH, F)					
T:	Si	5.821	5.854	5.742	5.844
	Al	0.179	0.146	0.258	0.156
B		3.000	3.000	3.000	3.000
Z:	Al	6.000	6.000	6.000	5.996
	Mg	0.000	0.000	0.000	0.004
	Cr	0.000	0.000	0.000	0.000
	Fe3+	0.000	0.000	0.000	0.000
Y:	Al	0.123	0.130	0.141	0.000
	Ti	0.165	0.144	0.142	0.172
	V	0.000	0.000	0.000	0.000
	Cr	0.000	0.000	0.000	0.000
	Fe3+	0.000	0.000	0.000	0.000
	Mg	0.746	0.970	0.985	0.928
	Mn	0.038	0.027	0.018	0.016
	Fe2+	1.870	1.586	1.662	1.794
	Zn	0.000	0.000	0.000	0.000
	Li*	0.059	0.143	0.052	0.090
∑Y		3.000	3.000	3.000	3.000
X:	Ca	0.075	0.095	0.101	0.118
	Ba	0.000	0.000	0.000	0.000
	Na	0.622	0.666	0.669	0.659
	K	0.013	0.015	0.014	0.012
	Rb	0.000	0.000	0.000	0.000
	Cs	0.000	0.000	0.000	0.000
	❒	0.290	0.224	0.215	0.211
OH		4.000	3.999	3.998	4.000
F		0.000	0.000	0.000	0.000
Cl		0.000	0.001	0.002	0.000

Label		T3 xl4 nose	T5 vein	T5 vein	T5 qtz?
Spot		rim	inter.	inter.	core
Texture		euh. c.g.	euh. c.g.	euh. c.g.	euh. c.g.
SiO2		34.420	35.140	34.540	35.510
TiO2		1.062	0.704	0.953	0.385
Al2O3		31.660	29.960	32.540	33.400
FeO		11.040	12.860	11.090	11.410
MnO		0.172	0.069	0.138	0.086
MgO		3.870	4.130	4.110	3.450
CaO		0.532	1.211	0.556	0.329
Na2O		2.116	1.841	1.974	1.795
K2O		0.062	0.054	0.060	0.080
F		0.000	0.000	0.000	0.000
Cl		0.001	0.013	0.000	0.000
Total		84.950	85.980	85.960	86.440
Structural formula based on 31 anions (O, OH, F)					
T:	Si	5.829	5.949	5.783	5.885
	Al	0.171	0.051	0.217	0.115
B		3.000	3.000	3.000	3.000
Z:	Al	6.000	5.927	6.000	6.000
	Mg	0.000	0.073	0.000	0.000
	Cr	0.000	0.000	0.000	0.000
	Fe3+	0.000	0.000	0.000	0.000
Y:	Al	0.149	0.000	0.203	0.408
	Ti	0.135	0.090	0.120	0.048
	V	0.000	0.000	0.000	0.000
	Cr	0.000	0.000	0.000	0.000
	Fe3+	0.000	0.000	0.000	0.000
	Mg	0.977	0.969	1.026	0.852
	Mn	0.025	0.010	0.020	0.012
	Fe2+	1.564	1.821	1.553	1.581
	Zn	0.000	0.000	0.000	0.000
	Li*	0.150	0.111	0.079	0.099
ΣY		3.000	3.000	3.000	3.000
X:	Ca	0.097	0.220	0.100	0.058
	Ba	0.000	0.000	0.000	0.000
	Na	0.695	0.604	0.641	0.577
	K	0.013	0.012	0.013	0.017
	Rb	0.000	0.000	0.000	0.000
	Cs	0.000	0.000	0.000	0.000
	❒	0.195	0.164	0.247	0.348
OH		4.000	3.996	4.000	4.000
F		0.000	0.000	0.000	0.000
Cl		0.000	0.004	0.000	0.000

Label		T5 qtz?	T5 zone	T5 zone	SM2 pt3 tour1zoning
Spot		rim	rim	inter.	edge
Texture		euh. c.g.	euh. c.g.	euh. c.g.	skel. f.g.
SiO2		34.900	34.710	35.190	36.060
TiO2		1.305	1.325	1.137	1.014
Al2O3		31.240	31.620	32.170	32.550
FeO		12.480	12.300	11.420	11.120
MnO		0.189	0.172	0.103	0.195
MgO		3.450	2.914	3.790	4.000
CaO		0.526	0.408	0.555	0.502
Na2O		1.977	1.966	1.888	1.894
K2O		0.098	0.094	0.052	0.067
F		0.000	0.000	0.000	0.012
Cl		0.000	0.000	0.001	0.000
Total		86.160	85.510	86.300	87.410
Structural formula based on 31 anions (O, OH, F)					
T:	Si	5.871	5.865	5.860	5.910
	Al	0.129	0.135	0.140	0.090
B		3.000	3.000	3.000	3.000
Z:	Al	6.000	6.000	6.000	6.000
	Mg	0.000	0.000	0.000	0.000
	Cr	0.000	0.000	0.000	0.000
	Fe3+	0.000	0.000	0.000	0.000
Y:	Al	0.065	0.161	0.174	0.197
	Ti	0.165	0.168	0.142	0.125
	V	0.000	0.000	0.000	0.000
	Cr	0.000	0.000	0.000	0.000
	Fe3+	0.000	0.000	0.000	0.000
	Mg	0.865	0.734	0.941	0.977
	Mn	0.027	0.025	0.015	0.027
	Fe2+	1.756	1.738	1.590	1.524
	Zn	0.000	0.000	0.000	0.000
	Li*	0.122	0.174	0.138	0.149
∑Y		3.000	3.000	3.000	3.000
X:	Ca	0.095	0.074	0.099	0.088
	Ba	0.000	0.000	0.000	0.000
	Na	0.645	0.644	0.609	0.602
	K	0.021	0.020	0.011	0.014
	Rb	0.000	0.000	0.000	0.000
	Cs	0.000	0.000	0.000	0.000
	❒	0.239	0.262	0.281	0.296
OH		4.000	4.000	4.000	3.994
F		0.000	0.000	0.000	0.006
Cl		0.000	0.000	0.000	0.000

Label		SM2 pt3 tour2zoning	SM2 pt3 tour3zoning	SM2 pt3 tour4zoning	SM2 pt3 tour5zoning
Spot		edge	inter.	inter.	arm
Texture		skel. f.g.	skel. f.g.	skel. f.g.	skel. f.g.
SiO2		35.770	35.640	35.530	36.250
TiO2		1.055	0.845	1.159	0.294
Al2O3		32.230	33.120	32.740	33.970
FeO		10.720	10.830	12.070	10.530
MnO		0.140	0.307	0.139	0.196
MgO		4.200	4.460	3.760	3.590
CaO		0.712	0.571	0.446	0.348
Na2O		1.892	1.760	1.707	1.798
K2O		0.049	0.065	0.040	0.047
F		0.000	0.154	0.000	0.000
Cl		0.000	0.000	0.017	0.000
Total		86.770	87.680	87.600	87.010
Structural formula based on 31 anions (O, OH, F)					
T:	Si	5.896	5.838	5.850	5.923
	Al	0.104	0.162	0.150	0.077
B		3.000	3.000	3.000	3.000
Z:	Al	6.000	6.000	6.000	6.000
	Mg	0.000	0.000	0.000	0.000
	Cr	0.000	0.000	0.000	0.000
	Fe3+	0.000	0.000	0.000	0.000
Y:	Al	0.158	0.231	0.203	0.464
	Ti	0.131	0.104	0.143	0.036
	V	0.000	0.000	0.000	0.000
	Cr	0.000	0.000	0.000	0.000
	Fe3+	0.000	0.000	0.000	0.000
	Mg	1.032	1.089	0.923	0.874
	Mn	0.020	0.043	0.019	0.027
	Fe2+	1.478	1.483	1.662	1.439
	Zn	0.000	0.000	0.000	0.000
	Li*	0.182	0.050	0.050	0.160
∑Y		3.000	3.000	3.000	3.000
X:	Ca	0.126	0.100	0.079	0.061
	Ba	0.000	0.000	0.000	0.000
	Na	0.605	0.559	0.545	0.569
	K	0.010	0.014	0.008	0.010
	Rb	0.000	0.000	0.000	0.000
	Cs	0.000	0.000	0.000	0.000
	❒	0.259	0.327	0.368	0.360
OH		4.000	3.920	3.995	4.000
F		0.000	0.080	0.000	0.000
Cl		0.000	0.000	0.005	0.000

APPENDIX G

ELECTRON MICROPROBE ANALYSIS OF TOURMALINE IN GRANITE

Label		SM1 1.1	SM1 1.2	SM1 1.3	SM1 1.4
Spot		rim	rim	inter.	inter.
Texture		skel. f.g.	skel. f.g.	skel. f.g.	skel. f.g.
SiO2		35.290	35.510	35.860	35.230
TiO2		0.598	0.735	0.948	1.043
Al2O3		31.560	32.120	31.590	32.190
FeO		10.270	11.560	10.680	10.850
MnO		0.183	0.173	0.164	0.283
MgO		4.040	4.120	4.180	4.070
CaO		0.523	0.570	0.426	0.536
Na2O		1.858	1.956	1.974	1.904
K2O		0.040	0.052	0.055	0.066
F		0.000	0.000	0.000	0.000
Cl		0.000	0.000	0.000	0.003
Total		84.360	86.800	85.880	86.180
Structural formula based on 31 anions (O, OH, F)					
T:	Si	5.965	5.891	5.968	5.865
	Al	0.035	0.109	0.032	0.135
B		3.000	3.000	3.000	3.000
Z:	Al	6.000	6.000	6.000	6.000
	Mg	0.000	0.000	0.000	0.000
	Cr	0.000	0.000	0.000	0.000
	Fe3+	0.000	0.000	0.000	0.000
Y:	Al	0.252	0.172	0.164	0.181
	Ti	0.076	0.092	0.119	0.131
	V	0.000	0.000	0.000	0.000
	Cr	0.000	0.000	0.000	0.000
	Fe3+	0.000	0.000	0.000	0.000
	Mg	1.018	1.019	1.037	1.010
	Mn	0.026	0.024	0.023	0.040
	Fe2+	1.452	1.604	1.486	1.511
	Zn	0.000	0.000	0.000	0.000
	Li*	0.176	0.089	0.170	0.128
ΣY		3.000	3.000	3.000	3.000
X:	Ca	0.095	0.101	0.076	0.096
	Ba	0.000	0.000	0.000	0.000
	Na	0.609	0.629	0.637	0.615
	K	0.009	0.011	0.012	0.014
	Rb	0.000	0.000	0.000	0.000
	Cs	0.000	0.000	0.000	0.000
	r	0.288	0.259	0.275	0.276
OH		4.000	4.000	4.000	3.999
F		0.000	0.000	0.000	0.000
Cl		0.000	0.000	0.000	0.001

Label		SM1 1.5	SM1 1.6	SM1 1.7	SM1 1.8
Spot		core	core	inter.	rim
Texture		skel. f.g.	skel. f.g.	skel. f.g.	skel. f.g.
SiO2		36.100	35.820	35.060	35.870
TiO2		0.241	0.535	1.034	0.381
Al2O3		32.580	31.900	32.310	33.510
FeO		10.410	11.390	12.200	10.840
MnO		0.137	0.009	0.118	0.219
MgO		4.060	4.060	3.600	3.790
CaO		0.401	0.504	0.488	0.253
Na2O		1.825	1.959	1.893	1.704
K2O		0.048	0.055	0.062	0.066
F		0.000	0.111	0.000	0.000
Cl		0.006	0.000	0.000	0.000
Total		85.810	86.300	86.770	86.630
Structural formula based on 31 anions (O, OH, F)					
T:	Si	5.988	5.959	5.839	5.912
	Al	0.012	0.041	0.161	0.088
B		3.000	3.000	3.000	3.000
Z:	Al	6.000	6.000	6.000	6.000
	Mg	0.000	0.000	0.000	0.000
	Cr	0.000	0.000	0.000	0.000
	Fe3+	0.000	0.000	0.000	0.000
Y:	Al	0.357	0.213	0.182	0.421
	Ti	0.030	0.067	0.129	0.047
	V	0.000	0.000	0.000	0.000
	Cr	0.000	0.000	0.000	0.000
	Fe3+	0.000	0.000	0.000	0.000
	Mg	1.004	1.007	0.894	0.931
	Mn	0.019	0.001	0.017	0.031
	Fe2+	1.444	1.585	1.699	1.494
	Zn	0.000	0.000	0.000	0.000
	Li*	0.145	0.128	0.079	0.076
ΣY		3.000	3.000	3.000	3.000
X:	Ca	0.071	0.090	0.087	0.045
	Ba	0.000	0.000	0.000	0.000
	Na	0.587	0.632	0.611	0.544
	K	0.010	0.012	0.013	0.014
	Rb	0.000	0.000	0.000	0.000
	Cs	0.000	0.000	0.000	0.000
	r	0.332	0.267	0.288	0.397
OH		3.998	3.941	4.000	4.000
F		0.000	0.059	0.000	0.000
Cl		0.002	0.000	0.000	0.000

Label		SM1 2.1	SM1 3.1redo	SM1 4.1	SM1 4.2
Spot		core	rim	arm	arm
Texture		skel. f.g.	skel. f.g.	skel. f.g.	skel. f.g.
SiO2		35.900	35.240	35.840	35.960
TiO2		0.884	0.888	0.254	0.402
Al2O3		31.620	31.160	31.820	31.530
FeO		11.520	10.840	10.640	10.770
MnO		0.073	0.082	0.128	0.110
MgO		4.390	4.320	4.350	4.540
CaO		0.639	0.526	0.551	0.519
Na2O		2.007	1.836	1.799	1.919
K2O		0.067	0.043	0.049	0.064
F		0.000	0.000	0.047	0.000
Cl		0.000	0.000	0.000	0.000
Total		87.090	84.930	85.460	85.810
Structural formula based on 31 anions (O, OH, F)					
T:	Si	5.931	5.947	5.993	5.997
	Al	0.069	0.053	0.007	0.003
B		3.000	3.000	3.000	3.000
Z:	Al	6.000	6.000	6.000	6.000
	Mg	0.000	0.000	0.000	0.000
	Cr	0.000	0.000	0.000	0.000
	Fe3+	0.000	0.000	0.000	0.000
Y:	Al	0.087	0.144	0.265	0.193
	Ti	0.110	0.113	0.032	0.050
	V	0.000	0.000	0.000	0.000
	Cr	0.000	0.000	0.000	0.000
	Fe3+	0.000	0.000	0.000	0.000
	Mg	1.081	1.087	1.084	1.129
	Mn	0.010	0.012	0.018	0.015
	Fe2+	1.592	1.530	1.488	1.502
	Zn	0.000	0.000	0.000	0.000
	Li*	0.120	0.116	0.113	0.110
ΣY		3.000	3.000	3.000	3.000
X:	Ca	0.113	0.095	0.099	0.093
	Ba	0.000	0.000	0.000	0.000
	Na	0.643	0.601	0.583	0.621
	K	0.014	0.009	0.011	0.014
	Rb	0.000	0.000	0.000	0.000
	Cs	0.000	0.000	0.000	0.000
	r	0.230	0.295	0.308	0.273
OH		4.000	4.000	3.975	4.000
F		0.000	0.000	0.025	0.000
Cl		0.000	0.000	0.000	0.000

Label		SM1 4.3	SM1 4.4	SM1 5.1	SM2 pt3 tour1zoning
Spot		arm	arm	arm	rim
Texture		skel. f.g.	skel. f.g.	skel. f.g.	skel. f.g.
SiO2		35.450	35.540	35.180	36.060
TiO2		0.846	0.689	0.761	1.014
Al2O3		31.360	31.430	31.840	32.550
FeO		10.670	10.010	10.410	11.120
MnO		0.000	0.164	0.119	0.195
MgO		4.320	4.470	4.530	4.000
CaO		0.476	0.577	0.569	0.502
Na2O		1.936	1.925	1.974	1.894
K2O		0.047	0.060	0.041	0.067
F		0.000	0.021	0.000	0.012
Cl		0.000	0.008	0.005	0.000
Total		85.110	84.880	85.430	87.410
Structural formula based on 31 anions (O, OH, F)					
T:	Si	5.956	5.968	5.893	5.910
	Al	0.044	0.032	0.107	0.090
B		3.000	3.000	3.000	3.000
Z:	Al	6.000	6.000	6.000	6.000
	Mg	0.000	0.000	0.000	0.000
	Cr	0.000	0.000	0.000	0.000
	Fe3+	0.000	0.000	0.000	0.000
Y:	Al	0.165	0.188	0.179	0.197
	Ti	0.107	0.087	0.096	0.125
	V	0.000	0.000	0.000	0.000
	Cr	0.000	0.000	0.000	0.000
	Fe3+	0.000	0.000	0.000	0.000
	Mg	1.082	1.119	1.131	0.977
	Mn	0.000	0.023	0.017	0.027
	Fe2+	1.499	1.406	1.458	1.524
	Zn	0.000	0.000	0.000	0.000
	Li*	0.147	0.177	0.118	0.149
∑Y		3.000	3.000	3.000	3.000
X:	Ca	0.086	0.104	0.102	0.088
	Ba	0.000	0.000	0.000	0.000
	Na	0.631	0.627	0.641	0.602
	K	0.010	0.013	0.009	0.014
	Rb	0.000	0.000	0.000	0.000
	Cs	0.000	0.000	0.000	0.000
	r	0.274	0.257	0.248	0.296
OH		4.000	3.987	3.999	3.994
F		0.000	0.011	0.000	0.006
Cl		0.000	0.002	0.001	0.000

Label		SM2 pt3 tour2zoning rim	SM2 pt3 tour3zoning inter.	SM2 pt3 tour4zoning rim	SM2 pt3 tour5zoning arm
Spot					
Texture		skel. f.g.	skel. f.g.	skel. f.g.	skel. f.g.
SiO2		35.770	35.640	35.530	36.250
TiO2		1.055	0.845	1.159	0.294
Al2O3		32.230	33.120	32.740	33.970
FeO		10.720	10.830	12.070	10.530
MnO		0.140	0.307	0.139	0.196
MgO		4.200	4.460	3.760	3.590
CaO		0.712	0.571	0.446	0.348
Na2O		1.892	1.760	1.707	1.798
K2O		0.049	0.065	0.040	0.047
F		0.000	0.154	0.000	0.000
Cl		0.000	0.000	0.017	0.000
Total		86.770	87.680	87.600	87.010
Structural formula based on 31 anions (O, OH, F)					
T:	Si	5.896	5.838	5.850	5.923
	Al	0.104	0.162	0.150	0.077
B		3.000	3.000	3.000	3.000
Z:	Al	6.000	6.000	6.000	6.000
	Mg	0.000	0.000	0.000	0.000
	Cr	0.000	0.000	0.000	0.000
	Fe3+	0.000	0.000	0.000	0.000
Y:	Al	0.158	0.231	0.203	0.464
	Ti	0.131	0.104	0.143	0.036
	V	0.000	0.000	0.000	0.000
	Cr	0.000	0.000	0.000	0.000
	Fe3+	0.000	0.000	0.000	0.000
	Mg	1.032	1.089	0.923	0.874
	Mn	0.020	0.043	0.019	0.027
	Fe2+	1.478	1.483	1.662	1.439
	Zn	0.000	0.000	0.000	0.000
	Li*	0.182	0.050	0.050	0.160
ΣY		3.000	3.000	3.000	3.000
X:	Ca	0.126	0.100	0.079	0.061
	Ba	0.000	0.000	0.000	0.000
	Na	0.605	0.559	0.545	0.569
	K	0.010	0.014	0.008	0.010
	Rb	0.000	0.000	0.000	0.000
	Cs	0.000	0.000	0.000	0.000
	r	0.259	0.327	0.368	0.360
OH		4.000	3.920	3.995	4.000
F		0.000	0.080	0.000	0.000
Cl		0.000	0.000	0.005	0.000

Label		SM2 pt3 tour6zoning	SM2 pt3 tour7zoning
Spot		arm	rim
Texture		skel. f.g.	skel. f.g.
SiO2		35.600	34.830
TiO2		0.416	1.129
Al2O3		32.390	32.140
FeO		10.440	11.510
MnO		0.154	0.098
MgO		4.550	3.830
CaO		0.458	0.525
Na2O		1.808	1.767
K2O		0.054	0.072
F		0.047	0.051
Cl		0.012	0.000
Total		85.900	85.940
Structural formula based on 31 anions (O, OH, F)			
T:	Si	5.925	5.838
	Al	0.075	0.162
B		3.000	3.000
Z:	Al	6.000	6.000
	Mg	0.000	0.000
	Cr	0.000	0.000
Fe3+		0.000	0.000
Y:	Al	0.278	0.187
	Ti	0.052	0.142
	V	0.000	0.000
	Cr	0.000	0.000
Fe3+		0.000	0.000
	Mg	1.129	0.957
	Mn	0.022	0.014
Fe2+		1.453	1.613
	Zn	0.000	0.000
	Li*	0.066	0.087
ΣY		3.000	3.000
X:	Ca	0.082	0.094
	Ba	0.000	0.000
	Na	0.583	0.574
	K	0.012	0.015
	Rb	0.000	0.000
	Cs	0.000	0.000
	r	0.324	0.316
OH		3.972	3.973
F		0.025	0.027
Cl		0.003	0.000

APPENDIX H

ELECTRON MICROPROBE ANALYSIS OF MICA

Label	SM1 Pt 4 bio	SM1 Pt 4 wm	SM1 Pt 4 bio2	SM1 Pt 4 wm2
Spot	granite	granite	granite	granite
Texture				
SiO2	35.360	45.730	35.570	44.930
TiO2	3.090	0.798	3.200	0.780
Al2O3	17.020	31.440	17.600	32.980
FeO	24.670	4.150	25.350	3.420
MnO	0.412	0.000	0.859	0.000
MgO	4.060	1.478	3.700	1.099
CaO	0.110	0.166	0.108	0.044
Na2O	0.074	0.260	0.042	0.308
K2O	9.060	11.080	9.500	10.880
F	0.251	0.000	0.214	0.000
Cl	0.000	0.000	0.053	0.000
Total	94.000	95.100	96.090	94.440
Number of ions on the basis of 11 O				
apfu				
Si	2.111	2.649	2.662	2.801
Ti	0.098	0.084	0.085	0.184
Al	2.000	1.662	1.655	1.589
Fe	2.464	2.095	2.100	1.634
Mn	0.000	0.000	0.013	0.028
Mg	0.439	0.365	0.338	0.480
Ca	0.014	0.012	0.012	0.009
Na	0.034	0.028	0.019	0.011
K	1.064	0.910	0.945	0.915
F	0.034	0.029	0.000	0.063
Cl	0.200	0.171	0.160	0.000
O	10.767	10.800	10.840	10.937
CatTot	8.457	8.005	7.988	7.715
Total	19.223	18.804	18.828	18.652

Label	SM1 Pt 3 bt1	SM1 Pt 3 wm1	SM1 Pt 3 bt1	SM1 Pt 3 bt2
Spot	granite	granite	granite	granite
Texture				
SiO2	45.090	46.240	34.150	35.350
TiO2	0.630	0.615	2.794	2.859
Al2O3	31.860	31.920	17.870	17.490
FeO	3.590	3.420	24.590	23.880
MnO	0.107	0.134	0.469	0.678
MgO	1.158	1.172	4.140	4.370
CaO	0.000	0.065	0.186	0.121
Na2O	0.129	0.315	0.062	0.163
K2O	11.120	11.220	8.030	9.060
F	0.000	0.000	0.312	0.415
Cl	0.000	0.038	0.000	0.000
Total	93.690	95.130	92.470	94.220
Number of ions on the basis of 11 O				
apfu				
Si	3.117	2.773	3.067	3.110
Ti	0.041	0.187	0.040	0.033
Al	2.525	1.617	2.654	2.590
Fe	0.236	1.652	0.195	0.207
Mn	0.000	0.057	0.000	0.006
Mg	0.150	0.430	0.112	0.119
Ca	0.012	0.009	0.003	0.000
Na	0.034	0.006	0.041	0.017
K	0.963	0.945	0.948	0.978
F	0.000	0.053	0.000	0.000
Cl	0.000	0.007	0.000	0.000
O	11.000	10.940	11.000	11.000
CatTot	7.079	7.737	7.060	7.060
Total	18.079	18.677	18.060	18.060

Label	SM1 Pt 3 bt2	SM1 Pt x wm in plag	SM1 Pt x2 wm in plag	SM1 Pt x3 wm in plag
Spot	granite	in plag	in plag	in plag
Texture				
SiO2	45.300	46.340	47.000	46.730
TiO2	0.610	0.807	0.593	0.310
Al2O3	31.290	27.840	26.970	33.550
FeO	4.470	4.540	5.270	2.706
MnO	0.080	0.268	0.134	0.054
MgO	1.420	1.923	2.308	1.085
CaO	0.031	0.204	0.275	0.055
Na2O	0.285	0.222	0.196	0.273
K2O	11.060	10.670	10.340	10.330
F	0.000	0.000	0.000	0.000
Cl	0.000	0.000	0.000	0.000
Total	94.550	92.810	93.080	95.090
Number of ions on the basis of 11 O				
apfu				
Si	3.138	2.740	2.783	3.112
Ti	0.031	0.169	0.169	0.032
Al	2.552	1.690	1.623	2.534
Fe	0.194	1.650	1.573	0.257
Mn	0.008	0.032	0.045	0.005
Mg	0.119	0.495	0.513	0.145
Ca	0.005	0.016	0.010	0.002
Na	0.041	0.010	0.025	0.038
K	0.972	0.822	0.910	0.969
F	0.000	0.079	0.103	0.000
Cl	0.004	0.000	0.000	0.000
O	10.996	10.921	10.897	11.000
CatTot	7.063	7.702	7.755	7.094
Total	18.059	18.623	18.652	18.094

Label	SM1 Pt 2 wm1	SM1 Pt 2 wm2	SM3 Pt 1 wm1	SM3 Pt 1 bt1
Spot	granite	granite	granite	granite
Texture				
SiO2	45.380	45.470	45.650	35.17
TiO2	0.731	0.669	0.628	3.54
Al2O3	32.580	32.370	31.890	18.55
FeO	3.170	2.676	3.660	23.11
MnO	0.187	0.107	0.053	0.6761
MgO	1.209	1.085	1.115	3.32
CaO	0.000	0.000	0.115	0
Na2O	0.370	0.343	0.173	0.0231
K2O	11.220	11.180	10.840	9.26
F	0.000	0.000	0.009	0.1634
Cl	0.024	0.000	0.052	0
Total	94.860	93.900	94.170	93.75
Number of ions on the basis of 11 O				
apfu				
Si	3.242	3.280	3.133	3.126
Ti	0.042	0.031	0.016	0.0323
Al	2.296	2.218	2.651	2.5734
Fe	0.265	0.308	0.152	0.2098
Mn	0.016	0.008	0.003	0.0031
Mg	0.201	0.240	0.108	0.1138
Ca	0.015	0.021	0.004	0.0085
Na	0.030	0.027	0.036	0.023
K	0.953	0.921	0.884	0.9469
F	0.000	0.000	0.000	0.0019
Cl	0.000	0.000	0.000	0.006
O	11.000	11.000	11.000	10.992
CatTot	7.059	7.053	6.986	7.044
Total	18.059	18.053	17.986	18.036

Label	SM3 Pt 2 bt1	SM3 Pt 2 bt1	SM4 pt1 bio	SM4 pt1 wm
Spot	granite	granite	granite	granite
Texture				
SiO2	35.57	45.06	35.56	45.55
TiO2	2.6961	0.5774	3.36	0.7963
Al2O3	17.82	32.5	17.56	32.59
FeO	25.62	3.34	23.32	3.63
MnO	0.7785	0.1069	0.6453	0.0705
MgO	4.47	1.1769	4.36	1.4016
CaO	0.0456	0	0.005	0.0017
Na2O	0.0701	0.1983	0.0503	0.0805
K2O	9.4	11.13	9.49	10.81
F	0.6675	0	0.5654	0.3918
Cl	0	0.0141	0	0.0024
Total	96.86	94.1	94.67	95.16
Number of ions on the basis of 11 O				
apfu				
Si	2.7734	2.7435	3.09	2.779
Ti	0.2101	0.1564	0.0298	0.1973
Al	1.724	1.6201	2.6269	1.617
Fe	1.5239	1.6522	0.1917	1.524
Mn	0.0452	0.0509	0.0062	0.0427
Mg	0.3899	0.5144	0.1203	0.5081
Ca	0	0.0038	0	0.0004
Na	0.0035	0.0105	0.0264	0.0076
K	0.9316	0.9245	0.9738	0.9457
F	0.0407	0.1628	0	0.1397
Cl	0	0	0.0016	0
O	10.959	10.837	10.998	10.86
CatTot	7.642	7.839	7.067	7.762
Total	18.602	18.676	18.066	18.622

Label	SM4 pt2 bio	SM4 pt2 wm	SM4 pt2 bio2	SM4 pt2 wm2
Spot	granite	granite	granite	granite
Texture				
SiO2	34.71	45.17	35.46	46.27
TiO2	2.7403	0.8223	2.7544	0.6603
Al2O3	17.59	32.08	17.95	33.1
FeO	25.49	3.66	25.33	3.32
MnO	0.6706	0.1269	0.9447	0.1129
MgO	4.15	1.2144	4.33	1.3352
CaO	0.0083	0.0309	0.0578	0
Na2O	0.0039	0.1611	0.0508	0.1828
K2O	9.34	10.96	9.19	10.85
F	0.4597	0	0.4887	0.1268
Cl	0	0	0.0207	0.0119
Total	94.96	94.23	96.36	95.91
Number of ions on the basis of 11 O				
apfu				
Si	3.08	2.7388	3.097	2.7469
Ti	0.0405	0.1626	0.0424	0.1605
Al	2.5972	1.6362	2.5923	1.6388
Fe	0.205	1.6819	0.2098	1.6412
Mn	0.004	0.0448	0.0074	0.062
Mg	0.1412	0.4877	0.1241	0.4998
Ca	0.0001	0.0007	0.0023	0.0048
Na	0.0106	0.0006	0.0214	0.0076
K	0.9319	0.9401	0.9583	0.9082
F	0.0838	0.1147	0	0.1197
Cl	0.0003	0	0	0.0027
O	10.916	10.885	11	10.878
CatTot	7.094	7.808	7.055	7.792
Total	18.01	18.693	18.055	18.67

Label	SM2 pt3 wm halo	SM2 pt3 wm2 halo
Spot	halo	halo
Texture		
SiO2	44.81	45.83
TiO2	0.8579	0.9423
Al2O3	33.72	31.89
FeO	2.8006	3.06
MnO	0.0988	0.0424
MgO	0.879	1.182
CaO	0.0241	0.0481
Na2O	0.1277	0.1121
K2O	10.69	10.14
F	0	0
Cl	0.0048	0
Total	94.02	93.25
Number of ions on the basis of 11 O		
apfu		
Si	3.099	3.057
Ti	0.0333	0.044
Al	2.6135	2.711
Fe	0.1857	0.1598
Mn	0.0064	0.0057
Mg	0.1333	0.0894
Ca	0	0.0018
Na	0.0237	0.0169
K	0.9269	0.9308
F	0.0269	0
Cl	0.0014	0.0006
O	10.972	10.999
CatTot	7.05	7.017
Total	18.022	18.017